




2023

CHEMICAL IMMOBILIZATION OF HELICOPTER-CAPTURED ELK (CERVUS CANADENSIS) AND SURVIVAL OF ELK CALVES IN SOUTHEASTERN KENTUCKY

Kathleen E. Williams

University of Kentucky, kathleen.williams126@gmail.com

Author ORCID Identifier:

 <https://orcid.org/0000-0003-0531-1847>

Digital Object Identifier: <https://doi.org/13023/etd.2023.353>

[Right click to open a feedback form in a new tab to let us know how this document benefits you.](#)

Recommended Citation

Williams, Kathleen E., "CHEMICAL IMMOBILIZATION OF HELICOPTER-CAPTURED ELK (CERVUS CANADENSIS) AND SURVIVAL OF ELK CALVES IN SOUTHEASTERN KENTUCKY" (2023). *Theses and Dissertations--Forestry and Natural Resources*. 72.

https://uknowledge.uky.edu/forestry_etds/72

This Master's Thesis is brought to you for free and open access by the Forestry and Natural Resources at UKnowledge. It has been accepted for inclusion in Theses and Dissertations--Forestry and Natural Resources by an authorized administrator of UKnowledge. For more information, please contact UKnowledge@lsv.uky.edu.

STUDENT AGREEMENT:

I represent that my thesis or dissertation and abstract are my original work. Proper attribution has been given to all outside sources. I understand that I am solely responsible for obtaining any needed copyright permissions. I have obtained needed written permission statement(s) from the owner(s) of each third-party copyrighted matter to be included in my work, allowing electronic distribution (if such use is not permitted by the fair use doctrine) which will be submitted to UKnowledge as Additional File.

I hereby grant to The University of Kentucky and its agents the irrevocable, non-exclusive, and royalty-free license to archive and make accessible my work in whole or in part in all forms of media, now or hereafter known. I agree that the document mentioned above may be made available immediately for worldwide access unless an embargo applies.

I retain all other ownership rights to the copyright of my work. I also retain the right to use in future works (such as articles or books) all or part of my work. I understand that I am free to register the copyright to my work.

REVIEW, APPROVAL AND ACCEPTANCE

The document mentioned above has been reviewed and accepted by the student's advisor, on behalf of the advisory committee, and by the Director of Graduate Studies (DGS), on behalf of the program; we verify that this is the final, approved version of the student's thesis including all changes required by the advisory committee. The undersigned agree to abide by the statements above.

Kathleen E. Williams, Student

Dr. John J. Cox, Major Professor

Dr. Jian Yang, Director of Graduate Studies

CHEMICAL IMMOBILIZATION OF HELICOPTER-CAPTURED ELK (*CERVUS CANADENSIS*) AND SURVIVAL OF ELK CALVES IN SOUTHEASTERN KENTUCKY

THESIS

A dissertation submitted in partial fulfillment of the requirements for the degree of Master of Science in Forest and Natural Resource Science in the Martin Gatton College of Agriculture, Food and Environment at the University of Kentucky

By

Kathleen E. Williams

Lexington, Kentucky

Co- Directors: Dr. John J. Cox, Associate Professor of Wildlife and Conservation Biology
and Dr. Matthew T. Springer, Assistant Extension Professor of Wildlife Management

Lexington, Kentucky

2023

Copyright © Kathleen E. Williams 2023
<https://orcid.org/0000-0003-0531-1847>

ABSTRACT OF THESIS

CHEMICAL IMMOBILIZATION OF HELICOPTER-CAPTURED ELK (*CERVUS CANADENSIS*) AND SURVIVAL OF ELK CALVES IN SOUTHEASTERN KENTUCKY

Safe and effective chemical immobilization is critical to minimize stress and risk of injury when capturing free-ranging, wild ungulates. Many traditionally favored high potency opioids have been phased out or become unavailable because of increased regulations, leading to the development of two pre-mixed combination drugs, butorphanol-azaperone-medetomidine (BAM) and nalbuphine-medetomidine-azaperone (NalMed-A). Both drugs have been used to chemically immobilize ungulates, but their efficacy has not been documented in elk captured and transported via helicopter. During 2020 – 2022, we chemically immobilized helicopter-captured female elk (*Cervus canadensis*) with a single IM-injection of BAM (n = 41) or NalMed-A (n = 78) and documented onset of action and physiological responses including heart rate, respiration, body temperature, and blood oxygen saturation. Mean induction times were 8.34 ± 0.03 minutes for BAM and 8.78 ± 0.08 minutes for NalMed-A. We reversed sedation with atipamezole (IM/IV) and naltrexone (IM), with comparable mean reversal times of 4.56 ± 0.09 and 4.14 ± 0.05 minutes for BAM and NalMed-A, respectively. All physiological responses decreased with induction of either drug, whereas post-induction heart rate and respiration were stable.

During these captures, we checked sedated female elk for signs of pregnancy to prepare for a 3-year calf survival study using vaginal implant transmitters to locate newborn calves across Kentucky's Elk Restoration Zone. During 2020 – 2022, we captured 81 elk neonates and monitored their survival to one year of age or until a mortality occurred, allowing us to estimate elk calf survival for three survival periods (neonatal, summer, and annual), determine cause-specific mortality, and elucidate how maternal characteristics, morphometrics, health metrics, and weather conditions influence survival. Because survival monitoring was not yet completed for calves captured in 2022, we only reported mean survival ranges for calves captured in 2020 and 2021. During these years, we documented 14 mortalities and 6 unknown fates, which were censored. The top proximate cause of mortality was predation or suspect predation by black bears and coyotes (n = 7), followed by trauma (n = 2), and emaciation or abandonment (n = 2). Mean neonatal survival ranged from 0.822 (SE \pm 0.057) to 0.844 (SE \pm 0.054) and was influenced by total precipitation during the first week of life. Mean summer survival ranged from 0.730 (SE \pm 0.067) to 0.772 (SE \pm 0.064) and was influenced by total precipitation during the first week of life and femur length. Lastly, mean annual survival ranged from 0.556 (SE \pm 0.074) to 0.681 (SE \pm 0.071) and was only influenced by femur length. No maternal characteristics and health metrics appeared to influence survival during any period. Although our mean annual survival range is lower than the survival rates previously reported in Kentucky and other eastern elk populations, it

is likely more representative of Kentucky's fully established and stabilized elk herd 20 years after the completion the state's reintroduction efforts.

KEYWORDS: *Cervus canadensis*, elk, Kentucky, chemical immobilization, calf survival, cause-specific mortality

Kathleen E. Williams
(Name of Student)

07/31/2023
Date

CHEMICAL IMMOBILIZATION OF HELICOPTER-CAPTURED ELK (*CERVUS CANADENSIS*) AND SURVIVAL OF ELK CALVES IN SOUTHEASTERN KENTUCKY

By
Kathleen E. Williams

John J. Cox

Co-Director of Dissertation

Matthew T. Springer

Co-Director of Dissertation

Jian Yang

Director of Graduate Studies

07/31/2023

Date

ACKNOWLEDGMENTS

It takes a village to complete a large, multi-year research project like this and I am thankful for all the wonderful people that helped make it possible. To start, I would like to thank my co-advisors, Dr. John Cox and Dr. Matthew Springer, for their evaluation and feedback on my thesis, guidance on project management, and their patience through all of my ideas for yet another side project or changes to my analysis. Next, I would like to thank my committee member, Dr. Philip Bridges, for his feedback on my thesis and first published paper, as well as for boosting my confidence in performing ultrasounds on female elk during our winter captures. I also want to extend a huge thank you to Nate Hooven, my fellow master's student on this project. From the start, Nate and I had a good rapport, making the transition into to my idea springboard, my partner in crime during our extensive fieldwork, and one of my closest friends, seamless. I greatly admire his dedication, knowledge, and passion for not only wildlife conservation, but the natural world in general, and I know he is going to change the world someday with his big, wrinkly-brain ideas.

This project could not have been completed without substantial support from the Kentucky Department of Fish and Wildlife Resources (KDFWR), which provided the funding and manpower that allowed us to complete this project. First, thank you to Dr. John Hast for his steady and calming support during project planning, fieldwork, and progress updates to the Kentucky Fish and Wildlife Commission. Thanks to Joe McDermott for his enthusiasm for this project and assistance with all the logistics, especially during winter captures. I also wish to express my gratitude to Dan Crank, Tristan Curry, Mark Peterson, Jonathan Fusaro, Kyle Sams, and David Yancy for their help with fieldwork, and to Gabe Jenkins, who offered me this opportunity. I am deeply grateful to Dr. Christine Casey for her guidance on chemical immobilization and blood collection. I would also like to thank her for her support, as my current supervisor and friend, in finishing my data analysis and writing so that I could finally complete my thesis. Lastly, thank you to all the biologists, technicians, and volunteers that helped us capture adult and neonatal elk each year. Specifically, I would like to acknowledge the efforts of the KDFWR technicians (Dustin

Brewster, Paula Clements, Jeran Lane, Abby Riggs, Jenny Wissmann, Zach Hahn, Sam Maywald, Austin Eversole, Connor Lykens, Cullen Whitaker, Aaron Smith, Erin McDaniel, McKenzie Clark, and Andrew Slear) and McKenzie Thornberry for her hard work in performing manual differentials on the mountain of elk blood smears collected during this project.

Additional thanks go to our University of Kentucky (UK) technicians and volunteers (Beth Evers, Kai Davis, Parker Wholstein, Sam McKinley, Maggie Abell, and Brittany Hughes) as well as the staff at UK's Robinson Forest and UK's Robinson Center for Appalachian Resource Sustainability for lodging and access to Robinson Forest. I am also incredibly grateful to Dr. Sean Murphy for his help developing and sorting through my statistical analyses, as well as his patience in answering all my questions about statistics and R. I would also like to acknowledge the efforts of both helicopter crews (Native Range Capture Services and Helicopter Wildlife Services) for their efforts to capture such a large sample of Kentucky elk, often in less-than-ideal conditions. Additional funding for this project came from the U.S. Department of Agriculture McIntire-Stennis Cooperative Forestry Research Program (project #10219360) with supplemental funding from the Rocky Mountain Elk Foundation, UK's Appalachian Center, and the Michael Gatton College of Agriculture, Food and Environment.

Finally, I would like to thank my friends and fellow graduate students Sarah Tomke and Briana Snyder for keeping me sane throughout this project, especially during the race toward the finish line. I am also deeply grateful to my previous supervisors and co-workers, many of whom became good friends during long days in the field and helped shape the experiences that prepared me for this project, and especially Dr. Taylor Ganz for helping me build my confidence in leading a project and feeling ready for graduate school. My final acknowledgment is for my family. I would like to thank my parents and grandparents, who may not have always known quite what I was doing out there in the woods but undoubtedly knew I would achieve whatever I set out to do.

TABLE OF CONTENTS

ACKNOWLEDGMENTS	iii
LIST OF TABLES	vii
LIST OF FIGURES	viii
CHAPTER 1. CHEMICAL IMMOBILIZATION OF HELICOPTER-CAPTURED ELK (<i>CERVUS CANADENSIS</i>) WITH BUTORPHANOL-AZAPERONE-MEDETOMIDINE VERSUS NALBUPHONE-MEDETOMIDINE-AZAPERONE.....	1
1.1 <i>Abstract</i>	1
1.2 <i>Introduction</i>	2
1.3 <i>Methods</i>	5
1.4 <i>Results</i>	10
1.4.1 <i>Onset of Action</i>	11
1.4.2 <i>Physiological Responses</i>	13
1.5 <i>Discussion</i>	18
1.5.1 <i>Onset of Action</i>	19
1.5.2 <i>Physiological Responses</i>	21
1.5.3 <i>Conclusions and Recommendations</i>	27
CHAPTER 2. SURVIVAL AND CAUSE-SPECIFIC MORTALITY OF ELK CALVES (<i>CERVUS CANADENSIS</i>) IN SOUTHEASTERN KENTUCKY	42
2.1 <i>Abstract</i>	42
2.2 <i>Introduction</i>	43
2.3 <i>Methods</i>	47
2.3.1 <i>Capture and monitoring</i>	47
2.3.2 <i>Blood and hair sample analysis</i>	52
2.3.3 <i>Weather data</i>	54
2.3.4 <i>Survival analysis and cause-specific mortality</i>	55
2.4 <i>Results</i>	58
2.5 <i>Discussion</i>	64
APPENDICES	83
APPENDIX 1. SUPPLEMENTAL MATERIALS FOR THE BAM VERSUS NALMED-A CHEMICAL IMMOBILIZATION ANALYSIS.....	84
APPENDIX 2. ELK CALF CAPTURE AND CAUSE-SPECIFIC MORTALITY DATA	146
REFERENCES	150

VITA..... 167

LIST OF TABLES

Table 1.1. Hypotheses, predictor variables, and response categories considered in an exploratory analysis to evaluate which factors influence onset of action and physiological responses in female elk chemically immobilized with BAM or NalMed-A.	30
Table 1.2. Summary of onset of action, processing time, and dose for “typical” single-injection events for helicopter-captured female elk in southeastern Kentucky chemically immobilized with BAM (n = 41) or NalMed-A (n = 78).	31
Table 1.3. Summary of onset of action, processing time, and dose for “atypical” multiple-injection events for helicopter-captured female elk in southeastern Kentucky chemically immobilized with BAM or NalMed-A.	32
Table 2.1. Covariates considered in Cox proportional hazard models to evaluate which factors influence neonatal, summer, and annual elk calf survival in 2020 - 2021.	68
Table 2.2. Summary of morphometrics of elk calves captured across southeastern Kentucky during 2020 - 2022.	70
Table 2.3. Comparison of elk calf morphometrics and health metrics by sex using Welch’s t-test.	71
Table 2.4. Neonatal elk health metrics from biological samples collected during calf captures in 2020 – 2022 in southeastern Kentucky.	72
Table 2.5. Causes of elk calf mortality in southeastern Kentucky in 2020 and 2021.	73
Table 2.6. Neonatal, summer, and annual survival estimates using the Kaplan-Meier estimator for elk calves captured in 2020 – 2021 in Kentucky.	74
Table 2.7. Model selection for stratified Cox proportional hazards models explaining factors influencing neonatal elk calf survival in Kentucky.	75
Table 2.8. Model selection for stratified Cox proportional hazards models explaining factors influencing summer elk calf survival in Kentucky.	76
Table 2.9. Model selection for stratified Cox proportional hazards models explaining factors influencing annual elk calf survival in Kentucky.	77
Table 2.10. Hazard ratios from the top stratified Cox proportional hazards model for the neonatal, summer, and annual survival periods in Kentucky using calf survival data from 2020 – 2021. ...	78
Table 2.11. Estimated cause-specific mortality probabilities for elk calves in Kentucky for the neonatal, summer, and annual survival periods using calf survival data from 2020 – 2021.	79

LIST OF FIGURES

Figure 1.1. Map of Kentucky Elk Restoration Zone in southeast Kentucky, USA. 33

Figure 1.2. Characteristics influencing induction of a single IM injection of BAM and NalMed-A in helicopter-captured female elk in southeastern Kentucky with associated 95% confidence intervals..... 34

Figure 1.3. Characteristics influencing reversal of a single IM-injection of BAM and NalMed-A in female elk in southeastern Kentucky, USA with the antagonists atipamezole and naltrexone, and the associated 95% confidence intervals. 35

Figure 1.4. Observed pre- and post-induction physiological responses for “typical” single IM-injection events in chemically immobilized helicopter-captured female elk. 36

Figure 1.5. Characteristics influencing pre-induction physiological responses of female elk in southeastern Kentucky, USA immobilized with a single IM-injection of BAM and NalMed-A and the associated 95% confidence intervals..... 37

Figure 1.6. Characteristics influencing post-induction heart rate in female elk in southeastern Kentucky, USA immobilized with a single IM-injection of BAM and NalMed-A and the associated 95% confidence intervals. 38

Figure 1.7. Characteristics influencing post-induction respiration in female elk in southeastern Kentucky, USA immobilized with a single IM-injection of BAM and NalMed-A and the associated 95% confidence intervals. 39

Figure 1.8. Characteristics influencing post-induction rectal body temperature in female elk in southeastern Kentucky, USA immobilized with a single IM-injection of BAM and NalMed-A and the associated 95% confidence intervals..... 40

Figure 1.9. Characteristics influencing post-induction blood oxygen saturation (SpO2) in female elk in southeastern Kentucky, USA immobilized with a single IM-injection of BAM and NalMed-A and the associated 95% confidence intervals. 41

Figure 2.1. Study area comprised of 16 counties in southeastern Kentucky and elk calf capture locations by year. 80

Figure 2.2. Ultrasonogram examples of confirmed-pregnant elk in Kentucky..... 81

Figure 2.3. Elk calf parturition season based on calf captures during 2020 – 2021 in southeastern Kentucky..... 82

Figure 2.4. Estimated annual survival for elk calves Kentucky during 2020 – 2021 using the Kaplan-Meier estimator. 83

CHAPTER 1. CHEMICAL IMMOBILIZATION OF HELICOPTER-CAPTURED ELK (*CERVUS CANADENSIS*) WITH BUTORPHANOL-AZAPERONE-MEDETOMIDINE VERSUS NALBUPHONE-MEDETOMIDINE-AZAPERONE

1.1 Abstract

Safe and effective chemical immobilization is critical to minimize stress and risk of injury when capturing free-ranging, wild ungulates. Many traditionally favored high potency opioids have been phased out or become unavailable because of increased regulations, leading to the development of two pre-mixed combination drugs, butorphanol-azaperone-medetomidine (BAM) and nalbuphine-medetomidine-azaperone (NalMed-A). Both drugs have been used to chemically immobilize ungulates, but their efficacy has not been documented in elk captured and transported via helicopter. During 2020 – 2022, we chemically immobilized 119 helicopter-captured female elk (*Cervus canadensis*) with a single IM-injection of BAM (n = 41) or NalMed-A (n = 78) and documented onset of action and physiological responses including heart rate, respiration, body temperature, and blood oxygen saturation. Mean induction times were 8.34 ± 0.03 minutes for BAM and 8.78 ± 0.08 minutes for NalMed-A. We reversed sedation with atipamezole (IM/IV) and naltrexone (IM), with comparable mean reversal times of 4.56 ± 0.09 and 4.14 ± 0.05 minutes for BAM and NalMed-A, respectively. All physiological responses decreased with induction of either drug, whereas post-induction heart rate and respiration were stable. Post-induction body temperature and blood oxygen saturation were more variable, and intervention to minimize hypo- or hyperthermia and respiratory depression should be considered for both drugs. Intrinsic factors (e.g. age, noticeable hemorrhage, initial body temperature) and weather had the most influence on induction, reversal, and physiological responses. However, NalMed-A was affected by less these factors and appears to be a better choice than BAM for immobilizing ungulates captured via helicopter net-gunning.

1.2 Introduction

Capturing wildlife provides a unique opportunity to collect biological information and prepare for longer-term data collection on demography, behavior, and ecology (Brivio et al. 2015). Commonly employed capture methods for large ungulates include helicopter net-gunning and darting, which can be more efficient than ground-based capture methods because of increased success in approaching potentially aggressive animals, improved access to remote or rugged terrain, and selection of a large number of individual target animals (Barrett et al. 1982, Andryk et al. 1983, Kock et al. 1987, Webb et al. 2008). However, helicopter-based methods can be costly and dangerous, even for experienced personnel, and can result in trauma or death of target animals due to injury and/or capture myopathy (Kock et al. 1987, Kreeger and Arnemo 2018). To reduce capture-related mortality, capture and restraint methods should minimize stress and risk of injury while promoting both human and animal safety, especially when capturing large animals (Shury 2007, Ellis et al. 2019). The ideal process should include elements of both physical and chemical restraint (Shury 2007), highlighting the need for experienced capture personnel and safe, consistent immobilization drugs.

The development, use, and regulation of safe and efficacious chemical immobilization drugs for wildlife capture and handling is constantly changing. Historically, wildlife managers used a variety of drugs to chemically immobilize large ungulates ranging from cyclohexane immobilants to high potency opioids, both of which were commonly combined with adjunct sedatives or tranquilizers to smooth induction and increase muscle relaxation (Kreeger et al. 2011, Monteith et al. 2012, Kreeger and Arnemo 2018, Ellis et al. 2019). Both of those drug categories have major drawbacks which led wildlife managers, researchers, and veterinarians to phase out their use. For instance, cyclohexanes, such as combinations of tiletamine-zolazepam and ketamine are not reversible and can cause convulsions that result in animal injury. Potent opioids are better because they induce immobilization from smaller doses and are reversible but pose a greater risk to human and animal safety through accidental exposure, overdose, and resedation (Kreeger and

Arnemo 2018). Additionally, many cyclohexanes and opioids are strictly regulated by the U.S. Drug Enforcement Administration (DEA) as controlled substances (schedule III and schedule II, respectively) due to their potential for abuse (Drug Enforcement Administration [DEA] 2020). As such, many of those drugs require careful documentation of use, special storage, and DEA registration in addition to a veterinarian prescription, which can be costly and prohibitive for field staff involved in the capture of large numbers of target animals (Kreeger and Arnemo 2018, Gettelman et al. 2022). Furthermore, in light of the opioid crisis in the United States (van Amsterdam et al. 2021), many derivatives of fentanyl have increased restrictions (e.g. thiafentanil) or are unavailable (e.g. carfentanil; Hansen and Beckmen 2018, Kreeger and Arnemo 2018, Levine et al. 2022). Thus, an increasing need exists for effective chemical immobilization alternatives that are immediately reversible and safer for both humans and target animals with less prohibitive restrictions. This need has fostered the development of compound or combination drugs, in which each drug works synergistically to produce effective immobilization and sedation (Wolfe et al. 2014a, b, 2017, Kreeger and Arnemo 2018). Compound drugs often have reduced dosages of each drug in the combination, thereby reducing the total dose and reducing the occurrence of adverse side effects that are often observed when each drug is administered individually (Kreeger and Arnemo 2018).

Two promising fixed-dose combination drugs for chemical immobilization of wildlife include butorphanol – azaperone – medetomidine (BAM; ZooPharm, Inc., Laramie, WY, USA) and nalbuphine – medetomidine – azaperone (NalMed-A; ZooPharm, Inc., Laramie, WY, USA). Both pre-mixed drug combinations contain a synthetic opioid agonist-antagonist that functions as an immobilant and analgesic, along with similar concentrations of medetomidine and azaperone (Wolfe et al. 2014a, b). Medetomidine is an alpha-2 adrenoceptor agonist that is a completely reversible potent sedative known to cause respiratory depression, bradycardia, and disrupt thermoregulation. Azaperone is a short-acting butyrophenone agonist and tranquilizer that smooths

induction and can increase respiration, but generally has minimal effects on heart rate or thermoregulation. Both drugs work synergistically with the opioid, which is the main difference between these drug combinations (Kreeger and Arnemo 2018). Butorphanol tartrate, the low-potency opioid in BAM, is a controlled substance (schedule IV) in the United States and Canada (Wolfe et al. 2014a, Kreeger and Arnemo 2018). Conversely, nalbuphine HCl, the opioid in NalMed-A, has a lower potential for human abuse and thus is not a controlled substance (unscheduled) even though it is ten-times more potent (Wolfe et al. 2014b, Kreeger and Arnemo 2018). This is mainly due to its agonist-antagonist “ceiling” effect on respiratory depression (Drug Enforcement Administration [DEA] 2019), meaning NalMed-A relies more upon the alpha-2 agonist for induction (Wolfe et al. 2014b). Both opioids and combination drugs are known to cause respiratory depression but are easily reversed with naltrexone (opioid antagonist) and atipamezole (alpha-2 antagonist). The effects of BAM and NalMed-A have been studied in wild ungulates (Siegal-Willott et al. 2009, Harms et al. 2018, Ellis et al. 2019, McDermott et al. 2020, Levine et al. 2022, Thomas et al. 2022), but they have not thus far been documented and compared in helicopter-based captures of elk.

In this study, we investigated and compared the effects of two commonly used combination immobilization drugs (BAM and NalMed-A) on female individuals of a commonly captured large ungulate in North America, the elk (*Cervus canadensis*), that were captured via helicopter net-gunning. Our objectives were to: 1) report observed onset of action and physiological responses, 2) determine what characteristics may influence onset of action and physiological responses, and 3) compare how these relationships differ in elk immobilized with either BAM or NalMed-A. We hypothesized that onset of action (induction and reversal times) would be similar between drug combinations because both drugs contain comparable concentrations of azaperone and medetomidine and are reversed with the same antagonists (Wolfe et al. 2014a, b). However, we expected induction time for NalMed-A to be slightly shorter than

BAM, since nalbuphine is a more potent opiate than butorphanol (Kreeger and Arnemo 2018). Additionally, we hypothesized that physiological responses (i.e. heart rate, respiration, body temperature, and blood oxygen saturation) would be similar between drug combinations. For both composites, we expected to see post-induction respiratory depression, resulting in hypoxemia (Read 2003) as evidenced by decreased blood oxygen saturation (SpO₂). We also expected heart rate, respiration, and body temperature to decrease with induction and then stabilize post-induction. Finally, we hypothesized that weather conditions would influence both pre-induction physiological responses and post-induction body temperature. Weather, especially in combination with physical exertion, may affect an animal's physiological responses (Harris et al. 1960, Cattet et al. 2003, Costa et al. 2017, Thompson et al. 2020), thus we expected to see higher physiological responses on capture days with higher ambient temperatures and more solar radiation. Overall, we posited that there would be no substantial differences in onset of action or physiological responses between BAM and NalMed-A since they are similar combination immobilization drugs.

1.3 Methods

We conducted this study across the 16-county Kentucky Elk Restoration Zone (KERZ) in southeastern Kentucky, USA (Figure 1.1), which has a mean temperature range from -1.2 – 8.3°C with mean of 31.7 cm of precipitation and 46.2 cm of snowfall (Jackson, KY, USA; National Oceanic and Atmospheric Administration [NOAA] 2022) during the winter months. We contracted a helicopter crew (Native Range Capture Services, Elko, NV, USA in 2020 and Helicopter Wildlife Services, Austin, TX, USA in 2021-2022) to capture elk via net-gun in late January of each year. Once captured, elk were blindfolded, hobbled, and removed from the net for transport back to a centralized workup location. We then weighed each elk before they were placed on a modified flatbed trailer by the helicopter for processing. Once sex, weight, and age category were known, we initiated a decision tree to determine if 1) the animal should be chemically immobilized or processed without drug and 2) what chemical immobilization drug

should be used. We processed juveniles, males of any age, and individuals experiencing extreme hyperthermia (usually > 41.0°C) without drug (physical restraint), but chemically immobilized most adult and yearling females to check pregnancy status. Immobilized female elk received either 1.2 ml etorphine HCl (Wildlife Pharmaceuticals, Inc., Windsor, CO, USA), 2 ml butorphanol tartrate (27.3 mg/ml) – azaperone (9.1 mg/ml) – medetomidine (10.9 mg/ml) (BAM, ZooPharm, Inc., Laramie, WY, USA) or 2 ml nalbuphine HCl (40.0 mg/ml) – medetomidine (10.0 mg/ml) – azaperone (10.0 mg/ml) (NalMed-A; ZooPharm, Inc., Laramie, WY, USA). During the induction period, all elk were monitored closely to determine when they reached an appropriate plane of sedation, based on their response to light stimulus including blinking, ear movements, swallowing, and/or spontaneous leg movements (Kreeger and Arnemo 2018). All doses were administered intramuscularly (IM), and several animals required additional drug to either reach or maintain an appropriate plane of sedation.

Once immobilized female elk reached this appropriate plane of sedation, we considered them fully induced, applied eye lubricant (Optixcare; Adventix, Burlington, ON, Canada), and removed their hobbles. Each animal was repositioned from lateral to sternal recumbency with continual support for their head to maintain the airway and prevent regurgitation (Caulkett and Arnemo 2007). We then shaved hair from the neck and collected ≤ 30 ml of blood via jugular venipuncture (University of Minnesota 2022). We checked pregnancy status in the field using real-time transrectal ultrasonography (Ibex Pro; E.I. Medical Imaging, Loveland, CO, USA), which was later confirmed via assays for serum pregnancy-specific protein B (PSPB; BioPRYN; Herd Health Diagnostics, Pullman, WA, USA) (Stephenson et al. 1995). Additionally, we assessed body condition (Gerhart et al. 1996) and either estimated age based on tooth replacement (Jenson 1999) or administered a local anesthetic (Lidocaine 2%; VetOne®, Boise, Idaho, USA) and extracted a lower canine tooth for lab-based aging by counting cementum layers (Hamlin et al. 2000). Field-confirmed pregnant female elk received a Vertex Plus GPS telemetry collar and paired vaginal

implant transmitter (VIT; Vectronic Aerospace, Berlin, Germany) following Hooven et al. (2022), while open or unchecked females received a LifeCycle Pro or GlobalstarTrack Pro GPS telemetry collar (Lotek Wireless, Newmarket, Ontario, Canada). All elk also received a health assessment to document and treat injuries, including the administration of ≤ 20 ml penicillin (Norocillin®; Norbrook, Lenexa, KS, USA) or 5 ml flunixin meglumine (Banamine; Merck, Rahway, NJ, USA), as needed in response to injury or hyperthermia, respectively. Once processing was complete, elk were either moved to a stock trailer for relocation within the KERZ or an on-site release location, where we reversed chemical immobilization with atipamezole (25 mg/ml, half given IM and half given intravenous or IV) (ZooPharm, Inc., Laramie, WY, USA) and naltrexone (50 mg/ml, IM) (ZooPharm, Inc., Laramie, WY, USA).

Monitoring of physiological responses (heart rate, respiration rate, body temperature, blood oxygen saturation, capillary refill time, and color of mucous membranes) began as soon as possible and occurred approximately every 5 minutes until the reversal of chemical immobilization. Body temperature was monitored using digital thermometers and continuous temperature monitors (DataTherm II; Geratherm Medical AG, Geschwenda, Geratal, Germany), and blood oxygen saturation (SpO_2) was monitored using pulse oximeters attached to the tongue (PM10N Nellcor Portable SpO_2 Patient Monitoring System; Covidien, Dublin, Ireland). Blood oxygen saturation $\leq 95\%$ was considered low (Fahlman 2014) and we administered supplemental oxygen via nasal insufflation when blood oxygen saturation decreased below 90%. Circulation was monitored via capillary refill time and the color of mucous membranes (Lian et al. 2014), which we monitored in the gums. Each monitoring time was recorded, as well as times for agonist/antagonist injection and induction. Following capture, we remotely monitored collared elk for 4 weeks for mortality associated with capture myopathy (Van de Kerk et al. 2020) using software (GPS Plus X; Vectronic Aerospace, Berlin, Germany) and online platforms (INVENTA; Vectronic Aerospace, Berlin, Germany or Lotek Web Service; Lotek Wireless, Newmarket,

Ontario, Canada), with all mortalities investigated as soon as possible. Capture and immobilization followed the American Society of Mammalogists (Sikes et al. 2016) guidelines and protocols were approved by the University of Kentucky Institutional Animal Care and Use Committee (IACUC #2019-3382).

We obtained variables of interest for the capture, therapeutics, and animal hypotheses (Table 1.1) from the data collected during captures. All data was collected in the same units between years except for body mass (pounds vs kilograms) and body temperature (rectal vs vaginal). To ensure continuity of data, we converted all body mass to kilograms and any vaginal body temperatures to rectal temperatures, which are typically higher than vaginal temperatures (Lees et al. 2018) by adding 2°F to account for based on observed differences (personal communication, C. Casey). Additionally, we calculated several times (in minutes), including induction time (agonist administered to full sedation), workup time (full sedation to reversal administered), reversal time (antagonist administered to walking away), and monitor time (monitor event to/from sedation) using event times recorded during capture for use in exploratory analysis and summary statistics. We calculated transport distance (transp_dist) using the spTransform function in the R package ‘sp’ (version 1.4-5; Pebesma and Bivand 2005) to compute Euclidean distance between each workup location (Figure 1.1) and capture location. Variables in the weather hypothesis, including mean daily ambient temperature (avg_temp), mean wind speed (wind) and daily solar radiation (solar; Table 1.1), were obtained from Kentucky Mesonet weather stations (Western Kentucky University Kentucky Climate Center 2022). Since none of the weather stations were located at our workup locations, we extracted weather data from the closest weather station for each immobilization event. We determined this using the spTransform function (Pebesma and Bivand 2005) to calculate the Euclidean distance between the workup location for each immobilization event and each weather station, assigning the weather station with the shortest distance. We then converted all ambient and rectal body temperatures from Fahrenheit to Celsius

using the R package ‘weathermetrics’ (version 1.2.2; Anderson et al. 2016). All data processing and analysis occurred in program R 4.0.3 (R Core Team 2020) within RStudio (RStudio Team 2021).

We removed all female elk immobilized with etorphine HCl or processed with only physical restraint to solely compare the effects of BAM and NalMed-A. Several of the remaining female elk immobilized with BAM or NalMed-A required additional drug to achieve or maintain sedation; however our goal was to understand “typical” single-injection chemical immobilization events. For this reason, we removed female elk that were euthanized prior to release and that were reversed with atypical routes of administration (e.g. all IM, instead of IV/IM) from all further analysis to achieve our final samples size reported in the results below. We also removed all “atypical” multiple-injection events in which additional immobilization drug was administered for separate reporting and analysis. Only one female was recaptured, but we retained both immobilization events because they were not in the same or consecutive capture seasons. We then compared induction times, reversal times, and observed physiological responses between immobilization drug before investigating what variables may affect these responses and if those relationships varied by drug.

Prior to modeling, we confirmed which distributions best characterized each response and attempted to improve normality of response residuals if possible, using log-transformation (Zuur et al. 2009). We checked all possible variable combinations for multicollinearity using Pearson’s correlation coefficient (continuous variables), the Kruskal-Wallis H test (continuous and categorical variables), and Cramér’s V (categorical variables). Due to issues with multicollinearity (Grueber et al. 2011), the breadth of our hypotheses, and the necessary incorporation of a relationship with time (monitor_min) for all physiological responses, we deemed an exploratory approach better than generating predictive models selected via an information theoretic approach. To accomplish this, we centered and scaled all continuous variables using the ‘scale’ function,

then fit individual models containing an interaction with immobilization drug for each applicable characteristic in each hypothesis, which resulted in nine response variable categories: 1) induction time, 2) reversal time, 3) pre-induction heart rate, 4) pre-induction respiration rate, 5) pre-induction body temperature, 6) post-induction respiration rate, 7) post-induction respiration rate, 8) post-induction body temperature, and 9) post-induction blood oxygen saturation (hereafter response category 1-9). We had too few observations of blood oxygen saturation prior to full sedation, and thus did not include that as a response category.

For response categories 1 and 2 (onset of action), we used linear regression to model the effects of characteristics in each hypothesis. For response categories 3-9 (physiological responses), we used mixed effects models to account for repeated measures from individual female elk. But first we investigated each physiological response's relationship with time by fitting both a linear mixed effects model and non-linear mixed effects model (with basis spline with quantile knots) using the 'glmmTMB' package (Brooks et al. 2022). We used Akaike's information criterion corrected for small sample sizes in the 'MuMIn' package (Bartoń 2023) to determine which model captured the most variation, then carried that model type forward for each response category to investigate the effects of characteristics in each hypothesis.

1.4 Results

During 2020 – 2022, we captured 177 female elk ($n_{\text{adult}} = 150$, $n_{\text{yearling}} = 22$, $n_{\text{calf}} = 5$) across the KERZ (Figure 1.1). Of these, four female elk were euthanized during or immediately after processing due to untreatable capture-related injuries (1 physical restraint, 1 BAM, 2 NalMed-A) and we removed them from consideration in the final data set. Two female elk immobilized with NalMed-A were found dead within the 4-week capture myopathy window, however their cause of death (exsanguination and trauma from falling off a cliff) did not appear related to chemical immobilization, so we kept them in our analysis. We also removed 28 individuals that were processed under physical restraint only, one individual that was never fully induced, 11 events

with incomplete records for induction or reversal, and three elk immobilized with Etorphine so as to only compare the effects of BAM and NalMed-A. These events were further classified as either “typical” single-injection events (41 BAM, 78 NalMed-A), when the combination drug was administered only once and “atypical” multiple-injection events. Atypical events were broken down into a booster (2 BAM, 5 NalMed-A), when additional drug was administered to achieve an appropriate plane of induction, and a top-off (4 NalMed-A), when additional drug was administered to maintain sedation during processing.

1.4.1 *Onset of Action*

For individuals immobilized with a single injection of BAM (n = 41) the mean dose received was 2.07 ml, mean induction time was 8.34 ± 0.03 minutes, and mean reversal time was 4.56 ± 0.09 minutes (Table 1.2). Induction time was more variable in yearlings and animals with noticeable hemorrhage (e.g. blood in nostrils or mouth from lacerations or unknown cause) and appeared to be influenced by select characteristics in the weather and animal hypotheses. The strongest influence was ambient temperature when induction time decreased sharply as average daily temperature increased. BAM induction times were also moderately influenced by body mass, wind speed, and hemorrhage. As such, we found that induction time decreased as body mass or average daily wind speeds increased but actually increased when hemorrhage was observed (Figure 1.2). The therapeutic hypothesis was not considered in our analysis of induction time because these drugs were typically not administered until after induction and thus were not relevant to this response category. Reversal times in elk immobilized with BAM were more variable in yearlings, animals with noticeable hemorrhage, when female elk received therapeutic drugs or when supplemental oxygen was administered and also appeared to be influenced by select characteristics in all hypotheses. The strongest influences were body mass, when reversal time decreased as body mass increased, and hemorrhage, where mean reversal time in elk with noticeable hemorrhage was longer. Lidocaine also appeared to have a strong relationship, when

mean reversal time was longer in animals that received the drug. Moderate influences included age, work-up duration, penicillin, supplemental oxygen administration, and wind speed when reversal times were shorter in yearlings, increased with longer workups and when penicillin or supplemental oxygen was administered, but decreased as average daily wind speeds increased (Figure 1.3).

For individuals immobilized with a single injection of NalMed-A (n = 78) the mean dose received was 2.0 ml, mean induction time was 8.78 ± 0.08 minutes, and mean reversal time was 4.14 ± 0.05 minutes (Table 1.2). Similar to BAM, induction times for NalMed-A were more variable in yearlings or elk with noticeable hemorrhage and were influenced by select characteristics in the animal and weather hypotheses. For instance, induction time was strongly influenced only by age with shorter induction times in yearlings than adults. NalMed-A induction times were also moderately influenced by hemorrhage, whereby induction time increased in animals with noticeable hemorrhage, and wind speed, when induction time decreased as average daily wind speed increased (Figure 1.2). Reversal times in elk immobilized with NalMed-A were generally more variable in female elk that did not receive supplemental oxygen and that had noticeable hemorrhage. Like the reversal of BAM, this response category appeared to also be influenced by select characteristics in all hypotheses. The only strong influence was body mass, in which reversal time decreased as body mass increased. Moderate influences included workup duration, the administration of supplemental oxygen and banamine, observed hemorrhage, and ambient temperature. Consequently, NalMed-A reversal times were longer when noticeable hemorrhage was observed, supplemental oxygen was administered or when workup duration and daily ambient temperatures increased, but shorter in female elk that received banamine (Figure 1.3).

There were notable differences in onset of action for female elk that required additional chemical immobilization drug to either achieve induction (booster, n = 9) or maintain sedation

(top-off, n = 2). Female elk that received a booster had longer processing times with means of 25.80 ± 6.34 minutes for NalMed-A and 25.50 ± 3.50 minutes for BAM. NalMed-A booster doses ranged from 0.2 – 0.4 ml with a mean dose 2.28 ± 0.04 ml to achieve successful immobilization. Induction and reversal times for these individuals were 16.20 ± 1.36 minutes and 4.20 ± 0.64 minutes, respectively. Female elk immobilized with BAM that required a booster received an additional 0.5 ml dose and had a mean induction time of 22.5 ± 0.50 minutes with a mean reversal time of 4.00 ± 0.00 minutes (Table 1.3). The four individuals that required a top-off were immobilized with NalMed-A and had the longest processing times, with a mean of 51.75 ± 11.44 minutes. In each case, these prolonged processing times were due to treatment of capture-related injuries including cleaning, sutures, and/or surgical glue. Despite a prolonged handling period and occurrence of injuries, the mean induction and reversal times were similar to NalMed-A individuals that did not have a top-off, at 9.75 ± 2.43 minutes and 4.75 ± 2.18 minutes respectively (Table 1.3). Mean body mass of elk that received either a booster, top-off or only a single injection did not appear to differ between groups or drug, and due to the small sample size, we did not investigate if any other factors influenced the variability in onset of action.

1.4.2 *Physiological Responses*

Physiological responses, including heart rate, respiration rate, rectal body temperature, and blood oxygen saturation, were recorded both prior to- and after induction. All measurements were recorded approximately every 5 minutes, starting as early as 27 minutes prior to induction until as long as 47 minutes after induction, but we curtailed the observations used for analysis to a pre-induction period of -15 – 0 minutes and a post-induction period of 0 – 30 minutes. Pre-induction physiological responses had linear relationships with time and were influenced by select characteristics within the capture, animal, and weather hypotheses. We did not investigate the influence of the therapeutics hypothesis on this response category because these drugs were typically administered post-induction, nor did we separate physiological responses by chemical

immobilization drug administered. Pre-induction physiological responses were generally more variable in yearlings, heavier animals, and female elk that were transported longer distances by helicopter, as well as when hemorrhage was observed, or initial body temperatures were lower. Additionally, these ranges were more variable on days with higher ambient temperature, wind speed, and solar radiation (Figure 1.5). Heart rate decreased slightly leading up to induction (Figure 1.4) and was only moderately influenced by observed hemorrhage, wind speed, and solar radiation whereby heart rate was lower when hemorrhage was observed and on days with lower average daily wind speeds, but higher on days with more solar radiation (Figure 1.5). Respiration decreased prior to induction and appeared to be strongly influenced by wind speed, in which respiration started notably higher on days with higher average daily wind speeds and decreased rapidly with induction. This vital rate was also moderately influenced by initial body temperature so that female elk with higher initial body temperatures had higher respiration rates (Figure 1.5). Body temperature generally remained steady or increased slightly with induction (Figure 1.4) and was correlated with initial body temperature. This led to a strong influence whereby an animal's body temperature remained high following higher initial temperatures or increased with induction following lower initial temperatures. Furthermore, body temperature was moderately influenced by helicopter transport distance, body mass, and hemorrhage. These influences showed that body temperature was lower in animals transported longer distances and in heavier animals but higher in lighter animals as well as lower, but increasing, in elk with noticeable hemorrhage. This response was also influenced by ambient temperature, wind speed, and solar radiation, where body temperature was higher on days with higher average daily wind speeds and ambient temperatures, and lower on days with higher daily solar radiation (Figure 1.5).

Post-induction physiological responses of female elk chemically immobilized with BAM were influenced by select characteristics in all hypotheses. These response ranges were generally more variable in animals transported longer distances by helicopter, female elk that received

penicillin or had noticeable hemorrhage, yearlings, and heavier animals, as well as on days with higher average daily ambient temperatures and wind speeds. Heart rate had a linear relationship with time, and appeared to be strongly influenced by wind speed, increasing over time when average daily wind speeds were higher. This response was moderately influenced by the administration of penicillin or lidocaine, when heart rate increased over time in female elk given either therapeutic drug, as well as noticeable hemorrhage, in which heart rate increased over time when we observed hemorrhage. Additionally, heart rate was moderately influenced by initial body temperature and solar radiation, increasing over time in animals with lower initial body temperatures and on days with lower daily solar radiation (Figure 1.6). Respiration also had a linear relationship with time and appeared to be moderately influenced by the administration of supplemental oxygen or banamine, age, and observed hemorrhage. Respiration rate started lower and increased slightly in animals that received supplemental oxygen but remained lower if animals did not receive supplemental oxygen. Respiration also increased when elk were not given banamine or had noticeable hemorrhage and was different between age classes (decreased in yearlings but increased in adults). Furthermore, this response was moderately influenced by ambient temperature, where respiration decreased over time in higher average daily ambient temperatures but started lower and slightly increased in lower ambient temperatures, and wind speed, where respiration decreased over time with higher wind speeds (Figure 1.7).

Post-induction body temperature in female elk immobilized with BAM had a non-linear relationship with time and was strongly influenced by the administration of supplemental oxygen administration or banamine, initial body temperature, and wind speed. In these instances, body temperature became more erratic over time without supplemental oxygen. Body temperature also started higher and remained higher in elk that received banamine or had higher initial body temperatures. Overall, body temperature was less stable in animals with lower initial body temperatures and increased dramatically halfway through processing on days with higher average

daily wind speeds. Furthermore, this response was moderately influenced by penicillin administration and observed hemorrhage whereby body temperature decreased initially in elk that received penicillin then stabilized before decreasing again prior to reversal. When hemorrhage was observed, body temperature initially spiked then stabilized before increasing sharply prior to reversal. Solar radiation also moderately influenced body temperature in female elk immobilized with BAM, which increased slightly around 5 minutes post-induction on days with less solar radiation but decreased around this time on days with higher solar radiation, before stabilizing and continuing to increase or decrease, respectively, after 20 minutes of sedation (Figure 1.8). Blood oxygen saturation (SpO_2) also had a non-linear relationship with time and almost always decreased initially in the first 5-10 minutes of sedation. This response was strongly influenced by supplemental oxygen administration, body mass, and ambient temperature. Female elk that received supplemental oxygen generally started with lower blood oxygenation, which increased sharply after the start of nasal insufflation, and remained higher until reversal while elk with no supplemental oxygen started just below 90% SpO_2 but became more erratic over time. Blood oxygen saturation in elk with higher body masses exhibited a wave pattern, starting high then decreasing dramatically in the first 10 minutes of sedation, while female elk with lower body mass generally started around 65% SpO_2 , which sharply increase before stabilizing around 90% SpO_2 . Ambient temperature appeared to have a similar effect, causing blood oxygen saturation to oscillate in female elk on days with higher average daily ambient temperatures, undulating between low (~60%) and moderate blood oxygen levels (~80%), but was more stable (~75% and higher) on days with lower ambient temperatures (Figure 9). Blood oxygen saturation was also moderately influenced by age, wind speed, and solar radiation. For instance, blood oxygen saturation in yearlings started low but dramatically increased before stabilizing around 90% SpO_2 and started higher, but was less stable, on days with higher average daily wind speeds. Additionally, on days with lower wind speeds or higher daily solar radiation, blood oxygen

saturation increased over time then decreased decreasing dramatically prior to reversal, but only increased over time on days with lower daily solar radiation (Figure 1.9).

Post-induction physiological responses of female elk chemically immobilized with NalMed-A were also influenced by select characteristics within all hypotheses. These response ranges were generally more variable in yearlings, animals with lower initial body temperatures, and when hemorrhage was observed, as well as on days with higher ambient temperatures and higher wind speeds. Heart rate had a linear relationship with time and appeared only to be moderately influenced by body mass, where heart rate decreased over time in heavier elk but remained steady in smaller elk, and solar radiation, where heart rate was generally steady but higher on days with more solar radiation (Figure 1.6). Respiration also had a linear relationship with time and appeared to be strongly influenced by solar radiation, in which respiration increased over time on days with more solar radiation but decreased on days with less. Additionally, respiration was moderately influenced by the administration of supplemental oxygen, initial body temperature, and wind speed. For instance, this vital rate remained steady in elk that received supplemental oxygen but decreased slightly over time in animals that did not receive oxygen. Post-induction respiration also increased in female elk with lower initial body temperatures but decreased slightly over time on days with higher average daily wind speeds (Figure 1.7).

Post-induction body temperature had a non-linear relationship with time and appeared to be strongly influenced by age, initial body temperature, and ambient temperature. For instance, body temperature was generally more variable over time in yearlings and remained higher in animals with high initial body temperatures, likely because these variables are correlated. Body temperature also generally remained higher throughout sedation, except on days with higher average daily ambient temperatures when body temperatures decreased rapidly prior to reversal. At lower initial body temperatures and lower ambient temperatures, body temperature was stable and generally started lower before increasing sharply prior to reversal (Figure 1.8). This vital rate

was also moderately influenced by banamine administration, wind speed, and solar radiation. Body temperature was generally higher throughout sedation in female elk given banamine, higher and more variable over time on days with higher average daily wind speeds, and lower on days with higher daily solar radiation, until just before reversal when body temperature began to increase sharply (Figure 8). Blood oxygen saturation also had a non-linear relationship with time and was strongly influenced by age, body mass, and wind speed. This response was more variable in yearlings and appeared to exhibit a quadratic relationship on days with higher average daily wind speeds, with lower levels following induction and prior to reversal and a peak around 90% SpO₂ in the middle. Blood oxygen saturation also appeared to have a weak relationship with lidocaine administration and body mass, where blood oxygen saturation decreased in the first 5 minutes of sedation before stabilizing in elk that did not receive lidocaine but not in elk that did not receive lidocaine. Finally, blood oxygen saturation in heavier animals spiked during the first 5 minutes of sedation, while lighter animals experienced a slight decrease before both stabilizing around 80-90% SpO₂ until reversal (Figure 1.9). Overall, post-induction physiological responses in female elk immobilized with NalMed-A appeared to be more stable and less influenced by as many intrinsic and extrinsic factors.

1.5 Discussion

Both butorphanol-azaperone-medetomidine (BAM) and nalbuphine-medetomidine-azaperone (NalMed-A) appear to be effective for chemical immobilization in helicopter-captured female elk. Indeed, of the instances when BAM or NalMed-A was administered, ~92% of individuals with complete records were effectively immobilized with a single injection and only one adult female never reached an appropriate plane of sedation. Although we did not score the level of sedation observed in each animal, we considered restrained elk effectively immobilized when they had no response (e.g. twitching or spontaneous movements) to light touch. As expected, both immobilization drugs caused sedation and muscle relaxation, however several elk failed to

achieve this plane of sedation 10-15 minutes after injection and required additional drug (booster) to be effectively immobilized (2 BAM, 5 NalMed-A). Elk that received NalMed-A generally retained more motor function in their legs and eyes, making them appear twitchy even when fully immobilized, which could account for the increased number of boosters for this drug. Meanwhile, additional drug to maintain sedation (topper) was only administered in elk immobilized with NalMed-A (n = 4), but this was more related to the length of sedation, which was on average 29.7 minutes longer than in single-injection events (Tables 1.2 and 1.3) to treat capture-related injuries that required more intensive care. These combination drugs, while safer for humans than high potency opioids (Kreeger and Arnemo 2018), also appeared to be safer for helicopter-captured female elk. Although 3 chemically immobilized elk were euthanized during processing or shortly after reversal and 2 elk died within the post-handling capture myopathy window, no mortalities appeared related to chemical immobilization, but rather to capture-related injuries or just random (e.g. trauma from falling).

1.5.1 *Onset of Action*

Our hypothesis that onset of action (induction and reversal times) would be similar between immobilization drugs was supported, as both pre-mixed combination drugs had similar means and ranges (Table 1.2). Mean induction times for BAM (8.34 ± 0.03 minutes) and NalMed-A (8.78 ± 0.08 minutes) were higher than previously reported for both drugs in captive elk (Wolfe et al. 2014a, b), but more similar to those reported in studies of captive bison (Wolfe et al. 2017) and free-ranging white-tailed deer and moose (McDermott et al. 2020, Levine et al. 2022). This deviation is likely influenced by differences in excitement and stress levels between captive and free-ranging wildlife (Kreeger and Arnemo 2018), and capture method. For instance, helicopter-based methods, which are commonly used to chase and capture ungulates in remote locations, can be highly stimulating and impact an animal's physiological responses (Cattet et al. 2003). This is likely more pronounced in net-gunning than darting because of the additional stimulation of being

awake during initial restraint and transport. Mean reversal times for BAM (4.56 ± 0.09 minutes) and NalMed-A (4.14 ± 0.05) were similar to times reported for captive bison and aoudad (Wolfe et al. 2017, Thomas et al. 2022) but were much lower than previously reported in captive elk (Wolfe et al. 2014*a, b*) and even in free-ranging cervids (McDermott et al. 2020, Levine et al. 2022). This variation is presumably due to differences in type of antagonists used, doses administered, and/or drug delivery method between studies and highlights the advantage in administering atipamezole half IM and half IV for quicker reversal times. BAM and NalMed-A also had higher induction times but comparable reversal times when compared to the high potency opioids that were traditionally used for darting free-ranging deer, elk, and moose (Meuleman et al. 1984, Wolfe et al. 2004, Hast 2019) suggesting that these combination drugs may be preferred for immobilizing ungulates that are confined or already restrained.

Induction time for either drug was influenced by characteristics in the animal and weather hypotheses and appeared to be moderately influenced by body mass, noticeable hemorrhage, and average daily wind speeds. Helicopter net-gunned elk can be expected to have longer induction times when hemorrhage is observed but shorter induction times on windier days. Body mass effects varied by drug and induction in heavier animals can be expected to take less time when using BAM but more time in when using NalMed-A (Figure 1.2). This aligns with the effect age appears to have on NalMed-A induction, which was longer on average in adults than yearlings. BAM induction was not influenced by age but was strongly influenced by ambient temperature and can be expected to decrease sharply as ambient temperatures increase. Overall, induction time did not appear to be influenced by helicopter transport distance, initial body temperature, or solar radiation.

Reversal times for both drugs were influenced by a wider variety of characteristics spanning all hypotheses, including a strong relationship with body mass and moderate relationships with work-up duration, supplemental oxygen administration, and observed

hemorrhage. As the antagonists and dosages were generally the same to reverse both BAM and NalMed-A, it appears that these influences would apply broadly to helicopter-captured elk immobilized with similar combination drugs. Reversal times for female elk captured in this manner can be expected to be much shorter in heavier animals but increase the longer the individual is sedated, when hemorrhage is observed, or when supplemental oxygen is administered. Additional characteristics only affected the reversal times of one drug but not the other (Figure 1.3). For instance, reversal times for elk immobilized with BAM can be expected to decrease when those individuals also receive a localized injection of the analgesic lidocaine but increase on windier days. These characteristics did not seem to affect elk immobilized with NalMed-A, who instead were impacted more by age, the administration of banamine, and average daily ambient temperatures. On average, elk immobilized with NalMed-A that received banamine or were younger can be expected to have shorter reversal times, but longer reversals on warmer days. We hypothesize that the administration of therapeutic drugs such as penicillin, banamine, or lidocaine do not directly interact with or affect the onset of action of BAM or NalMed-A but could instead represent influences by confounding factors such as increased stress from tooth removal and injury, or elevated body temperature. Overall, reversal times for either immobilization drug did not appear to be influenced by initial body temperature or solar radiation.

1.5.2 *Physiological Responses*

Helicopter-captured female elk immobilized with either BAM or NalMed-A exhibited similar trends across all monitored physiological responses. As expected, these responses decreased during induction then stabilized following induction (Figure 1.4) and generally remained within normal ranges reported for domestic cattle (Jackson and Cockcroft 2002) and cervids (Caulkett and Arnemo 2007). However, we did record vitals outside of these normal ranges for either drug for body temperature or blood oxygen saturation (Figure 1.4). Body temperatures were generally more hyperthermic ($>40.5^{\circ}\text{C}$) early in the work-up and decreased

around 5-10 minutes post-induction to more normal or hypothermic ($<37^{\circ}\text{C}$) ranges. This was likely influenced by the transrectal ultrasound used for checking pregnancy rather than an immobilization drug effect. Post-induction blood oxygen saturation began below acceptable levels ($>85\%$, Caulkett and Arnemo 2014) in female elk immobilized with either drug but began to increase around 3 minutes after induction in BAM individuals and around 5 minutes in NalMed-A individuals due to the administration of supplemental oxygen and repositioning from lateral to sternal recumbency (Caulkett and Arnemo 2007) until it stabilized between 85-90% SpO_2 . Prior to induction, elk immobilized with NalMed-A started with and maintained higher heart rates, respiration, body temperatures, and blood oxygen saturation (Figure 1.5), and consequently started with higher, stronger vitals when an acceptable plane of sedation was achieved. This difference could be due to the larger sample size for NalMed-A or differences in physical exertion, but ultimately demonstrates the effective sedation this newer combination drug can produce, especially when wild ungulates are captured using active methods such as helicopter net-gunning (Wolfe and Miller 2016). Additionally, individuals immobilized with NalMed-A also appeared to have less variable post-induction physiological responses, than individuals immobilized with BAM, which indicates that less intervention may be needed with this drug to prevent capture myopathy or other undesirable effects from sedation.

All physiological responses decreased during induction, with the sharpest decline occurring in respiration, but more mild declines in heart rate and body temperature. On average, physiological responses appeared to be influenced by characteristics in all hypotheses. For instance, female elk that were captured closer to the processing site and thus were transported only a short distance unexpectedly had higher body temperatures than those that were captured further away, with no major differences in heart rate or respiration (Figure 1.5). This indicates that capturing and transporting female elk from further away may not necessarily increase the likelihood of capture myopathy, perhaps because they had more time to overcome the effects

physical exertion or reduce their body temperature via convection during transport below the helicopter. In the animal hypothesis, female elk with higher initial body temperatures maintained higher body temperatures through induction, yearlings had more variable pre-induction physiological responses overall, and larger animals tended to have lower body temperatures. Unexpectedly, animals with observed hemorrhage had lower physiological responses than animals that did not, which could indicate that the initial injury that caused the hemorrhage were likely not severe enough to strongly influence physiological responses. And lastly, as expected, pre-induction physiological responses were influenced by all characteristics in the weather hypothesis (Figure 1.5). Ambient temperature only influenced body temperature and solar radiation only influenced heart rate, but wind appeared to impact all vital rates. As such, helicopter-captured female elk immobilized with either BAM or NalMed-A can be expected to have higher heart rates on sunnier days, dramatically higher respiration on windy days, and higher body temperatures on days that are warmer, windier, or with more cloud cover.

Post-induction physiological responses generally started lower in female elk immobilized with BAM and were more easily influenced by our characteristics of interest. When looking at the capture hypothesis, we did not investigate the effects of helicopter transport distance but rather of supplemental oxygen administration because it had a more direct impact on an immobilized animal following induction. In these individuals, supplement oxygen did not appear to influence heart rate, but caused a slight increase in respiration over time. Without supplemental oxygen, elk immobilized with BAM had highly variable body temperatures, resulting in alternating periods of temporary hypo- or hyperthermia (Figure 1.8) that increased their risk of capture myopathy, and maintained lower blood oxygen saturation for longer periods post-induction, which increased the risk of hypoxia (Caulkett and Arnemo 2007). Supplemental oxygen insufflation stabilized body temperature and blood oxygen saturation, minimizing these risks (Fahlman 2014). Therapeutic drug administration potentially influenced physiological responses in BAM individuals but could

also be indicative of the underlying effects of trauma or stress. For instance, female elk with more severe, but treatable injuries received penicillin and generally had heart rates that increased over time and body temperatures that initially dropped in the first 5 minutes of processing before stabilizing (Figures 1.6 and 1.8). Female elk that received banamine had more stable respiration but appeared to start with and maintain higher body temperatures, thus banamine did not appear to cause any decrease in body temperature despite being administered intravenously to shorten the absorption time (Zhou et al. 2015). Lidocaine appeared to influence blood oxygen saturation (Figure 1.9), which was generally lower in individuals that received a local injection of lidocaine prior to having a tooth extracted than individuals that did not. This drug also appeared to influence heart rate, which increased slightly over time instead of decreasing like in elk that did not receive lidocaine. The reason for this difference is unknown, but it appears that these therapeutic drugs do not have any major impacts on the vital rates of elk immobilized with BAM.

In helicopter-captured elk immobilized with BAM, post-induction physiological responses were highly influenced by characteristics in the animal and weather hypotheses. For instance, in the animal hypothesis, age influenced respiration and blood oxygen saturation, which was also influenced by body mass. When using this drug to immobilize female elk, post-induction respiration can generally be expected to increase adults but not yearlings. Blood oxygen saturation will likely start very low in yearlings then increase and remain in an acceptable range (>85%, Caulkett and Arnemo 2014) until reversal. This trend was also observed in elk with lower body mass, which are likely to be yearlings, while heavier individuals are likely to start higher SpO₂ levels that drop significantly in the initial minutes after induction and may never quite reach healthy, acceptable levels for the duration of processing. Female elk with intermediate body mass can be expected to start at slightly low blood oxygen saturation levels (~80%) that increased back into acceptable levels approximately 5 minutes after induction (Figure 1.9), likely due to supplemental oxygen insufflation. All vital rates were influenced by the presence of noticeable

hemorrhage, thus injured animals given BAM can be expected to have heart rates that increase throughout processing, more variable body temperatures that peak at the beginning and end of processing, and more variable blood oxygen saturation, but steadier respiration. Finally, initial body temperature influenced heart rate, which increased over time in BAM individuals with lower initial body temperatures, and of course body temperature. Body temperature and initial body temperature were correlated, so we expected female elk with lower initial body temperatures to start and generally remain lower or less stable during processing and elk with higher initial body temperatures to maintain higher temperatures (Figure 1.8). This is likely because both drugs contained medetomidine, which is known to impact thermoregulation (Kreeger and Arnemo 2018).

Weather characteristics were highly influential to the post-induction physiological responses of helicopter-captured female elk immobilized with BAM, with wind speed and solar radiation impacting all or almost all vital rates. Thus, on windier days, female elk can be expected to have heart rates that dramatically increase but a slight decrease in respiration, body temperatures that are steady immediately after induction then increase dramatically, causing hyperthermia, and blood oxygen saturation levels that are higher but more variable, oscillating over time during processing. The effects of solar radiation were less distinct and generally the opposite. On sunnier days, heart rate and body temperature are likely to be steady or slightly decrease over time and blood oxygen saturation was lower than acceptable levels throughout processing. However, on cloudier days, heart rate increased, body temperature spiked around 5-minutes post-induction and then stabilized, and blood oxygen saturation generally remained within acceptable levels. Unexpectedly, ambient temperature did not appear to influence post-induction body temperature in female elk immobilized with BAM, but it did influence respiration and blood oxygen saturation (Figures 1.7 and 1.9). Thus, on warmer days, respiration can be expected to decrease over time and blood oxygen saturation is likely to generally be below acceptable levels and more variable, with

greater amplitude between the expected maximum and minimum saturation levels. This indicates that supplemental oxygen would be more important to administer to female elk immobilized with BAM on warmer, sunnier, or windier days.

Post-induction physiological responses were generally more stable in female elk chemically immobilized with NalMed-A and were influenced by a smaller number of characteristics across all hypotheses. The effects of capture were variable, with no effects of supplemental oxygen on heart rate or body temperature, but a stabilizing effect on respiration, and positive impact blood oxygen saturation until it could be maintained within more accepted levels (>85%, Caulkett and Arnemo 2014). The administration of therapeutic drugs appeared to have very little influence, as penicillin or lidocaine did not have any effect. Like individuals immobilized with BAM, female elk that received both NalMed-A and banamine appeared to start with and maintain higher body temperatures and thus, this drug did not appear to cause any decrease in body temperature, despite being administered IV. In the animal hypothesis, yearlings immobilized with NalMed-A had more variable vital rates than adults, heart rate decreased in heavier individuals over time, and respiration increased in female elk with lower initial temperatures. However, animals with higher initial temperatures started higher and generally stayed hyperthermic throughout processing (Figure 1.8), likely due to the loss of thermoregulatory abilities caused by medetomidine (Kreeger and Arnemo 2018). Select weather characteristics influenced all post-induction physiological responses in female elk immobilized with NalMed-A. For instance, heart rate was influenced by solar radiation, respiration was influenced by wind and solar radiation, and body temperature was influenced by all weather characteristics. This shows that helicopter-captured female elk immobilized with NalMed-A can be expected to have slightly higher heart rates that decreases throughout processing on sunnier days and respiration that increases over time on sunnier days but decreases on cloudier or windier days. As expected, body temperature was highly influenced by weather and can be expected to decrease slightly over time

on windier days and remain relatively steady during the first 20 minutes of processing before sharply decreasing on warmer days or sharply increasing on colder or sunnier days. Finally, blood oxygen saturation was strongly influenced by wind and can be expected to start very low on windier days, peak within acceptable levels after 10-20 minutes of processing, then decrease again prior to reversal, indicating that elk immobilized with NalMed-A on windier days should invariably receive supplemental oxygen to prevent hypoxemia.

1.5.3 *Conclusions and Recommendations*

Onset of action and physiological responses can be influenced by any number of biological and environmental factors, many of which we were unable to document or quantify, so we chose to assess the influence of each characteristic individually and were able to identify general trends to compare BAM and NalMed-A. Induction and reversal times were similar between drugs, although more individuals required boosters to achieve an acceptable plane of sedation when immobilized with NalMed-A than BAM. We hypothesize that this may be due to differences in the additive effects of each opioid in combination with medetomidine, which causes muscle relaxation, whereby butorphanol increases this effect but nalbuphine generally does not (Grimm et al. 2015, Kreeger and Arnemo 2018). This likely causes elk immobilized with NalMed-A to potentially retain more muscle movement in their legs and thus other indicators of sedation are more valuable in determining if immobilization is successful with this drug. Induction times for either drug appeared to be influenced more by animal characteristics, such as body mass and hemorrhage, than weather or capture characteristics. However, we did not have helicopter transport distances for all animals and were not able to investigate the effects of chase time, thus these characteristics may have more influence than we realize. Conversely, reversal times for either drug were influenced by capture characteristics like work-up duration and supplemental oxygen insufflation along with animal characteristics like body mass and hemorrhage. This indicates that even though female elk immobilized with either drug were generally induced and

reversed with standard doses, differences in onset of action between age groups (yearlings versus adults) or injury status could cause differences in onset of action, especially when using NalMed-A. We also highly recommend administering atipamezole, one of the antagonist drugs used to reverse these composite immobilization drugs, half IM/half IV to reduce reversal times (Zhou et al. 2015), especially if individuals have physiological responses that increase the risk of capture myopathy such as hyperthermia or severe hypoxia.

All pre-induction physiological responses (categories 3-5) decreased as female elk reached an appropriate plane of sedation, with respiration decreasing sharply during induction of both BAM and NalMed-A. These vital rates were mainly influenced by age and the presence of observable hemorrhage, although not always as expected, as female elk without hemorrhage appeared to have higher heart rates, respiration, and body temperatures. However, all characteristics in the animal and weather hypotheses appeared to have some influence. Post-induction physiological responses were generally stable for female elk immobilized with either drug, except for blood oxygen saturation, which started below acceptable levels indicating that respiratory depression resulting in hypoxemia seems to occur with either drug. This was expected, as one of the components of both drug combinations is medetomidine, which in addition to impacting blood pressure, heart rate, and thermoregulatory capabilities can cause respiratory depression that can be exacerbated by the opioid components butorphanol or nalbuphine (Kreeger and Arnemo 2018). To minimize these effects, in addition to maintaining a clear airway through proper head positioning, we recommend repositioning female elk from lateral to sternal recumbency and administration of supplemental oxygen via nasal insufflation as soon as possible following successful immobilization (Caulkett and Arnemo 2007). This is supported by the influence of the capture hypothesis, in which the supplemental oxygen improved respiration in elk immobilized with either drug also had a strong stabilizing effect on body temperature and blood oxygen saturation in elk immobilized with BAM, but a milder effect in elk immobilized with

NalMed-A. Other characteristics that influenced vital rates in female elk immobilized with either drug include initial body temperature, wind, and solar radiation, indicating that weather characteristics are important to consider when immobilizing helicopter-captured female elk regardless of what drug is used. Lastly, while banamine appeared to influence body temperature, it did not work as expected because elk that started with higher body temperatures were generally maintained throughout processing, thereby suggesting that banamine should not be considered effective for immediate intervention in chemically immobilized elk are hyperthermic. Overall, post-induction vital rates in helicopter-captured female elk chemically immobilized with NalMed-A were less likely to be influenced by both intrinsic and extrinsic factors than individuals immobilized with BAM. This, in combination with NalMed-A's similarities to BAM and less prohibitive restrictions, indicating that NalMed-A may be a better option than BAM for chemically immobilizing female elk captured via helicopter net-gun.

Table 1.1. Hypotheses, predictor variables, and response categories considered in an exploratory analysis to evaluate which factors influence onset of action and physiological responses in female elk chemically immobilized with BAM or NalMed-A.

Hypothesis	Variable	Levels	Response Category
	Workup Duration (Workup)	Continuous (minutes)	2
CAPTURE	Supplemental Oxygen (Supp_O2)	Yes or No	2, 6-9
	Helicopter Transport Distance (Transp_Dist)	Continuous (km)	1, 3-5
THERAPEUTICS	Penicillin Administered (Pen)	Yes or No	2, 6-9
	Banamine Administered (Bana)	Yes or No	2, 6-9
	Lidocaine Administered (Lido)	Yes or No	2, 6-9
ANIMAL	Age Class (Age)	Adult or Yearling	1-9
	Body Mass (Mass)	Continuous (kg)	1-9
	Observed Hemorrhage (Hem_Obs)	Yes or No	1-9
	First Temperature Taken (1Temp)	Continuous (°C)	1-9
WEATHER	Avg Daily Ambient Temperature (Avg_Temp)	Continuous (°C)	1-9
	Avg Daily Wind Speed (Wind)	Continuous (miles/hour)	1-9
	Avg Daily Solar Radiation (Solar)	Continuous (MJ/m2)	1-9

These hypotheses represent the broad categories each intrinsic or extrinsic factor of interest below to and the response categories include: 1) induction time, 2) reversal time, 3) pre-induction heart rate, 4) pre-induction respiration rate, 5) pre-induction body temperature, 6) post-induction respiration rate, 7) post-induction respiration rate, 8) post-induction body temperature, and 9) post-induction blood oxygen saturation.

Table 1.2. Summary of onset of action, processing time, and dose for “typical” single-injection events for helicopter-captured female elk in southeastern Kentucky chemically immobilized with BAM (n = 41) or NalMed-A (n = 78).

Metric	NalMed-A		BAM	
	Mean (\pm SE)	Range	Mean (\pm SE)	Range
Induction (minutes)	8.34 (\pm 0.03)	3.00 - 16.00	8.78 (\pm 0.08)	3.00 - 16.00
Workup (minutes)	22.10 (\pm 0.08)	9.00 - 41.00	22.61 (\pm 0.24)	4.00 - 55.00
Reversal (minutes)	4.14 (\pm 0.05)	1.00 - 19.00	4.56 (\pm 0.09)	1.00 - 13.00
Dose (ml)	2.00 (\pm 0.00)	2.00 - 2.00	2.07 (\pm 0.00)	1.50 - 2.50

Table 1.3. Summary of onset of action, processing time, and dose for “atypical” multiple-injection events for helicopter-captured female elk in southeastern Kentucky chemically immobilized with BAM or NalMed-A.

Event Type	Metric	NalMed-A		BAM	
		Mean (\pm SE)	Range	Mean (\pm SE)	Range
Booster	Induction (minutes)	16.20 (\pm 1.39)	13.00 – 23.00	22.50 (\pm 0.50)	22.00 – 23.00
	Workup (minutes)	25.80 (\pm 6.34)	18.00 – 51.00	25.50 (\pm 3.50)	22.00 – 29.00
	Reversal (minutes)	4.20 (\pm 0.64)	1.00 – 12.00	4.00 (\pm 0.00)	4.00 – 4.00
	Final Dose (ml)	2.28 (\pm 0.004)	2.20 - 2.40	2.50 (\pm 0.00)	2.50 - 2.50
Top-off	Induction (minutes)	9.75 (\pm 2.43)	7.00 – 17.00		
	Workup (minutes)	51.75 (\pm 11.44)	28.00 – 78.00		
	Reversal (minutes)	4.75 (\pm 2.18)	1.00 – 11.00		
	Final Dose (ml)	2.35 (\pm 0.09)	2.20 - 2.50		

Multiple-injection events were classified as a booster (5 NalMed-A, 2 BAM; additional drug administered to achieve induction) and topper (4 NalMed-A; additional drug administered to maintain full sedation during processing). No elk was administered both a booster and a top-off.

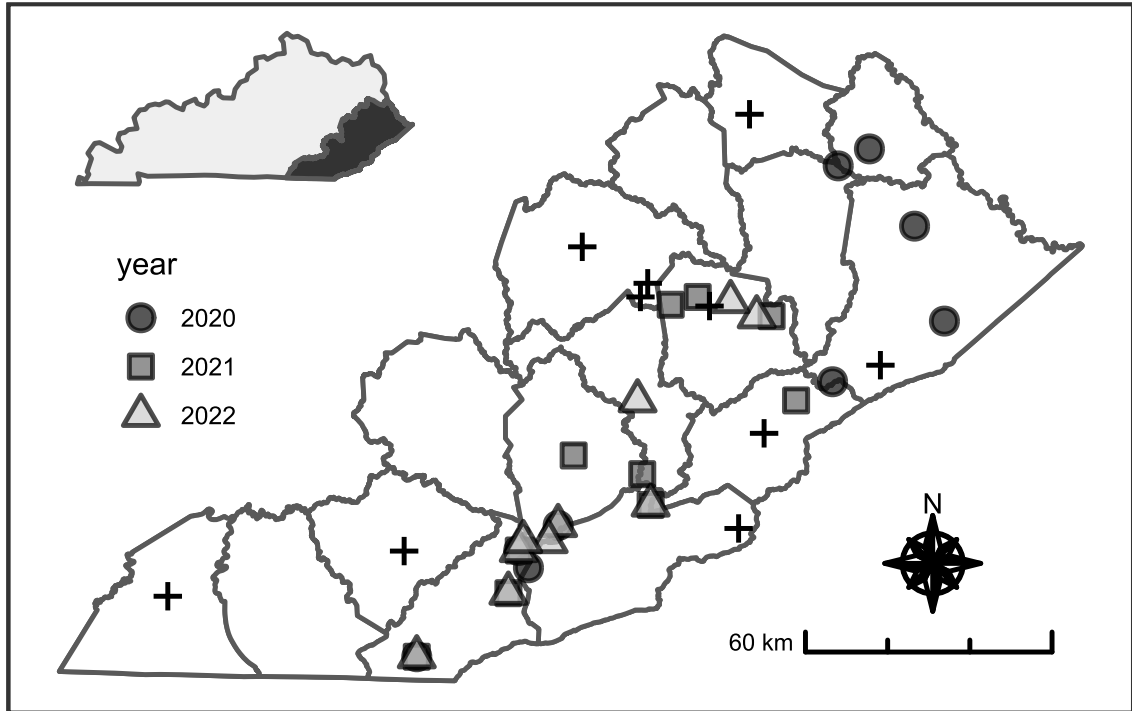


Figure 1.1. Map of Kentucky Elk Restoration Zone in southeast Kentucky, USA. The filled shapes represent each helicopter capture workup location by year and pluses represent all possible Kentucky Mesonet weather stations that recorded the weather characteristics used in the analysis.

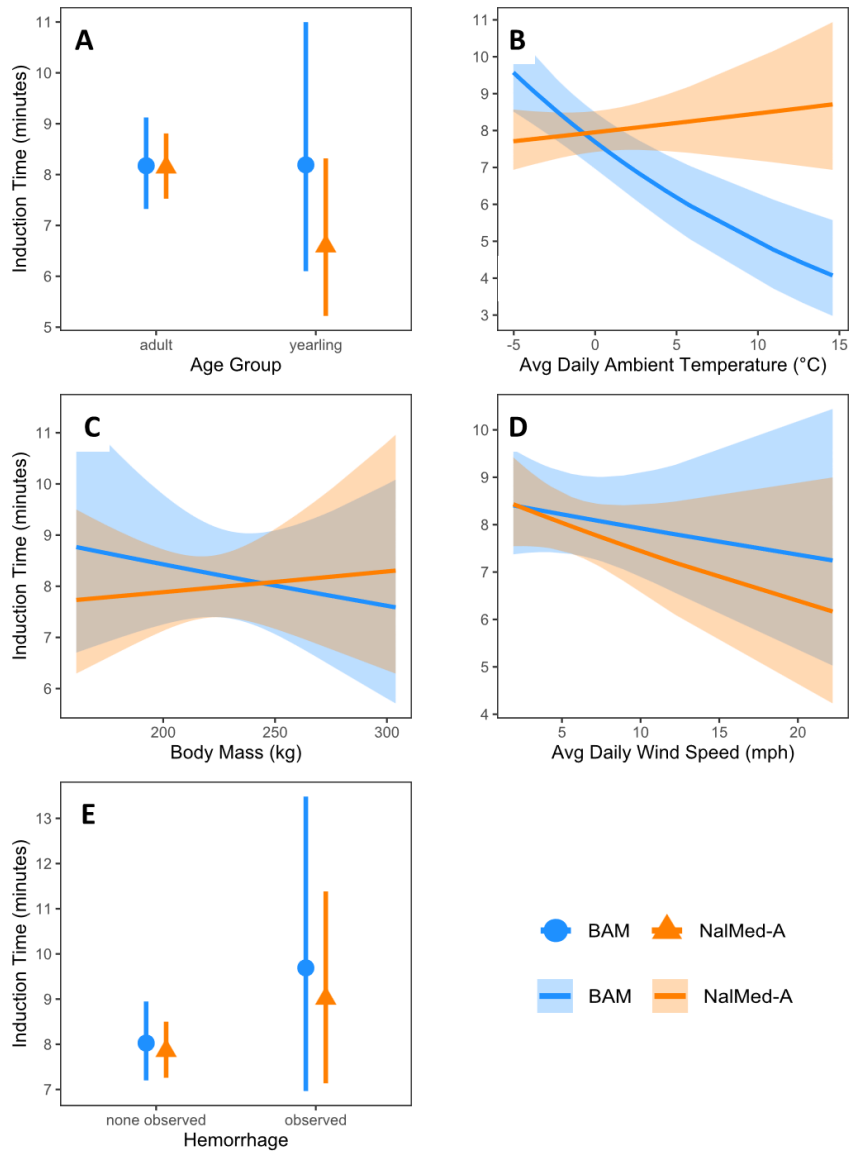


Figure 1.2. Characteristics influencing induction of a single IM injection of BAM and NalMed-A in helicopter-captured female elk in southeastern Kentucky with associated 95% confidence intervals. Influential intrinsic characteristics included age (A), body mass (C), and observed hemorrhage (E), while influential extrinsic characteristics included average daily ambient temperature (B) and average daily wind speed (D).

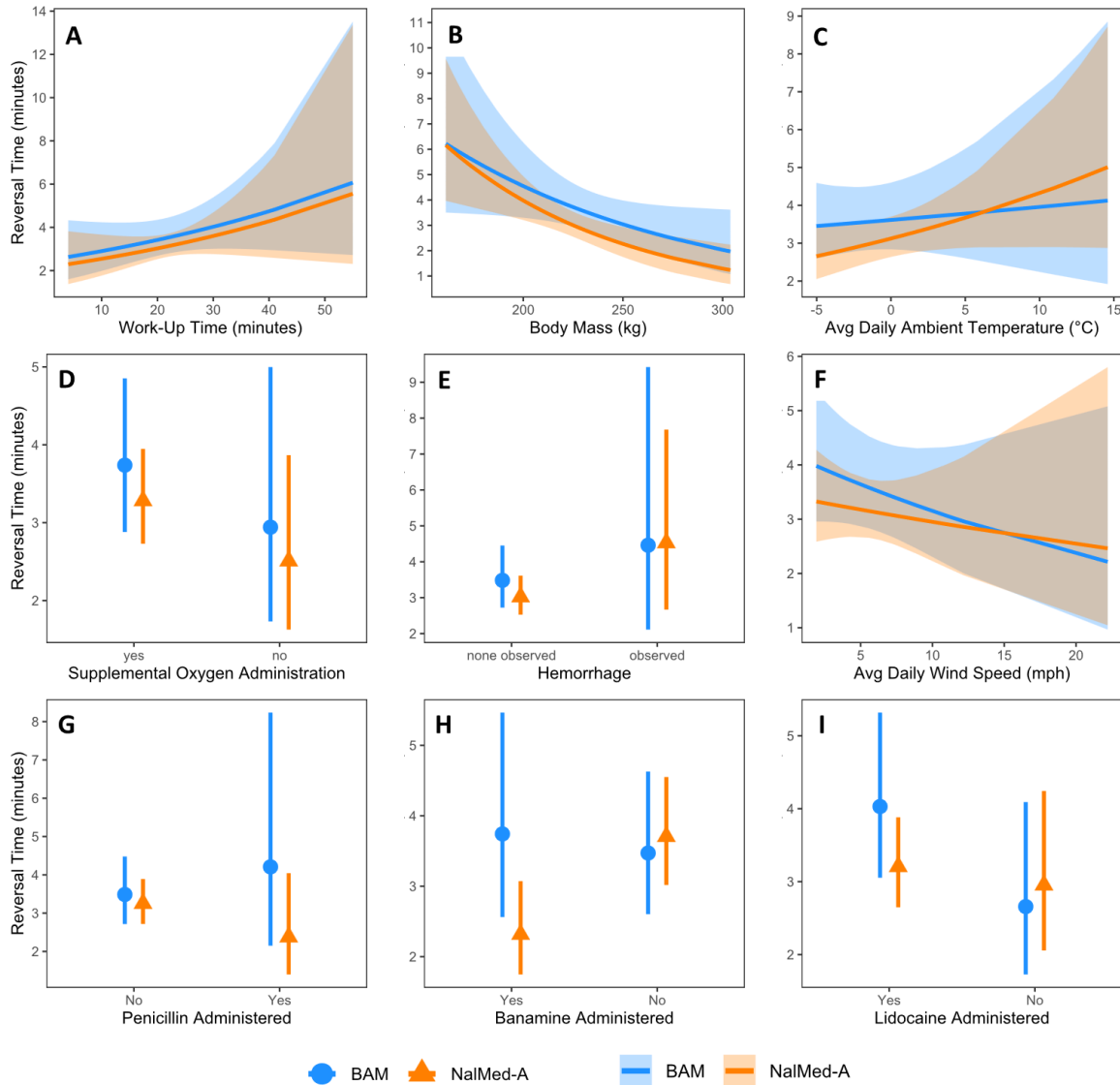


Figure 1.3. Characteristics influencing reversal of a single IM-injection of BAM and NalMed-A in female elk in southeastern Kentucky, USA with the antagonists atipamezole and naltrexone, and the associated 95% confidence intervals. Influential intrinsic characteristics included body mass (B) and observed hemorrhage (E). Influential extrinsic characteristics included workup duration (A), administration of supplemental oxygen (D), average daily ambient temperature (C), and average daily wind speed (F). Reversal times also appear to be influenced by the administration of therapeutic drugs including penicillin (G), banamine (H), and lidocaine (I).

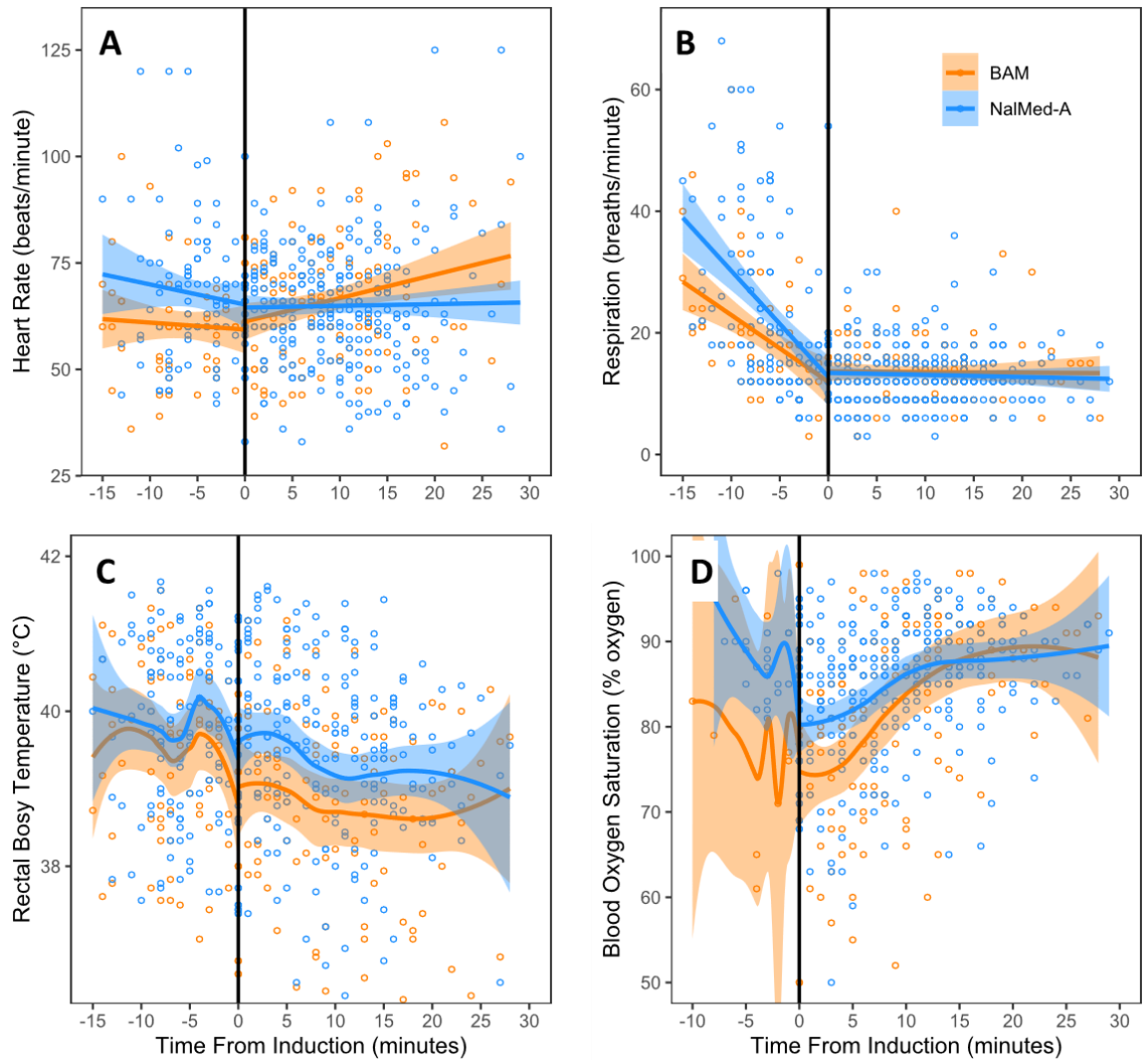


Figure 1.4. Observed pre- and post-induction physiological responses for “typical” single IM-injection events in chemically immobilized helicopter-captured female elk. These responses included heart rate (A), respiration (B), body temperature (C), and blood oxygen saturation (D) female elk chemically immobilized with NalMed-A (n = 78) or BAM (n = 41) in southeastern Kentucky, USA. All pre-induction physiological responses decreased with induction, but heart rate and respiration were generally stable following induction. Post-induction body temperature and blood oxygen saturation were more variable.

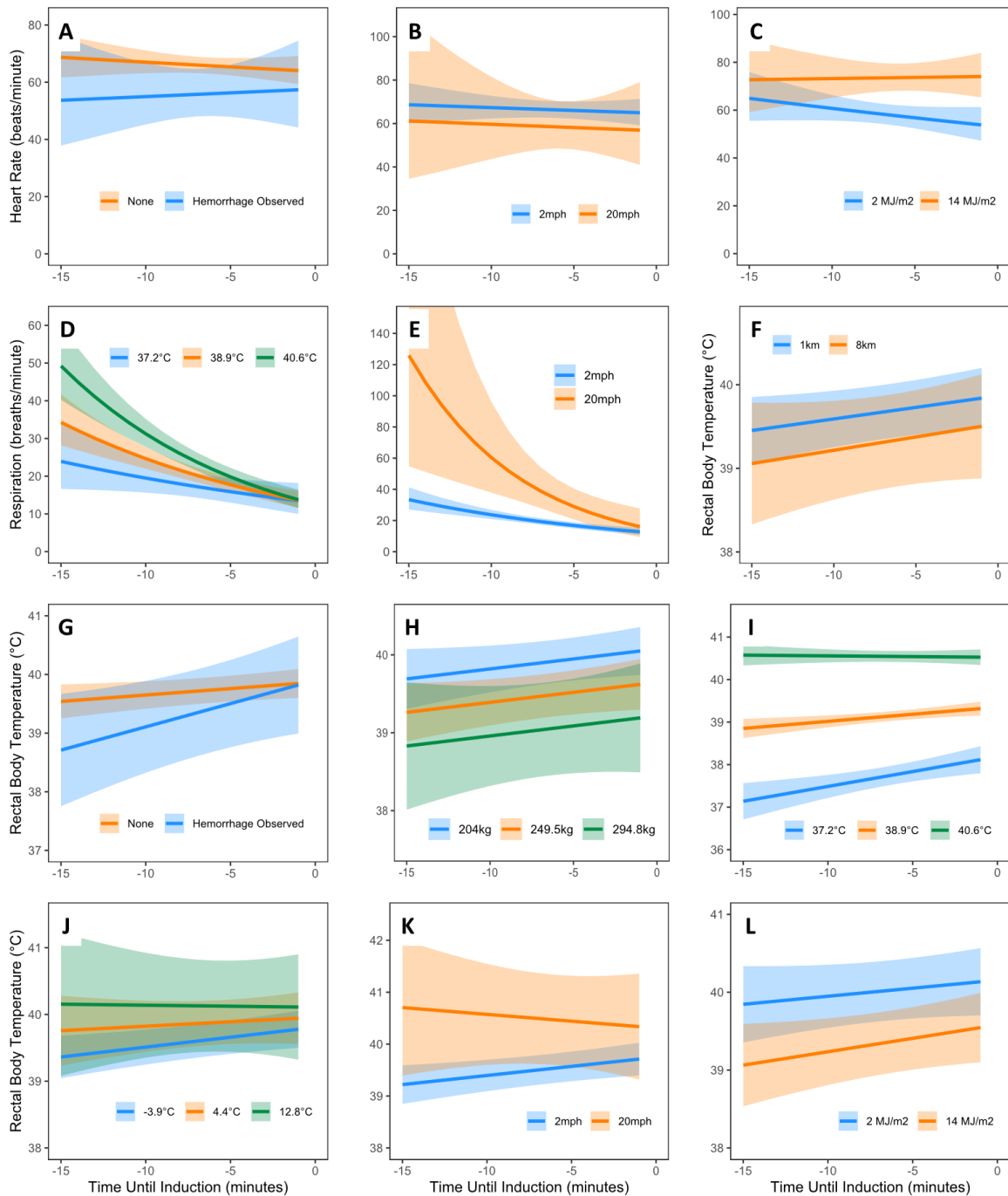


Figure 1.5. Characteristics influencing pre-induction physiological responses of female elk in southeastern Kentucky, USA immobilized with a single IM-injection of BAM and NalMed-A and the associated 95% confidence intervals. Influential intrinsic characteristics included observed hemorrhage (A, G), body mass (H), and initial body temperature (D, I). Influential extrinsic characteristics included helicopter transport distance for a subset of female elk (F), average daily ambient temperature (J), average daily wind speed (B, E, K), and daily solar radiation (C, L).

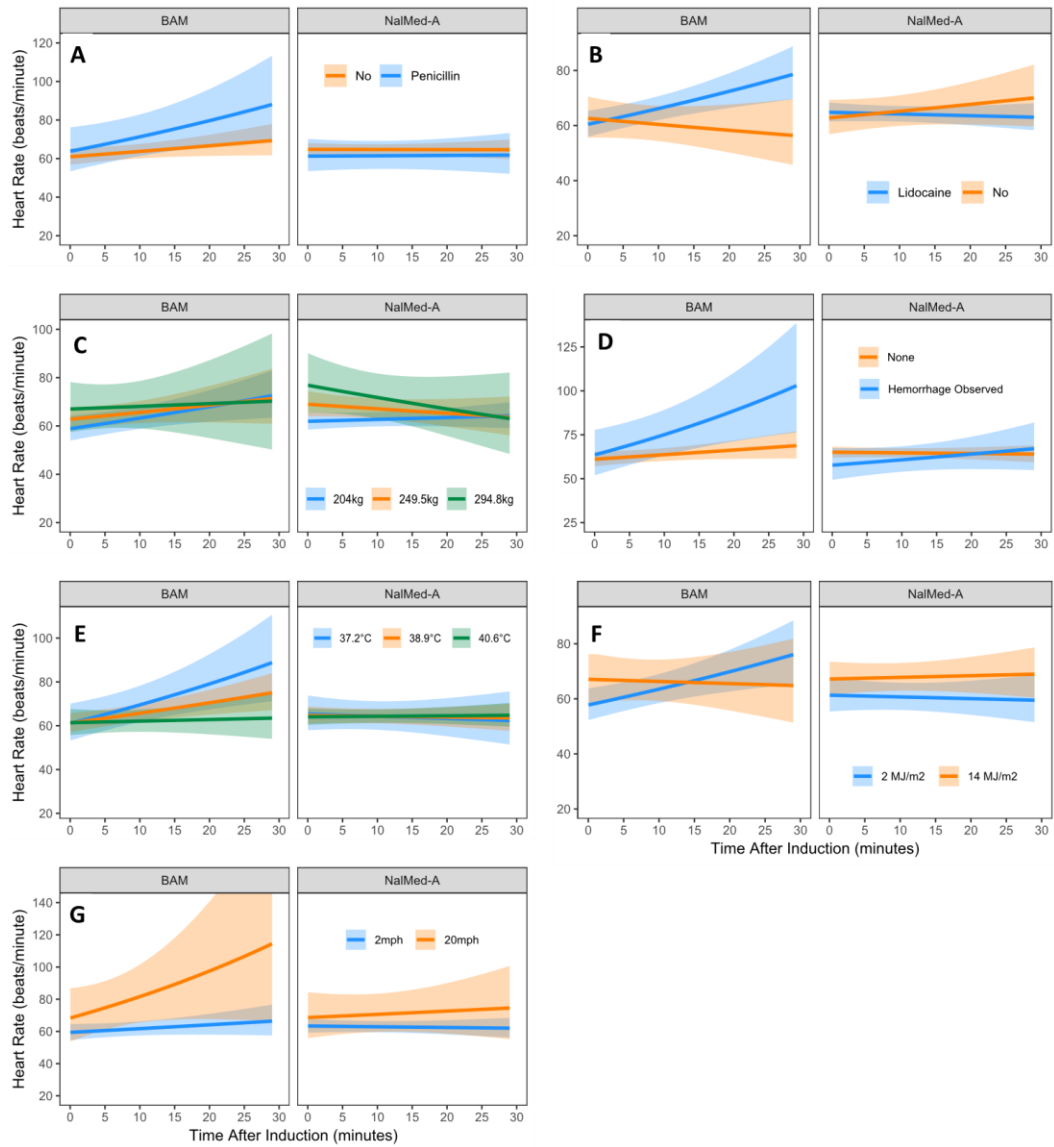


Figure 1.6. Characteristics influencing post-induction heart rate in female elk in southeastern Kentucky, USA immobilized with a single IM-injection of BAM and NalMed-A and the associated 95% confidence intervals. Influential intrinsic characteristics included body mass (C), observed hemorrhage (D), and initial body temperature (E). Influential extrinsic characteristics included the administration of the therapeutic drugs penicillin (A) and lidocaine (B), daily solar radiation (F), and average daily wind speed (G).

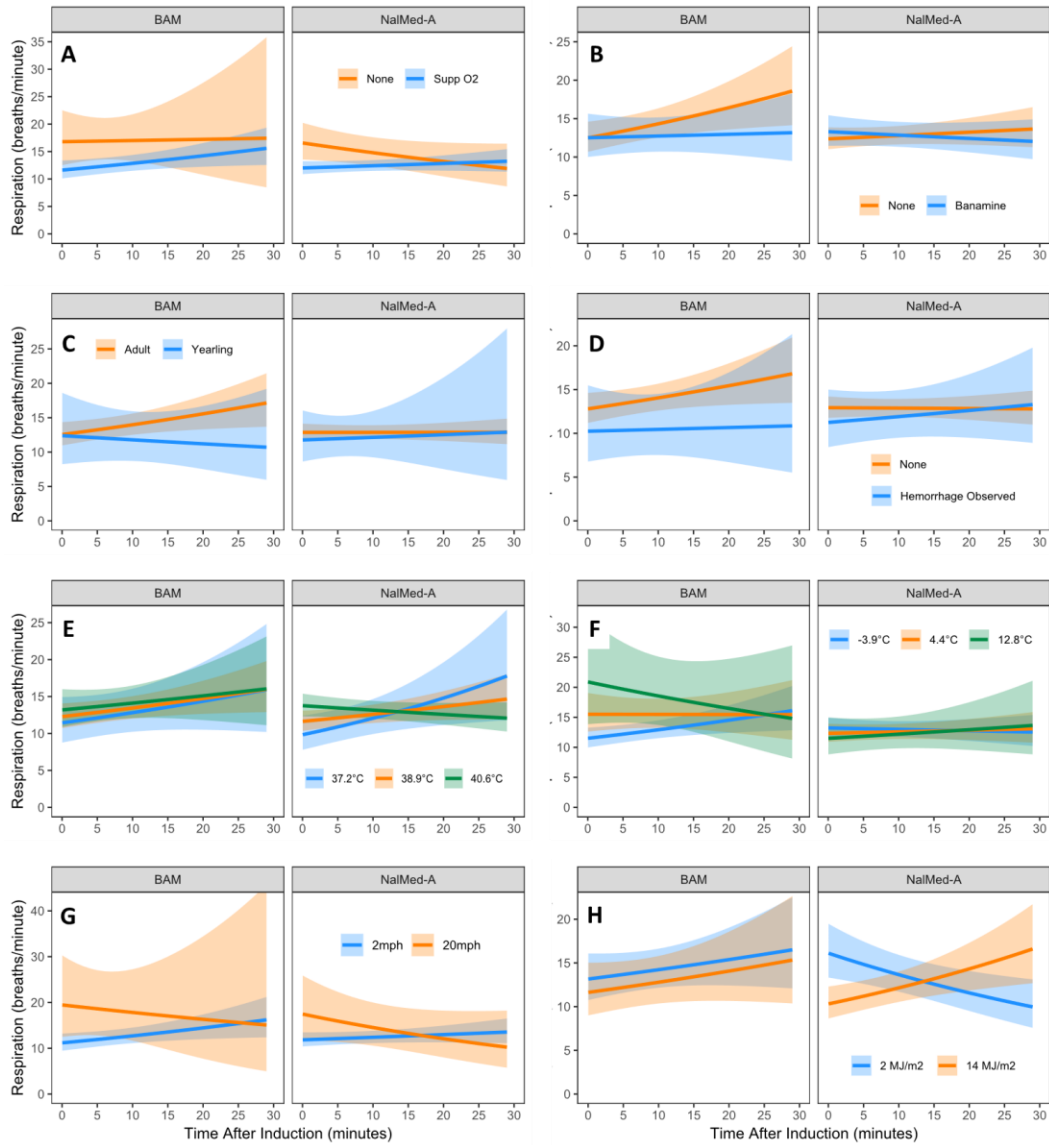


Figure 1.7. Characteristics influencing post-induction respiration in female elk in southeastern Kentucky, USA immobilized with a single IM-injection of BAM and NalMed-A and the associated 95% confidence intervals. Influential intrinsic characteristics included age class (C), observed hemorrhage (D), and initial body temperature (E). Influential extrinsic characteristics included the administration of supplemental oxygen (A) and banamine (B), average daily ambient temperature (F), average daily wind speed (G), and daily solar radiation (H).

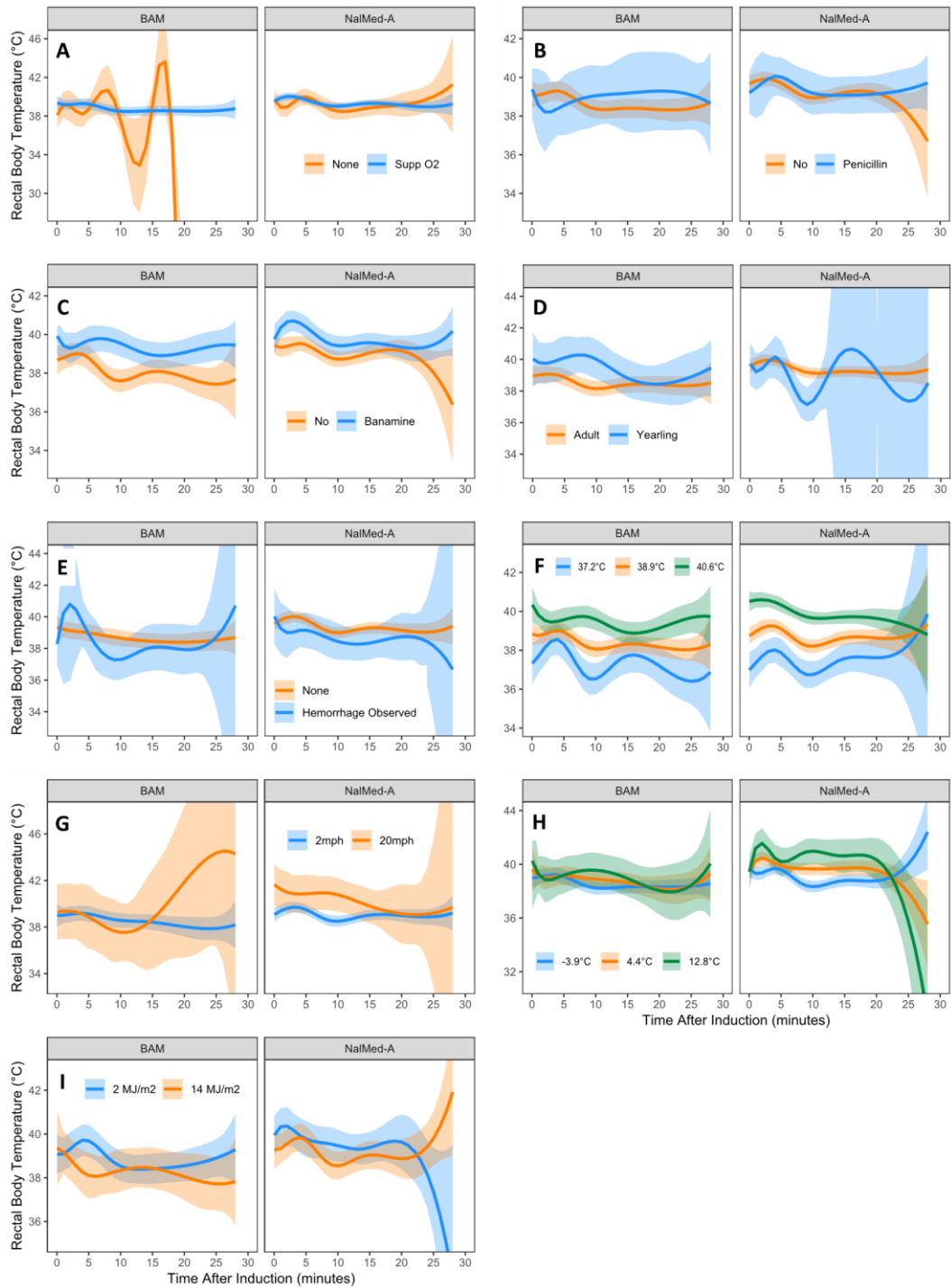


Figure 1.8. Characteristics influencing post-induction rectal body temperature in female elk in southeastern Kentucky, USA immobilized with a single IM-injection of BAM and NalMed-A and the associated 95% confidence intervals. Influential intrinsic characteristics included age class (D), observed hemorrhage (E), and initial body temperature (F). Influential extrinsic characteristics included the administration of supplemental oxygen (A), penicillin (B) or banamine (C), average daily wind speed (G), average daily ambient temperature (H), and daily solar radiation (I).

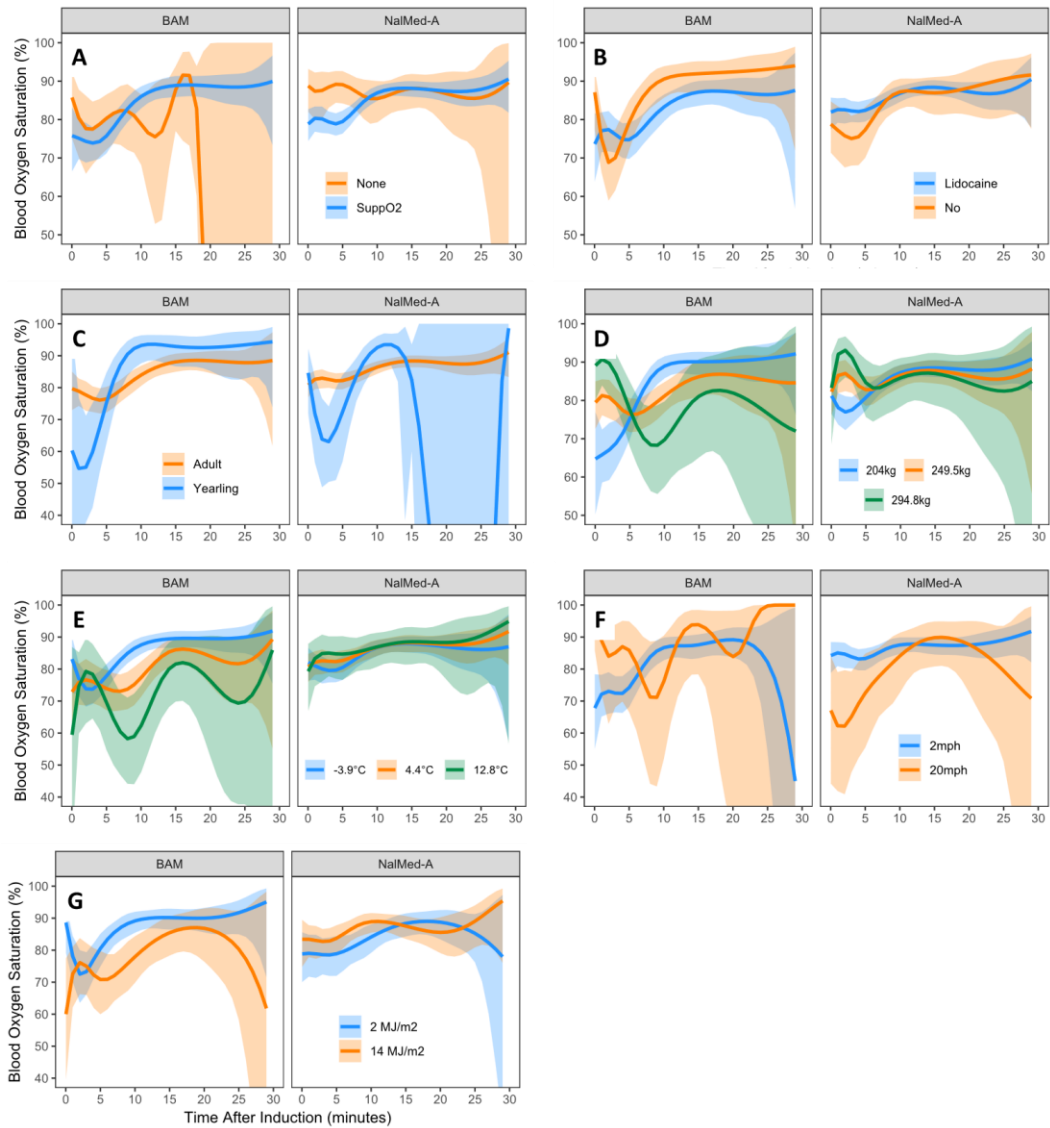


Figure 1.9. Characteristics influencing post-induction blood oxygen saturation (SpO₂) in female elk in southeastern Kentucky, USA immobilized with a single IM-injection of BAM and NalMed-A and the associated 95% confidence intervals. Influential intrinsic characteristics included age class (C), and body mass (D). Influential extrinsic characteristics included the administration of supplemental oxygen (A) or lidocaine (B), average daily ambient temperature (E), average daily wind speed (F), and daily solar radiation (G).

CHAPTER 2. SURVIVAL AND CAUSE-SPECIFIC MORTALITY OF ELK CALVES (*CERVUS CANADENSIS*) IN SOUTHEASTERN KENTUCKY

2.1 Abstract

Juvenile ungulate survival is a key population metric that should be periodically updated because it often has high annual variation and is influenced by a variety of intrinsic and extrinsic factors. To update this metric for a reintroduced population of elk (*Cervus canadensis*) in southeastern Kentucky, we conducted a 3-year calf survival study using vaginal implant transmitters to locate newborn calves across Kentucky's Elk Restoration Zone. During 2020 – 2022, we captured 81 elk neonates and monitored their survival to one year of age or until a mortality occurred, allowing us to estimate neonatal, summer, and annual elk calf survival, determine cause-specific mortality, and elucidate how maternal characteristics, morphometrics, health metrics, and weather conditions influence survival. Because monitoring was not yet completed for calves captured in 2022, we only reported mean survival ranges for calves captured in 2020 and 2021. During these years, we documented 6 unknown fates and 14 mortalities, with the top proximate cause of mortality being suspected predation by black bears and coyotes ($n = 7$), followed by trauma ($n = 2$), and emaciation or abandonment ($n = 2$). Mean neonatal survival ranged from 0.822 (SE \pm 0.057) to 0.844 (SE \pm 0.054) and was influenced by total precipitation during the first week of life. Mean summer survival ranged from 0.730 (SE \pm 0.067) to 0.772 (SE \pm 0.064) and was influenced by total precipitation during the first week of life and femur length. Lastly, mean annual survival ranged from 0.556 (SE \pm 0.074) to 0.681 (SE \pm 0.071) and was only influenced by femur length. Although this mean annual survival range is lower than survival rates previously reported in Kentucky and other eastern elk populations, this updated metric is more representative of the current population dynamics in Kentucky's established elk herd.

2.2 Introduction

Fundamental population metrics like survival and reproductive success need to be periodically updated to effectively manage large ungulate populations. In many cases, adult female survival is the main driver of ungulate population dynamics, but juvenile survival may have a significant impact if adult female survival is high and annually consistent but juvenile survival has high annual variation (Gaillard et al. 1998, Raithel et al. 2007, Eacker et al. 2017). Juvenile survival can be influenced by weather (Portier et al. 1998, Dion et al. 2020), maternal nutrition (Duquette et al. 2014, Tatman et al. 2018), predator communities and densities (Griffin et al. 2011, Eacker et al. 2016, Tatman et al. 2018), intrinsic characteristics such as body size (DeVivo et al. 2011), and physiological stress (Carstensen et al. 2009), especially during the first weeks of life. These effects can be exacerbated in reintroduced populations, which are already more vulnerable because of interrupted social structures (Le Gouar et al. 2012), novel predator communities (Kindall et al. 2011), disease (Viggers et al. 1993), and deleterious effects from genetic isolation (Groombridge et al. 2012). Such influences and juvenile mortality causes have been documented in several reintroduced elk (*Cervus canadensis*) populations in the eastern United States (Popp et al. 2014, Keller et al. 2015) during translocation efforts and once populations were established. As a result, some of these reintroduction efforts have failed, underscoring the need for periodic updates to gauge success and understand how key population metrics change over time.

Following in the footsteps of successful eastern states (Larkin et al. 2003b), Kentucky initiated its own elk reintroduction program from 1997 – 2002. In just five years, the Kentucky Department of Fish and Wildlife Resources (KDFWR) translocated ~1,550 Rocky Mountain elk (*Cervus canadensis nelsoni*) from six western source states to southeastern Kentucky (Crank et al. 2022). During this time, rigorous post-release monitoring was conducted around several release sites to document key population metrics and their potential impacts on reintroduction success and population viability. Key population metrics investigated included breeding success and adult survival (Cox 2003, Larkin et al. 2003b), the impacts of meningeal worm (*Parelaphostrongylus*

tenuis) on mortality rates (Larkin et al. 2003a, Alexy 2004), and calf survival (Seward 2003). Another round of monitoring and research occurred after Kentucky's elk population was established (> 4 years post-release, following Keller et al. 2015), including studies on adult elk survival (Slabach 2018, Hast 2019) and the effects of meningeal worm on juvenile survival (Bowling 2009), although no calf survival estimates were published from this research. Today, Kentucky is home to the largest elk herd in the eastern United States with a reported population estimate of ~10,000 individuals (Crank et al. 2022). However, concerns over data quality and its influence on the accuracy of Kentucky's population estimate prompted renewed research and monitoring efforts, especially for juvenile survival rates, which were last published almost two decades ago (KDFWR Elk Program 2020) before Kentucky's elk herd was established.

Previous studies of elk calf survival in Kentucky documented high survival rates surrounding several of the original release sites using a variety of methods. The earliest study, captured 27 elk calves in 2001 and 2002 around the Addington Wildlife Management Area release site, primarily using opportunistic ground searches based upon maternal observations and behavior following extensive vaginal implant transmitter failures (Seward 2003). The mean search time for this opportunistic capture method was 34.5 hours and the mean estimated age at capture was 4.18 days (SE \pm 0.51 days), based on body size, mobility, hoof wear, and umbilical scar healing (Johnson 1951). Calves were monitored until one year of age, allowing researchers to investigate mortality sources and document a mean annual survival rate of 0.766 (SE \pm 0.103) with a survival range of 0.564 – 0.967. Top mortality causes included coyote (*Canis latrans*) and domestic dog (*Canis lupus familiaris*) predation, meningeal worm, and hunter harvest. These survival estimates were comparable to the mean annual calf survival rates reported for other eastern elk herds around this time, including Pennsylvania (0.820, SE \pm 0.040; DeVivo et al. 2011), Michigan (0.870, SE \pm 0.050; Bender et al. 2002), and Tennessee (0.592, SE \pm 0.109; Murrow et al. 2009). A second elk calf study was conducted in the same location from 2004 – 2006, in which 97 neonates were

captured opportunistically. Capture methods included use of observation of maternal behavior, ground searches in locations where calves were previously observed, and location of calves via infrared scope from a helicopter (Bowling 2009). Collectively, the mean estimated age at capture was 5.40 days (SE \pm 0.30 days) and a subset of 62 calves were monitored until two years of age. No calf survival rates or mortality causes, aside from one death due to meningeal worm, were published from this study, but a mean 2-year-old survival rate of 0.92 was reported from the unpublished data (KDFWR Elk Program 2020).

Despite taking place in the same location, said past calf survival studies in Kentucky are not comparable because of the different survival time periods, were severely limited in their population inference due to the limited geographical scope, and relied upon opportunistic capture methods. Opportunistic methods are traditionally used to locate neonates but introduce bias into survival modeling, producing inaccurate survival estimates that can influence population estimates. These methods often rely on observations of maternal behavior or the neonate itself, which can be extremely labor-intensive because neonatal ungulates are cryptic and employ a “hiding” strategy (Barbknecht et al. 2011), and result in the capture of a neonate of unknown age. There are several metrics that have been used to estimate age in neonatal ungulates including subjective classifications and measurements of tooth eruption or hoof growth (Johnson 1951, Grovenburg et al. 2014), however estimates are highly variable and increase uncertainty in time-to-event survival estimation (Brackel et al. 2021). Opportunistic capture methods also introduce bias through left truncation, whereby some individuals die before they can be detected, which can artificially inflate survival estimates and limit our knowledge of mortality risks (Gilbert et al. 2014, Chitwood et al. 2017). However, with the development of specially designed vaginal implant transmitters (VIT), researchers are able to capture neonates of known age earlier and in variable habitat types. Modified from controlled internal drug release (CIDR) devices, a hormone delivery system commonly used to sync estrus in cattle, VITs have flexible wings to hold them in

place in the vaginal canal until expulsion due to a parturition event (Johnson et al. 2006, Barbknecht et al. 2009). In addition to reducing left truncation, using VITs aids in birth site detection and can drastically reduce search times, especially in less-open habitats (Barbknecht et al. 2009). Consequently, studies based on captures from VIT expulsions should lead to a more accurate estimate of elk calf survival compared to opportunistic methods that rely on visually detectable individuals that are often older and larger.

We used VITs to conduct a 3-year elk calf survival and cause-specific mortality study to update our understanding of one of the key demographic metrics that influences population growth. Our objectives were to 1) estimate survival, 2) investigate the influence of select intrinsic and extrinsic factors on survival, and 3) determine cause-specific mortality probabilities for elk calves in southeastern Kentucky during three survival periods (neonatal, summer, and annual). We hypothesized that use of VITs to locate calves would result in lower elk calf survival estimates than past estimates using opportunistic methods, but that predation would still be the leading cause of mortality. Based on the results of other juvenile ungulate survival studies across the eastern United States (Baxter et al. 2008, DeVivo et al. 2011), we expected intrinsic factors relating to body size (e.g. body mass and proportionality) to positively influence survival, as larger and more proportional neonates are more likely to survive. We also expected indicators of health, such as immune system function and stress, to negatively influence calf survival when immune function is low and cortisol concentrations are higher, as has been found in white-tailed deer fawns (Sams et al. 1996, Carstensen et al. 2009). Lastly, because neonates' poor thermoregulatory abilities and susceptibility to hypothermia (Mercer et al. 1979, Mota-Rojas et al. 2022), which can affect their metabolism and thus their nutritional status, we hypothesized that conditions that promote hypothermia such as increased precipitation and low minimum ambient temperatures could negatively impact survival.

2.3 Methods

We conducted this study across the 16-county Elk Restoration Zone (KERZ) in southeastern Kentucky, USA (Figure 2.1). This region has as a humid temperate climate (Hill 1976) with annual mean temperatures ranging from 8.7 – 19.3°C and 131.8 cm of mean precipitation annually as well as mean temperature ranges from -1.2 – 8.3°C with a mean of 31.7 cm precipitation and 46.2 cm of snow fall in the winter months (December – February). During late spring and summer (May – August), the mean annual temperature ranges from 18.6 – 27.8°C with a mean of 12.6 cm precipitation (Jackson, KY, USA; National Oceanic and Atmospheric Administration [NOAA] 2022). Located within the Cumberland Plateau physiographic region, the KERZ is characterized by steep, narrow valleys with large patches of mixed-mesophytic forest (McFarlan 1943) interspersed with areas of low-density development, timber harvest, and shrub-bordered grasslands. These grasslands were generated by reclamation efforts following intensive mountain-top removal and valley fill practices used in coal mining across Appalachia, which generated open areas less variable terrain and ample forage, mimicking traditional elk habitat found in many western states (Larkin et al. 2001, Cox 2011). Forested areas contain a mixture of oak species (*Quercus spp.*), maple species (*Acer spp.*), yellow poplar (*Liriodendron tulipifera*), American beech (*Fagus grandifolia*), and eastern redbud (*Cercis canadensis*). Shrubby areas and grasslands contain patches of autumn olive (*Elaeagnus umbellata*) mixed with or bordering areas of minimal topography containing bush clover (*Lespedeza spp.*), crown vetch (*Coronilla varia*), and Kentucky-31 tall fescue (*Lolium arundinaceum*; Hast 2019).

2.3.1 Capture and monitoring

To prepare for neonate searches in the summer, we captured adult and yearling female elk across the KERZ via helicopter net-gunning (Native Range Capture Services, Elko, NV, USA and Helicopter Wildlife Services, Austin, TX, USA) in January 2020 – 2022. Once captured, the helicopter crew applied a blindfold and hobbles before removing the elk from the net and

transporting non-sedated individuals to a designated workup location. Once each elk was weighed using the helicopter and placed on a modified flat-bed trailer, we assessed injury status and began monitoring vitals including heart rate, respiration, and body temperature for early warning signs of conditions that increase the chance of capture myopathy, such as hyperthermia (Paterson 2007). We then chemically immobilized any adult or yearling female elk with “safe” body temperatures (<40.5°) by hand-injecting either 2 ml of butorphanol tartrate (27.3 mg/ml) – azaperone (9.1 mg/ml) – medetomidine (10.9 mg/ml) (BAM; ZooPharm, Inc., Laramie, WY, USA), 2 ml of nalbuphine HCl (40.0 mg/ml) – medetomidine (10.0 mg/ml) – azaperone (10.0 mg/ml) (NalMed-A, ZooPharm, Inc., Laramie, WY, USA), or 1.2 ml of etorphine HCl (Wildlife Pharmaceuticals, Inc., Windsor, CO, USA). Once an appropriate plane of sedation was achieved, we applied eye lubricant, removed the hobbles, and repositioned each elk into sternal recumbency to improve vital rates and airway maintenance (Caulkett and Arnemo 2007).

Once each elk was sternal, we took a chest girth measurement and assessed body condition (Gerhart et al. 1996). Since aging elk based on tooth wear is not reliable, only age category was determined from observations of tooth replacement (Jenson 1999). In adults with stable vital rates, we extracted one of the lower canine teeth following administration of a local anesthetic (Lidocaine 2%; VetOne®, Boise, Idaho, USA) for lab-based aging (Matson’s Laboratory, Manhattan, MT, USA) which analyzes cementum annuli layers from a cross-section of each tooth (Hamlin et al. 2000). We drew ≤30 ml of blood via jugular venipuncture for health assessments, including pregnancy status based on pregnancy-specific protein B (PSPB; BioPRYN; Herd Health Diagnostics, Pullman, WA, USA) (Stephenson et al. 1995), and used real-time transrectal ultrasonography (Ibex Pro; E.I. Medical Imaging, Loveland, CO, USA) to check pregnancy in the field. If we observed a pocket of amniotic fluid with a placentome or visible fetus (Figure 2.2; Stephenson et al. 1995, Romano et al. 2006), then we considered that female to be pregnant and deployed the first half of the Vectronic natal-linked system, consisting of a Vertex Plus GPS

telemetry collar and paired vaginal implant transmitter (VIT; Vectronic Aerospace, Berlin, Germany). Following Hooven et al (2022), we inserted all VITs using a modified applicator made from 3/4 inch-diameter polyvinyl chloride (PVC) containing a 1/2 inch-diameter PVC plunger. One end of the applicator was cut to approximately a 45° angle and sanded to maintain a rounded edge thereby preventing injury, and liberal application of an all-purpose, non-spermicidal veterinary obstetrical lubricant jelly (Neogen Corporation, Lansing, MI, USA) was used to facilitate insertion. We then measured the amount of antenna protruding from the vagina before moving the individual a short distance to a release location, and hand injecting 4 ml of atipamezole (25 mg/ml, half given IM and half given intravenous or IV) (ZooPharm, Inc., Laramie, WY, USA) and 0.5 ml of naltrexone (50 mg/ml, IM) (ZooPharm, Inc., Laramie, WY, USA) to reverse the chemical immobilization.

We remotely monitored the survival, movement, and VIT status of all female elk that received a Vertex Plus GPS telemetry collar and paired VIT using a desktop program (GPS Plus X 10.7.1, Vectronic Aerospace, Berlin, Germany) and/or a web interface (INVENTA, Vectronic Aerospace, Berlin, Germany). All collars were programmed to send GPS relocations every 13 hours from time of deployment (January) until the start of calving season (May), when they began sending GPS relocations every 7 hours. These collars also continually searched for a specific ultra-high frequency (UHF) beacon over short distances that was pre-programmed into each VIT, allowing us to remotely track VIT status. When two biological thresholds, an activity level of 0 and a drop in temperature records well below normal body temperature (<34°C), were simultaneously met, each VIT began emitting a “mortality” beacon prompting the Vertex Plus collar to send a new status (expelled) and notification of a possible parturition event via e-mail and short message service (SMS; Rice 2016). We ensured a minimum of 3 hours had passed since VIT expulsion to reduce disturbance of critical maternal bonding (Livezey 1990), then tracked to the expelled VIT to locate the birth site and neonate. If the neonate was not found in or adjacent to the

birth site, we initiated a search, moving in circular transects approximately 5m apart until the calf was found or three hours had passed, returning the next day, for a maximum of three days. If a calf was not located after three days, we ended all search efforts for that cow/calf pair.

Once located, we physically restrained the elk calf, then applied a blindfold to reduce stress and moved the calf approximately 2-3m from the original capture location, wearing nitrile gloves throughout processing, to reduce scent transfer and thus, the risk of abandonment (Livezey 1990). We then shaved hair from the neck, swabbed the area with an alcohol swab, and collected ≤ 20 ml of blood via jugular venipuncture (University of Minnesota 2022). This blood sample was stored in a 2 ml ethylenediamine tetra acetic acid (EDTA) purple-top tube to prevent clotting and two 10 ml red-top blood collection tubes, then placed in a cooler with ice packs until processing. Next, we deployed an expandable VHF telemetry collar with an 8-hour mortality sensor and pre-programmed UHF beacon (Vectronic Aerospace, Berlin, Germany), which we paired to the dam's Vertex Plus collar using GPS Plus X following release of the calf. We also collected a series of morphometrics, including total body length (a curvilinear measurement from the tip of the nose, following the spine, to the base of the tail), neck circumference, chest girth, femur length, hind foot length (tip of hoof to tip of calcaneus), new hoof growth, and first incisor eruption (tip of tooth to gum; Johnson 1951). Lastly, we inserted two uniquely numbered plastic stud ear tags (National Band and Tag, Newport, KY, USA) and weighed each calf using a digital hanging scale before releasing the calf where we found it. Capture and handling protocols for both winter and summer captures were approved by the University of Kentucky Institutional Animal Care and Use Committee (IACUC #2019-3382) and followed the American Society of Mammalogists (Sikes et al. 2016).

We monitored each calf's survival through the first year of life or until mortality occurred, dividing survival data into three overlapping periods: neonatal (birth – 14 days), summer (birth – until the start of elk archery season on September 11th), and annual (birth – 1 year of age). Similar

to the paired VITs, calf survival was monitored remotely using GPS Plus X 10.7.1 and INVENTA (Vectronic Aerospace, Berlin, Germany). Depending on the dam's distance from the calf, and thus the calf collar, we could receive three possible status messages at each check-in: 1) alive and received indicating that the GPS collar is close enough to detect the calf collar and the calf was moving in the last 8 hours, 2) separation – no contact, indicating that the GPS collar is not close enough to detect the calf collar, but last time it was in contact the calf was moving, and 3) separation – mortality, indicating that the GPS collar is close enough to detect the calf collar and the calf has not moved in the last 8 hours, so the mortality beacon has been switched on. All separation – mortality statuses were investigated immediately to determine cause of death. When we received two separation – no contact statuses back-to-back without re-connecting, we attempted to locate the calf and check survival status via ground telemetry. However, the predictive ability of these statuses for indicating mortality were harder to parse out as calves became more mobile, especially once the fix rate was switched back to 13 hours approximately 2 weeks after birth. This prompted a change in our protocol from attempting to locate all calves and/or initiating a mortality investigation following two separation – no contact statuses, to three or four statuses. Once the following year's calving season began, monitoring became opportunistic as needed and final survival status was determined by re-connection with the dam after calving season in late summer.

We investigated all female elk and calf mortalities as soon as possible to determine cause of death following the receipt of a separation – mortality notification or detection via ground telemetry. Upon finding a “mortality scene”, we searched the immediate area for any remains and sign, documenting and photographing all findings. Additionally, we noted the orientation and condition of the carcass, as well as environmental cues, including any signs of predation or scavenging including tracks, scat, disturbed areas, and caching (Elbroch and McFarland 2019, Cristescu et al. 2022). If the carcass was fresh (< 1 day), intact, and close enough to an accessible

road, we collected it whole for necropsy by KDFWR's wildlife veterinarian or a diagnostic laboratory (e.g. the Southeastern Cooperative Wildlife Disease Study at the University of Georgia). If the calf had been dead for more than 1 day or if the carcass was not intact, we performed a field necropsy. This included skinning the carcass to look for hemorrhage and bruising corresponding to puncture marks or scratches, broken bones, and other characteristics unique to specific predators such as a peeled hide, intact rumen, clipped or plucked hair, and/or disarticulated limbs (Elbroch and McFarland 2019, Nigon 2020, Ganz et al. 2023). We also collected tissue samples for histological analysis to elucidate contributing morbidities if needed. All mortalities were assigned a preliminary cause of death, which we reviewed periodically upon receipt of additional necropsy or diagnostic results, then a final cause of death which was used in our cause-specific mortality analysis.

2.3.2 *Blood and hair sample analysis*

All blood samples were kept cold with ice packs during transport, processed within 24 hours of collection, and then fixed in 10% neutral buffered formalin or frozen to maintain quality and prevent cell degradation. We allowed blood collected in the red top blood collection tubes to clot for a minimum of an hour before the tubes were spun at 5,000 rpm for 15 minutes in a benchtop centrifuge (Ultra 8V, LW Scientific, Lawrenceville, GA, USA) to separate the serum, spinning tubes for an extra 5 minutes if the clot was not fully separated out. A drop of serum was then dropped on a handheld refractometer (Protein/Specific Gravit Model; LW Scientific, Lawrenceville, GA, USA) to obtain a measurement of total solids, an estimate of total protein in the serum (Cornell University College of Veterinary Medicine 2020a). The remaining serum was placed in sterile 2.0 ml cryovials (ExtraGene, Taichung City, Taiwan) and frozen. Unclotted whole blood from the purple top EDTA tube was used to measure packed cell volume (PCV) and create blood smears. To measure PCV, we placed a small amount of whole blood in 40 mm hematocrit tubes (LW Scientific, Lawrenceville, GA, USA) and spun the tubes for 3 minutes at 10,000 rpm in

a micro-centrifuge (ZipCombo, LW Scientific, Lawrenceville, GA, USA), using the provided card to measure the height of the packed red blood cells in each tube (Cornell University College of Veterinary Medicine 2020b). To make blood smears, we used a pipette to drop a small amount of blood at the end of a microscope slide (Karter Scientific Labware Manufacturing, Lake Charles, LA, USA) and used a second slide, pushed at a 30-40° angle, to spread the blood droplet and create a feathered edge (Cornell University College of Veterinary Medicine 2016). Once dried, we fixed each slide in methanol (VetOne® Rapid Differential Stain Kit; MWI, Boise, Idaho, USA) for 1 minute to prevent cellular degradation and stored all smears until they could be read. All remaining whole blood was frozen.

Due to funding constraints and distance from any veterinary diagnostic laboratories during the summer field work, all blood smears were manually analyzed by the KDFWR Wildlife Health Program instead of an automated cell counter. Each slide was dipped 10x for 1 second each in an eosinophilic stain, then the procedure was repeated for a basophilic stain methanol (VetOne® Rapid Differential Stain #1; MWI, Boise, Idaho, USA) and rinsed off with water until the water was clear, then allowed to dry (AMR Vet Collective n.d.). Once stained, the monolayer of each smear was first examined at 10x using a systematic approach for all types of white blood cells, including “normal” leukocytes (neutrophils, eosinophils, basophils, lymphocytes, and monocytes) and “abnormal” leukocytes (reactive lymphocytes and band or immature neutrophils). The smear was then examined at 100x with oil using a systematic approach to identify all observed leukocytes until 100 have been counted (Cornell University College of Veterinary Medicine 2020c). The output is a tally of each type of leukocyte found in the 100 observed white blood cells and is treated as a representation of the percentage of each cell type circulating in that elk calf when captured.

Hair samples were placed in labeled coin envelopes and stored in a sealed container with desiccant beads until we could send them to Murray State University for analysis. Each hair

sample was processed following Caslini et al. (2016) prior to extraction by cutting hair into 5mm pieces and placing it into a tared glass vial. The sample was washed by vortexing for 10 seconds in 3 ml of 100% methanol, then all alcohol was immediately removed with a pipettor. Next, 3 ml/40mg of hair of 100% methanol was added to the sample, then the vial was vortexed for 5 seconds and left on a plate shaker (level 6) for 24 hours. Each sample was subsequently spun for 10 minutes at 2400g in a benchtop centrifuge and the resulting supernatant was pipetted into a new glass vial, then air dried using a fume hood for approximately 24 hours, sealed, and stored at -20° C. When enough samples were prepared for extraction using a DetectX[®] Enzyme Immunoassay Kit (Arbor Assays, Ann Arbor, MI, USA), they were thawed to room temperature and reconstituted 10-fold in 3 ml of assay buffer. Each sample was then vortexed again for 1 minute and shaken for approximately 30 minutes using a plate shaker (level 5) while the assay was prepared following a protocol generated by Arbor Assays (Arbor Assays 2009). Once the assay plate was loaded, a plate reader generated reading optical densities generated for each well, which was used to calculate the cortisol concentration in each sample.

2.3.3 *Weather data*

We obtained all weather variables (precipitation, minimum temperature, and solar radiation) from Kentucky Mesonet weather stations (Western Kentucky University Kentucky Climate Center 2022) located across the Elk Restoration Zone. However, as none of the weather stations were located exactly where we captured elk calves, we extracted data from the closest station. To determine which station was closest, we transformed all capture and weather station locations from latitude/longitude to UTM's using the `spTransform` function in the R package 'sp' (version 1.6-1; Pebesma et al. 2005). Next, we calculated the Euclidean distance between them using the `gDistance` function in the 'rgeos' R package (Bivand et al. 2023) and extracted all pertinent weather data and converted all ambient temperatures from Fahrenheit to Celsius using the R package 'weathermetrics' (version 1.2.2; Anderson et al. 2016). Weather conditions,

especially precipitation and minimum temperatures which can contribute to hypothermia in neonates (Mercer et al. 1979), likely have the most impact when elk calves are less mobile, so we restricted the weather metrics extracted to the first week of life (birth date – 7 days or death date). All variables were either summed or averaged, producing metrics of total precipitation (cm), average daily minimum temperature (°C), and average daily solar radiation (MJ/m²) experienced by each elk calf during the first 7 days of life or until their death if they died in the first week.

2.3.4 *Survival analysis and cause-specific mortality*

We used two types of known-fate, time-to-event modeling to estimate elk calf survival and explore the influence of a variety of intrinsic and extrinsic factors during three survival periods. In this case, the event of interest is mortality and individuals that survived or had unknown fates because we lost the ability to monitor their survival status prior to the end of the designated survival period due to collar failure or the location of a collar with no evidence of mortality were right-censored (Fox and Weisberg 2011). This analysis approach is common in neonatal ungulate survival studies (McDermott 2017, Shuman et al. 2017, Wright et al. 2019, Dion et al. 2020), but we diverged from this typical approach by performing each modeling approach twice for three survival periods, once following traditional survival modeling approaches where elk calves with unknown fates were right-censored (hereafter referred to as the “traditional censor” data set), and again where calves with unknown fates are treated as mortalities to model the worst-case scenario (hereafter referred to as the “censor as dead” data set) to generate a survival probability range. This divergent modeling approach applies only to our survival analysis, not our assessment of competing risks for specific mortality causes. All survival analysis was completed with the R package “survival” (version 3.4-0; Therneau et al. 2022) using program R 4.2.2 (R Core Team 2020) within RStudio (RStudio Team 2021). Lastly, because monitoring of calves captured in 2022 was not yet complete, only elk calves captured in 2020 and 2021 were included in this analysis.

We used the Kaplan-Meier estimator (KM) with staggered entry to generate elk calf survival estimates and their associated 95% confidence intervals by year and overall, for 2020 and 2021 combined. This non-parametric model estimates the probability that an elk calf will survive to time t by dividing the number of remaining individuals by the number of starting individuals (Pollock et al. 1989, Kishore et al. 2010). Although this type of survival modeling can be used to assess the influence of factors on survival, it can only compare the impacts of a single categorical variable at a time, limiting its usefulness. For this reason, we used the Cox proportional hazards (CPH) models with staggered entry and stratified by year to investigate the influence of a suite of categorical and continuous factors simultaneously on the probability of an event occurring at time t . This semiparametric model generates hazard ratios for each variable or “hazard,” representing the proportional effect each variable has on a baseline hazard function over time (Fox and Weisberg 2011, George et al. 2014). We performed both the KM and CPH approaches for three overlapping time periods: a neonatal survival period from birth to 14 days old, a summer survival period from birth to the start of elk archery season on September 11 of each year because calves are eligible to be harvested, and an annual survival period from birth to one year of age.

We investigated the influence of several intrinsic and extrinsic factors on elk calf survival including hunt unit, maternal condition during winter captures, calf morphometrics and health metrics, and weather experienced during the first week of life (Table 2.1), although not all factors were considered for every survival period. For instance, we considered all variables for the neonatal survival period, but removed the health metrics from the manual differential from analysis of the summer and annual survival periods because hematological parameters change rapidly with development during the first weeks and months of life (Mohri et al. 2007), and thus are less likely to influence survival. Similarly, we included weather variables such as the total amount of precipitation (Nprecip), average minimum temperature (Navg_mintemp), and average daily solar radiation (Navg_solar) each calf experienced during their first week of life in our

analysis of the neonatal and summer survival periods but removed them from the annual survival period analysis because it was unlikely to have a proportional effect over a much longer survival period.

To determine which of these intrinsic and extrinsic variables of interest influenced elk calf survival, we employed a multi-stage information-theoretic approach using Akaike's information criterion corrected for small sample sizes (AICc; Burnham et al. 2011) using the 'AICcmodavg' package (version 2.3-1; (Mazerolle 2020) to select the best CPH model for each survival period. First, we fit univariate models for each variable of interest, comparing them to a null model and moving variables/models to the next stage only if they had a lower AICc value than the null model and did not contain uninformative parameters (Burnham et al. 2002, Arnold 2010). We then checked for multicollinearity, removing any variables with a Spearman's rank correlation coefficient (ρ) > 0.5 and a variance inflation factor (VIF) > 10 from further consideration. If Spearman's ρ was > 0.5 but the VIF was < 2, we retained the variable/model but kept the variables separate in future model selection. In the second stage, we fit CPH models in their respective variable category (Table 2.1) with all possible combinations of the variables retained from the first stage, removing models with a Δ AICc > 7 and uninformative parameters from further consideration (Arnold 2010, Burnham et al. 2011). We followed a similar approach in the final model selection stage, fitting all possible combinations of the candidate models retained in each variable category from the second stage. During this final stage of model selection, we considered all remaining models with no uninformative parameters and Δ AICc < 7 to be potentially supported. However, we only considered models with Δ AICc < 2 to be competitive (Burnham et al. 2011), selecting the model with the lowest Δ AICc as the top model for each survival period. We then assessed the hazard proportionality using the coxzph function in the R package "survival" (version 3.4-0; (Therneau et al. 2022) and reported the hazard ratios for all variables in the final models for each modeling type for each survival period.

Conversely, we used cumulative incidence functions (CIFs) to analyze cause-specific mortality during all survival time periods for the traditional censor data set. This method of analysis commonly used in survival studies (Slabach et al. 2018, Forrester and Wittmer 2019) because there can be more than one “event of interest” that may disproportionately impact wildlife populations. Thus, CIFs augment output from CPH models, which only designates two fates for monitored individuals (mortality and censored due to survival or a failed transmitter) by diversifying the number fates considered to assess competing risks from different sources of mortality and estimate cause-specific mortality probabilities (Heisey and Patterson 2006, Logan et al. 2006). In this study, we generally grouped fates into 7 categories: survived, censored due to an unknown fate (i.e. slipped collar or broken transmitter), mortality due to predation (as evidence by wounds with associated hemorrhage; Ganz et al. 2023), trauma (i.e. vehicle strike or other irrecoverable injuries), emaciation or abandonment, disease, or unknown causes (i.e. mortality, but did not have enough evidence to definitively categorize cause of death). Using the cuminc function in the R package “cmprsk” (version 2.2-11; Gray 2021), we then estimated the cumulative sub-hazard function, which represents the probability that a mortality is due to that specific cause, and the associated 95% confidence intervals for each category at the end of each survival period.

2.4 Results

During 2020 – 2022, we captured and chemically immobilized 137 female elk across 9 counties in southeastern Kentucky to confirm their reproductive status. We deployed GPS telemetry collars and paired VITs in 97 field-confirmed pregnant female elk (adults = 93, yearlings = 4) based upon observation of potential signs of pregnancy, which was later confirmed or contradicted by analysis of serum PSPB levels (95 confirmed pregnant, 2 not pregnant). Prior to calving season, we documented 7 unknown fates because 4 VITs broke (2020 = 1, 2022 = 3) and 3 VITs were expelled early with no signs of a fetus or calf (2020 = 1, 2021 = 2), preventing further monitoring and/or capture of a live-born calf. Additionally, we documented 3 known fates when

an aborted fetus was expelled early in 2021 and 2 female elk and their fetuses died (2020 = 1, 2021 = 1) prior to parturition. The remaining 84 VITs were remotely monitored through calving season and used to locate calves following parturition.

Calving season ranged from mid-May to early August with the earliest birth occurring in 2020 on May 17, the median birth date on June 7, and the latest birth occurring in 2021 on August 3 (Figure 2.3). During this time, we captured 81 live-born elk calves (2020 = 21, 2021 = 24, and 2022 = 36) following notification of a VIT expulsion. We also found 1 stillborn calf in 2021 and documented 3 unknown fates during this period when we were unable to locate an elk calf from a broken, but expelled, VIT in 2020, a functioning VIT that was expelled in 2022, and a VIT that was not expelled by the start of hunting season in 2021. A second VIT was also not expelled by the start of hunting season in 2021 but was retained and later expelled during a parturition event the following year, allowing us to capture a live-born calf in 2022. Of the live-born calves we captured, 39 were female and 42 were male with a sex ratio of 1:1.08 females to males. Mean age at capture, which was the average amount of time between VIT expulsion and capture, for all years was ~11.0 hours (range 1.9 – 43.7 hours). Across all years, the mean distance between newborn calves and the birth site or VIT was 34.97 m (range 0 – 1327.8 m). Mean search time, which we defined as the time between locating the VIT or female elk and locating the calf or ending our search if unsuccessful, was approximately 28 minutes (range 0 – 4.4 hours), and mean handling time was 24.1 minutes (range 15 – 36 minutes).

We recorded morphometrics for all live-born elk calves, except one which was found dead and never collared in 2022 (n = 80). We reported the means and ranges for total body length, neck circumference, chest girth, femur length, hind foot length, capture mass, and ponderal index, which is a calculated metric for body proportionality (body length (m)/mass (kg)³), by year and for all calves (Table 2.2). Based upon a significance threshold of $p < 0.05$, there were no significant differences between male and female calf morphometrics, except for neck circumference ($p =$

0.007; Table 2.3) where mean neck circumference was 26.2 cm (SE \pm 0.5) for male calves and 24.7 cm (SE \pm 0.3) for female calves. While we reported all morphometrics, only capture mass, femur length, and ponderal index were included in survival modeling due to high correlation ($\rho > 0.5$) between many of these measurements.

We collected blood and hair samples from all live-born elk calves, except one which was found dead and never collared in 2022. We reported the results of manual differentials for calves captured in all years with adequate blood samples and readable blood smears ($n = 74$) and hair cortisol concentrations for calves captured in 2020 and 2022 ($n = 22$; Table 2.4). We did not report hair cortisol concentrations for calves captured in 2022 because extraction results were not yet available and excluded them from our overall mean and range hair cortisol concentrations. There were no significant differences between continuous health metrics (% neutrophils, % eosinophils, % lymphocytes, and cortisol concentration; Table 2.4) by sex. Reactive lymphocytes were observed in all blood samples, but at difference concentrations, with a low concentration (< 5) observed per 100 white blood cells in 63 calves and a medium concentration (5 – 14) in 11 calves. Additionally, band or immature neutrophils were observed in 29 calves (Table 2.4). We used all health metrics in survival modeling, but only for the neonatal survival period because health metrics, including hematological values, can change very rapidly with growth and development (Mohri et al. 2007).

We monitored the survival of all live-born calves for up to one year or until mortality occurred. Herein, we only report the monitoring results, survival, and mortality probabilities for calves captured in 2020 and 2021 ($n = 46$) because survival monitoring had not yet been completed for calves captured in 2022. During the first two years of this study, we documented 20 total events including 14 mortalities (2020 = 4 and 2021 = 10) and 6 slipped collars or transmitter failures (2020 = 1 and 2021 = 5), which were right-censored because the calf's fate was unknown. We reported mortalities by survival period (Table 2.5) with the highest concentration of mortalities

occurring during the neonatal period (birth – 14 days) and most censor events occurring after the end of the summer survival period (September 11th). Despite not documenting any predation events in 2020, predation was the top proximate cause of mortality across all survival periods (Table 2.5). Coyotes were responsible for 57.1% of predation events (n = 4) and black bears (*Ursus americanus*) were responsible for 42.9% of predation events (n = 3). On average, calves killed by black bears were 6.7 days old (SE \pm 2.7, range 4 – 12 days) and calves killed by coyotes were 155.3 days old (SE \pm 49.2, range 59 – 243 days). We also documented consumption of elk calves by a bobcat (*Lynx rufus*, n = 1) and a black bear (n = 1), although the proximate cause of death was ultimately unknown. Additional causes of mortality included trauma (n = 2), hunter harvest (n = 1), bacterial pneumonia from an *Escherichia coli* (*E. coli*) infection (n = 1), emaciation or abandonment (n = 2), and unknown causes (n = 1).

For each survival period, we generated mean survival probability ranges from Kaplan-Meier survival estimates (Figure 2.4) and hazard ratios (hereafter HR) for influential factors using Cox proportional hazards models for both the traditional censor (TC) and the censor as dead (CD) data sets. At the end of the neonatal survival period, we estimated mean survival to range from 0.822 (SE \pm 0.057, 95% CI = 0.718 – 0.942) for the CD data set to 0.844 (SE \pm 0.054, 95% CI = 0.744 – 0.957) for the TC data set (Table 2.6). We considered all intrinsic and extrinsic factors of interest (Table 1) in the first state of model selection for this survival period and out of all the maternal, calf, and health characteristics considered in our CPH model selection process, the only factor that influenced neonatal calf survival was total precipitation during the first week of life (Table 2.7). This weather metric had a positive influence on survival, whereby for each additional centimeter of precipitation a calf experiences during its first week of life the chances of surviving increased 98.23% (HR 0.018) based on the TC data set and 98.59% (HR 0.014; Table 2.10) based on the CD data set. Maternal characteristics, calf characteristics, and health metrics such as

estimates for immune function obtained from manual differentials and hair cortisol did not appear to influence neonatal survival in calves captured in 2020 and 2021.

Mean survival estimates for the summer survival period ranged from 0.730 (SE \pm 0.067, 95% CI = 0.610 – 0.873) for the CD data set to 0.772 (SE \pm 0.064, 95% CI = 0.657 – 0.907) for the TC data set (Table 2.6). We considered all intrinsic and extrinsic variables of interest except the manual differential results because they can change very rapidly and are likely not representative of calf health later in the summer. CPH model selection for this survival period revealed that the total precipitation experienced during the first week of life and femur length positively influenced summer survival probabilities (Table 2.8). Using the TC data set, we found that each additional centimeter of precipitation during the first week of life increased the chances an elk calf survival by 86.8% (HR 0.132) and each additional centimeter of femur length increased the chances of survival by 64.3% (HR 0.3571). The magnitude of these influences increased slightly when based on the CD data set, such that the chances of survival for each calf increased to 90.0% for each additional centimeter of precipitation (HR 0.100) and to 68.3% (HR 0.3171; Table 2.10) per unit increase of femur length. Summer calf survival did not appear to be influenced hunt unit, maternal characteristics, other calf characteristics (i.e. sex, birthdate, and body mass), or average minimum temperature during the first week of life.

Finally, we estimated mean annual survival probability ranges from 0.556 (SE \pm 0.074, 95% CI = 0.428 – 0.721) for the CD data set to 0.681 (SE \pm 0.071, 95% CI = 0.556 – 0.834) for the TC data set (Table 2.6). We did not consider any weather or manual differential results in our investigation into factors influencing annual calf survival because of the extended duration of this survival period and the likelihood that early influences would be diluted by the conclusion of monitoring. We did investigate the influence of hunt unit, mid-winter maternal characteristics and other select calf characteristics but only femur length was shown to influence annual calf survival probabilities (Table 2.9). Based on data from calves captured in 2020 and 2021, femur length had

a positive influence on survival, whereby for each additional centimeter of precipitation a calf experiences during its first week of life the chances of surviving increased 77.2% (HR 0.228) based on the TC data set and 72.8% (HR 0.272; Table 2.10) based on the CD data set. Finally, we assessed the CPH assumption of proportional hazards for each variable the top model in all final model sets for each survival period using chi-square significance tests, finding that all models upheld this assumption (Table 2.10).

We also generated probabilities for specific categories of mortality for each survival period using CIFs, allowing us to identify the sources of mortality that are most likely to occur. Out of the seven categories of mortality causes we observed, predation (which includes both predation and suspected predation events) had the highest probability of occurring across all survival periods: 6.7% for the neonatal period, 11.4% for the summer period, and 16.0% during the first year of life (Table 2.11). We did not document any mortalities due to disease during the neonatal and summer survival periods (Table 2.5), nor any hunter harvested individuals because both survival periods ended prior to the state of hunting season. We did document mortalities due to trauma (1 calf appeared to have been stepped on and 1 calf also had a congenital vertebral malformation; Williams et al. 2023) and emaciation or abandonment ($n = 2$), resulting in annual mortality probabilities of 2.2% for mortality due to trauma and 4.4% for mortality due to abandonment (Table 2.11). However, both calves that died due to abandonment were small and either the first-born or last-born calf of their respective calving seasons, thus this mortality probability is most likely to affect the chances survival for calves born outside of peak calving season (Figure 2.3). We did not calculate cause-specific mortality probabilities by sex because of limited sample size and minimal differentiation between the number of male calf mortalities ($n = 8$) and female calf mortalities ($n = 6$).

2.5 Discussion

Population metrics, particularly those used to estimate population size, can be highly variable and are easily influenced by a variety of intrinsic and extrinsic factors. Consequently, estimates of age class-specific metrics, such as neonate survival, are a critical part of the routine long-term monitoring necessary for adaptive management of free-ranging ungulates. Furthermore, it is important to capture and monitor a statistically robust number of neonates at an appropriate geographic scale, to ensure that these survival estimates are as accurate and representative of the current population as possible (Rice 2016, Engebretsen et al. 2023). This can be difficult to accomplish, especially for Kentucky's elk population, which is spread across a 16-county area with portions of rugged terrain. Our use of paired vaginal implant transmitters greatly improved our ability to locate neonatal elk earlier and with less manpower compared to previous studies in Kentucky where calves were captured (Seward 2003, Bowling 2009). We were also able to gather information about fetal survival and early reproductive success (Hooven et al. 2022), including an aborted fetus and a stillbirth, which have not previously been documented in Kentucky.

By using paired expandable VHF calf collars, we optimized our post-parturition monitoring, allowing us to document mortalities as soon as possible to increase our chances of determining cause specific mortality, especially when calves were less mobile and generally in closer proximity to its mother (Rice 2016). However, as calf mobility increased and calves stray out of UHF range, remote monitoring became more difficult. Despite this, we were able to document 14 elk calf mortalities in first two years of this study and determine a proximate cause of death in ~93% of mortality investigations (13/14 mortalities). Consequently, we have documented new causes of mortality compared to previous elk calf survival studies in Kentucky including predation by black bears ($n = 3$), a bacterial infection caused by *E. coli*, and emaciation or abandonment ($n = 2$), one of which was born to a cow with a confirmed aberrant meningeal worm infection. We were also able to discern patterns in predation and scavenging, with mortality risk

from black bear and possibly bobcats occurring earlier during the neonatal period and mortality risk from coyotes occurring later in life when calves are more mobile.

Our mean annual elk calf survival range ($0.556 \pm \text{SE } 0.074$ to $0.681 \pm \text{SE } 0.071$) was higher than those reported for established elk populations in the west (Eacker et al. 2016, Tatman et al. 2018) but lower than most calf survival rates reported for other reintroduced elk populations in the eastern United States (Bender et al. 2002, DeVivo et al. 2011). The difference between western elk calf survival can be attributed to differences in predator communities, human population densities, and Kentucky's milder climate, especially as relates to winter severity which can be a major mortality source in for western populations (Keller et al. 2015); however, these factors tend to be similar between eastern states and do not explain the differences between eastern elk calf survival rates, suggesting that variation in other factors such as habitat change or availability, nutritional status, or disease could be contributing factors. Additionally, our hypothesis that current elk calf survival rates would be lower than previously reported in Kentucky was supported, as our observed (TC) and worst-case (CD) survival estimates were both lower than the mean annual survival rate of $0.766 (\pm \text{SE } 0.103)$ reported in a previous calf survival study (Seward 2003). This is likely due to our more successful use of VITs to locate known age calves, thus reducing bias from left-truncation and unreliable age estimation (Gilbert et al. 2014, Grovenburg et al. 2014) but could also be attributed to a variety of other factors including changes in habitat succession from decreased coal mining in southeastern Kentucky, nutrition, changes in predator abundance and utilization of elk calves as a food resource, and/or unknown health or disease impacts.

The effects of maternal nutrition and experience, parturition date, calf morphometrics, and weather conditions on juvenile ungulate survival are well documented (Baxter et al. 2008, Tatman et al. 2018, Dion et al. 2020). Nevertheless, we found that elk calf survival across all survival periods in Kentucky appears to only be influenced by a limited number of factors: femur length

and total precipitation during the first week of life. Increases in femur length, which is a representative metric of body size, increased the chances survival during the summer and annual survival periods by 64.3 – 68.3% and 72.8 – 77.2%, respectively. While this does meet our expectations that body size would positively influence survival, we had originally expected body mass and not femur length to be the most influential morphometric. We were also surprised by the influence of weather conditions, which positively influenced the chances of a calf surviving during the neonatal and summer survival periods, because we expected weather conditions associated with hypothermia, such as precipitation and/or average minimum daily ambient temperature to negatively influence survival (Mercer et al. 1979). However, since each additional centimeter of precipitation due the first week of life seemed to improve the chances of survival (neonatal = 98.2 – 98.6% increase, summer = 86.8 – 90.0% increase), it is possible that this variable may actually represent the benefits of additional precipitation in the growing season on vegetation quantity or quality, which could impact maternal nutrition in the critical period that follows parturition. Mid-winter maternal characteristics and calf health metrics did not have any influence on survival, possibly indicating that female elk and their newborn calves are generally good enough nutritional condition to give birth to calves that are health and not immune-compromised or chronically stressed.

Because we only used survival data from two of the three years in this study was conducted, inference from this survival analysis is limited and likely to change with the addition of data from elk calves captured in 2022. However, since calves were captured in more discrete clusters across the eastern and central parts of the Elk Restoration Zone, data from these years could be used to determine if survival or mortality risks differ between more localized groups of elk in different parts of the zone. We also documented temporal and geographic differences in mortality risks for elk calves, suggesting that predation may be more of a risk for elk calves in the central part of the Elk Restoration Zone, but we can't definitively say this without more

information about predator presence, distribution, and expansion throughout southeastern Kentucky. Additionally, through the analysis of three overlapping survival periods, we posit that the first two weeks of life are a critical survival period and thus any management actions taken to improve calf survival in Kentucky should be planned accordingly to produce the most benefits during this time period for the highest impact.

Table 2.1. Covariates considered in Cox proportional hazard models to evaluate which factors influence neonatal, summer, and annual elk calf survival in 2020 - 2021.

Category	Variable (units)	Abbrev.	Survival Period
COW	Age (category)	Age_cat	N, S, A
	Mid-Winter Body Condition Score	MW_BCS	N, S, A
	Mid-Winter Body Mass (kg)	MW_mass	N, S, A
CALF	Sex	Sex	N, S, A
	Birth Date (julian date)	Birth_date	N, S, A
	Capture Mass (kg)	Cap_mass	N, S, A
	Calf Ponderal Index (mass/body length ³)	Calf_PI	N, S, A
	Femur Length (cm)	Femur	N, S, A
	Neutrophils (%)	Neutro	N
	Eosinophils (%)	Eosin	N
	Lymphocytes (%)	Lympho	N
	Reactive Lymphocytes (present or absent)	Rxn_Lympho	N
	Band Neutrophils (present or absent)	B_Neutro	N
	Hair Cortisol (pg/mg)	Cortisol	N, S, A
WEATHER	Total Precipitation in First Week (cm)	Nprecip	N, S
	Avg Min. Temperature in Wk 1 (°C)	Navg_mintemp	N, S
	Avg Daily Solar Radiation in Wk 1 (MJ/m ²)	Navg_solar	N, S

Table 2.1 (continued)

These predictor variables were considered in the Cox proportional hazards models to determine what factors influence the survival of elk calves captured in 2020 – 2021 in southeastern Kentucky. Survival period denotes which period, and thus which model sets, each variable was used: neonatal (N; birth – 14 days), summer (S; birth – September 11th), and/or annual (A; birth – 1 year of age).

Table 2.2. Summary of morphometrics of elk calves captured across southeastern Kentucky during 2020 - 2022.

Morphometric	2020	2021	2022	All Years
Body Mass (kg)	16.1 (6.3 – 20.0)	14.4 (7.2 – 17.6)	15.3 (7.0 – 20.0)	15.2 (6.3 – 20.0)
Total Body Length (cm)	101.6 (79.1 – 112.0)	97.5 (77.0 – 112.0)	98.8 (71.0 – 112.0)	99.1 (71.0 – 112.0)
Chest Girth (cm)	59.3 (43.6 – 65.0)	55.8 (42.5 – 63.5)	56.0 (42.0 – 63.5)	56.8 (42.0 – 65.0)
Hind Foot Length (cm)	41.7 (34.5 – 44.0)	40.8 (33.0 – 44.0)	40.4 (34.0 – 44.0)	40.9 (33.0 – 44.0)
Femur Length (cm)	21.5 (15.0 – 32.0)	20.2 (14.0 – 30.5)	18.9 (15.5 – 23.0)	20.0 (14.0 – 32.0)
Neck Circumference (cm)	26.3 (18.4 – 31.6)	25.1 (21.0 – 29.8)	25.2 (15.5 – 30.5)	25.5 (15.5 – 31.6)
Incisor (cm)	2.77 (0.76 – 7.76)	0.26 (0.43 – 6.28)	2.83 (0.82 – 4.78)	2.04 (0.09 – 7.76)
Hoof Growth (cm)	4.39 (2.18 – 6.46)	0.41 (0.25 – 0.64)	3.97 (1.80 – 6.70)	3.01 (0.25 – 6.70)
Calf Ponderal Index	15.3 (10.7 – 20.0)	15.7 (11.9 – 27.6)	15.8 (13.0 – 21.0)	15.6 (10.7 – 27.6)

Summary (mean and range) of elk calf morphometrics and calculated body proportionality from across the Elk Restoration Zone (KERZ) in southeastern Kentucky (n = 80; 2020 = 21, 2021 = 24, and 2022 = 35). These measurements were collected from each elk calf during capture and include total body length (curvilinear measurement from tip of nose to base of tail), chest girth, neck circumference, femur length, hind foot length (from tip of hoof to end of calcaneus), first incisor (amount of I1 incisor erupted from gums), new hoof growth, and body mass at capture (Johnson 1951). Calf body proportionality was determined by calculating the ponderal index (body mass (kg)/ total body length (m)³).

Table 2.3. Comparison of elk calf morphometrics and health metrics by sex using Welch’s t-test.

Metric	Males (Mean ± SE)	Females (Mean ± SE)	t	df	p-value
Total Body Length (cm)	99.0 (± 1.4)	99.3 (± 0.8)	-0.144	63.09	0.886
Neck Circumference (cm)	26.2 (± 0.5)	24.7 (± 0.3)	2.791	65.73	0.007*
Chest Girth (cm)	57.0 (± 0.8)	56.6 (± 0.6)	0.476	70.66	0.635
Femur Length (cm)	19.7 (± 0.4)	20.2 (± 0.5)	-0.797	71.61	0.428
Hind Foot Length (cm)	41.0 (± 0.4)	40.8 (± 0.3)	0.401	69.40	0.690
Body Mass (kg)	15.66 (± 0.51)	14.78 (± 0.31)	1.475	65.36	0.145
% Neutrophils	80.58 (± 1.38)	77.42 (± 1.44)	1.580	71.6	0.119
% Eosinophils	0.52 (± 0.14)	1.53 (± 0.60)	-1.613	38.73	0.115
% Lymphocytes	16.74 (± 1.21)	18.08 (± 1.23)	-0.781	71.87	0.437
Hair Cortisol (pg/mg)	2.43 (± 0.13)	2.15 (± 0.13)	1.560	51.97	0.125

The results (test statistic, degrees of freedom, and p-value) of comparing the morphometrics and health metrics for neonatal elk calves in southeastern Kentucky captured in 2020 – 2022 by sex with significance determined by a threshold of $p < 0.05$ (*). We found no significant differences for any metric between male and female calves except for neck circumference, where male calves had larger mean circumferences than females.

Table 2.4. Neonatal elk health metrics from biological samples collected during calf captures in 2020 – 2022 in southeastern Kentucky.

Health Metric	2020	2021	2022	All Years
Neutrophils (%)	77.39 (61.00 – 91.00)	83.55 (73.00 – 93.00)	77.00 (54.00 – 92.00)	79.04 (54.00 – 93.00)
Eosinophils (%)	2.78 (0 – 18.00)	0.14 (0 – 1.00)	0.65 (0 – 36.00)	1.01 (0 – 18.00)
Lymphocytes (%)	18.28 (6.00 – 35.00)	13.69 (5.00 – 21.00)	19.38 (7.00 – 36.00)	17.39 (5.00 – 36.00)
Reactive Lymphocytes (n)				
Low	14	21	28	63
Medium	4	1	6	11
Band Neutrophils (n)				
Yes	9	8	12	29
No	9	14	22	45
Hair Cortisol (pg/mg)	2.28 (1.19 – 4.01)	2.45 (1.00 – 4.03)		2.37 (1.00 – 4.03)

Summary (mean and range or number of individuals) of elk calf health data from across the Elk Restoration Zone (KERZ) in southeastern Kentucky. This health data consists of whole blood analysis obtained from manual differentials of blood smears (n = 74; 2020 = 18, 2021 = 22, and 2022 = 34) and hair cortisol (n = 42; 2020 = 21 and 2021 = 21). Hair cortisol concentrations in calves captured in 2022 were not included because not all extractions have been completed. Whole blood analysis values include the percentage of neutrophils, eosinophils, and lymphocytes as well as the presence of reactive lymphocytes and band or immature neutrophils. Hair cortisol was extracted from hair shaved each elk calf’s neck prior to blood collection.

Table 2.5. Causes of elk calf mortality in southeastern Kentucky in 2020 and 2021.

Cause of Death	Neonatal	Summer	Annual
Disease	0	0	1
Harvest	0	0	1
Emaciation/Abandonment	2	2	2
Predation	3	5	7
Trauma	2	2	2
Unknown (died)	0	1	1
Unknown (censored)	1	2	6
TOTAL	8	12	20

Fates observed during the neonatal (birth – 14 days), summer (birth – start of elk archery season on September 11), and annual (birth – 1 year old) survival periods for elk calves captured and monitored during 2020 – 2021 across the Elk Restoration Zone (KERZ) in southeastern Kentucky. The survival periods overlap, this mortality counts within each period are cumulative (i.e. summer mortalities are equal to the number of mortalities in each respective category that occurred during the neonatal period plus those that occurred between 15 days and the start of archery season). Fates of elk calves captured in 2022 were not included for any survival period because monitoring has not yet been completed.

Table 2.6. Neonatal, summer, and annual survival estimates using the Kaplan-Meier estimator for elk calves captured in 2020 – 2021 in Kentucky.

Survival Period	Year	Traditional Censor			Censor as Dead		
		n _{events}	Survival Probability (\pm SE)	95% CI	n _{events}	Survival Probability (\pm SE)	95% CI
Neonatal	2020	2	0.905 (\pm 0.064)	0.788 - 1.000	2	0.905 (\pm 0.064)	0.788 - 1.000
	2021	5	0.789 (\pm 0.084)	0.641 - 0.972	6	0.750 (\pm 0.088)	0.595 - 0.945
	Combined	7	0.844 (\pm 0.054)	0.744 - 0.957	8	0.822 (\pm 0.057)	0.718 - 0.942
Summer	2020	2	0.905 (\pm 0.064)	0.788 - 1.000	2	0.905 (\pm 0.788)	0.788 - 1.000
	2021	8	0.645 (\pm 0.102)	0.473 - 0.880	10	0.572 (\pm 0.103)	0.402 - 0.815
	Combined	10	0.772 (\pm 0.064)	0.657 - 0.907	12	0.730 (\pm 0.067)	0.610 - 0.873
Annual	2020	4	0.810 (\pm 0.086)	0.658 - 0.996	5	0.762 (\pm 0.093)	0.600 - 0.968
	2021	10	0.561 (\pm 0.105)	0.389 - 0.810	15	0.375 (\pm 0.099)	0.224 - 0.629
	Combined	14	0.681 (\pm 0.071)	0.556 - 0.834	20	0.556 (\pm 0.074)	0.428 - 0.721

74

Kaplan-Meier estimate, standard errors, and ranges for elk calves captured in 2020 and 2021 in southeastern Kentucky during three survival time periods: neonatal (birth – 14 days), summer (birth – start of elk archery season on September 11th), and annual (birth – 1 year of age). The “traditional censor” data set treats censored individuals as an unknown fate but does not impact the actual survival rate, while the “censor as dead” data set treats censored individuals as a mortality to model the worst-case scenario. Elk calves captured in 2022 were not included in this analysis because monitoring has not yet been completed.

Table 2.7. Model selection for stratified Cox proportional hazards models explaining factors influencing neonatal elk calf survival in Kentucky.

Data Set	Model	K	AICc	Δ AICc	AICcWt
Traditional Censor	Femur + Nprecip*	2	22.40	0.00	0.57
	Nprecip	1	24.28	1.87	0.22
	Cap_mass + Nprecip*	2	24.47	2.07	0.20
Censor as Dead	Femur + Nprecip*	2	22.70	0.00	0.56
	Nprecip	1	24.46	1.76	0.23
	Cap_mass + Nprecip*	2	24.71	2.01	0.21

Top Cox proportional hazards models used to determine what intrinsic and/or extrinsic factors influence neonatal survival (birth – 14 days) in elk calves captured in 2020 – 2021 in southeastern Kentucky. Elk calves captured in 2022 were not included in this analysis because monitoring has not yet been completed. We used Akaike’s Information Criterion corrected for small samples sizes to rank models, report only those $< 7 \Delta$ AICc from the top model and denote models with uninformative parameters (*).

Table 2.8. Model selection for stratified Cox proportional hazards models explaining factors influencing summer elk calf survival in Kentucky.

Data Set	Model	K	AICc	Δ AICc	AICcWt
Traditional Censor	Femur + Nprecip	2	41.48	0.00	0.66
	Cap_mass + Nprecip*	2	43.78	2.31	0.21
	Nprecip	1	44.70	3.23	0.13
Censor as Dead	Femur + Nprecip	2	44.40	0.00	0.77
	Cap_mass + Nprecip	2	47.27	2.86	0.18
	Nprecip	1	49.91	5.51	0.05

Top Cox proportional hazards models used to determine what intrinsic and/or extrinsic factors influence summer survival (birth – September 11th) in elk calves captured in 2020 – 2021 in southeastern Kentucky. Elk calves captured in 2022 were not included in this analysis because monitoring has not yet been completed. We used Akaike’s Information Criterion corrected for small samples sizes to rank models and note models with uninformative parameters (*).

Table 2.9. Model selection for stratified Cox proportional hazards models explaining factors influencing annual elk calf survival in Kentucky.

Data Set	Model	K	AICc	Δ AICc	AICcWt
Traditional Censor	Femur	1	72.18	0.00	0.64
	Cap_mass* + Femur	2	73.50	1.32	0.33
	Cap_mass	1	78.25	6.07	0.03
Censor as Dead	Cap_mass* + Femur	2	101.10	0.00	0.54
	Femur	1	101.56	0.47	0.43
	Cap_mass	1	107.14	6.05	0.03

Top Cox proportional hazards models used to determine what intrinsic and/or extrinsic factors influence annual survival (birth – 1 year of age) in elk calves captured in 2020 – 2021 in southeastern Kentucky. Elk calves captured in 2022 were not included in this analysis because monitoring has not yet been completed. We used Akaike’s Information Criterion corrected for small samples sizes to rank models, report only those $< 7 \Delta$ AICc from the top model and denote models with uninformative parameters (*).

Table 2.10. Hazard ratios from the top stratified Cox proportional hazards model for the neonatal, summer, and annual survival periods in Kentucky using calf survival data from 2020 – 2021.

Data Set	Survival Period	Variable	Model Output			Schoenfeld Residuals	
			Beta (\pm SE)	Hazard Ratio	95% CI	Chi Square	P-value
Traditional Censor	Neonatal	Nprecip	-4.032 (1.734)	0.018	0.001 - 0.531	2.810	0.094
	Summer	Femur	-1.030 (0.482)	0.357	0.139 - 0.918	0.367	0.540
		Nprecip	-2.026 (0.721)	0.132	0.032 - 0.541	1.995	0.160
	Annual	Femur	-1.479 (0.510)	0.228	0.084 - 0.618	0.222	0.640
Censor as Dead	Neonatal	Nprecip	-4.260 (1.670)	0.014	0.001 - 0.373	2.850	0.091
	Summer	Femur	-1.148 (0.463)	0.317	0.128 - 0.786	0.015	0.900
		Nprecip	-2.301 (0.706)	0.100	0.025 - 0.399	1.834	0.180
	Annual	Femur	-1.302 (0.417)	0.272	0.120 - 0.616	1.310	0.250

Regression coefficients and hazard ratios generated by the top cox proportional hazards model for each 2020 – 2021 data set for the neonatal survival period (0 – 14 days), summer survival period (0 ~ 118 days), and annual survival period (0 – 365 days) and the associated 95% confidence intervals. These ratios indicate how the influencing variable of interest or hazard is different from an unspecific baseline hazard rate and how that particular hazard affects the chances of survival. A hazard ratio >1 negatively influences survival, while a hazard ratio <1 positively influences survival and a hazard ratio of 1 has no effect.

Table 2.11. Estimated cause-specific mortality probabilities for elk calves in Kentucky for the neonatal, summer, and annual survival periods using calf survival data from 2020 – 2021.

Cause of Death	Neonatal	Summer	Annual
Disease	0	0	0.023 (0.002 - 0.108)
Harvest	0	0	0.023 (0.002 - 0.109)
Emaciation/Abandonment	0.022 (0.002 - 0.103)	0.022 (0.002 - 0.103)	0.022 (0.002 - 0.103)
Predation	0.067 (0.017 - 0.167)	0.114 (0.041 - 0.227)	0.160 (0.070 - 0.285)
Trauma	0.044 (0.008 - 0.135)	0.044 (0.008 - 0.135)	0.044 (0.008 - 0.135)
Unknown	0.022 (0.002 - 0.103)	0.045 (0.008 - 0.136)	0.045 (0.008 - 0.136)

79

These probabilities were calculated using the cumulative incidence function for the neonatal survival period (0 – 14 days), summer survival period (0 ~ 118 days), and annual survival period (0 – 365 days) and the associated 95% confidence intervals. The top cause of mortality for all three survival periods using calf survival data from 2020 – 2021 is predation, followed by trauma and unknown causes. Elk calves captured in 2022 were not included in this analysis because monitoring has not yet been completed.

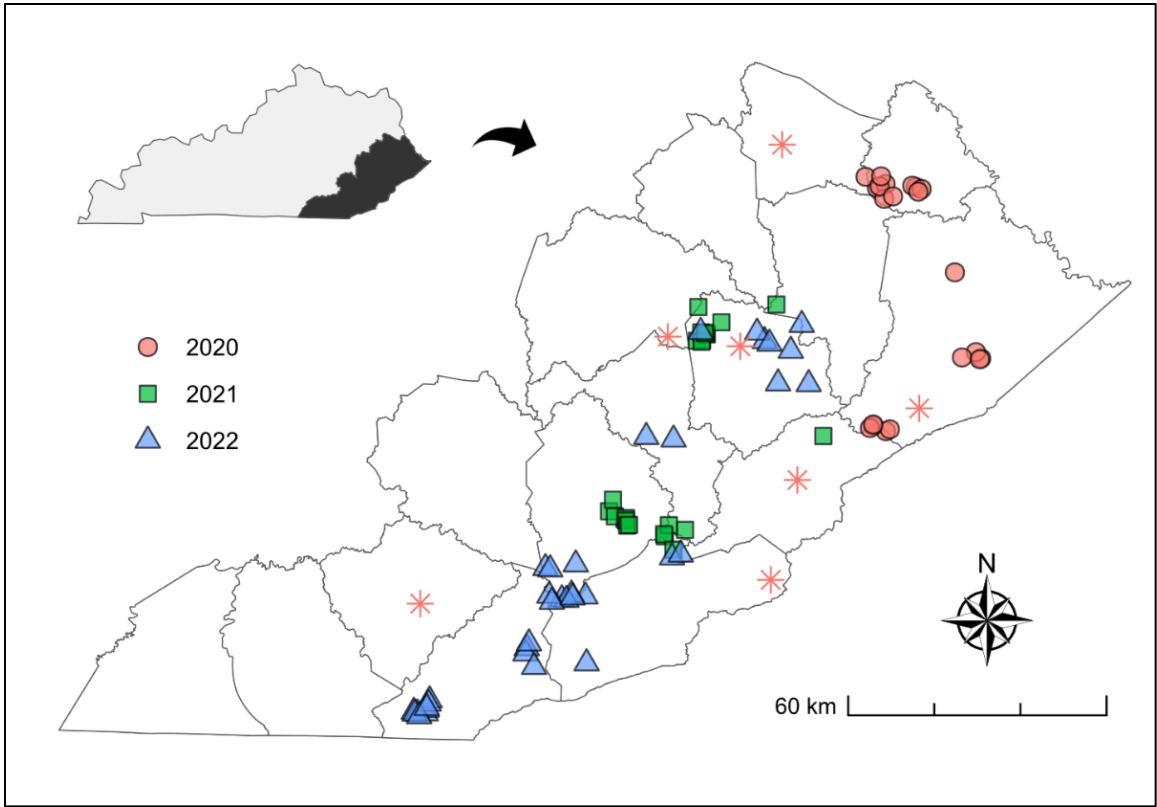


Figure 2.1. Study area comprised of 16 counties in southeastern Kentucky and elk calf capture locations by year. Locations of calf captures by year across the sixteen-county Elk Restoration Zone (KERZ) in southeastern Kentucky, with filled shapes representing calf captures by year and red stars representing Kentucky Mesonet weather stations.

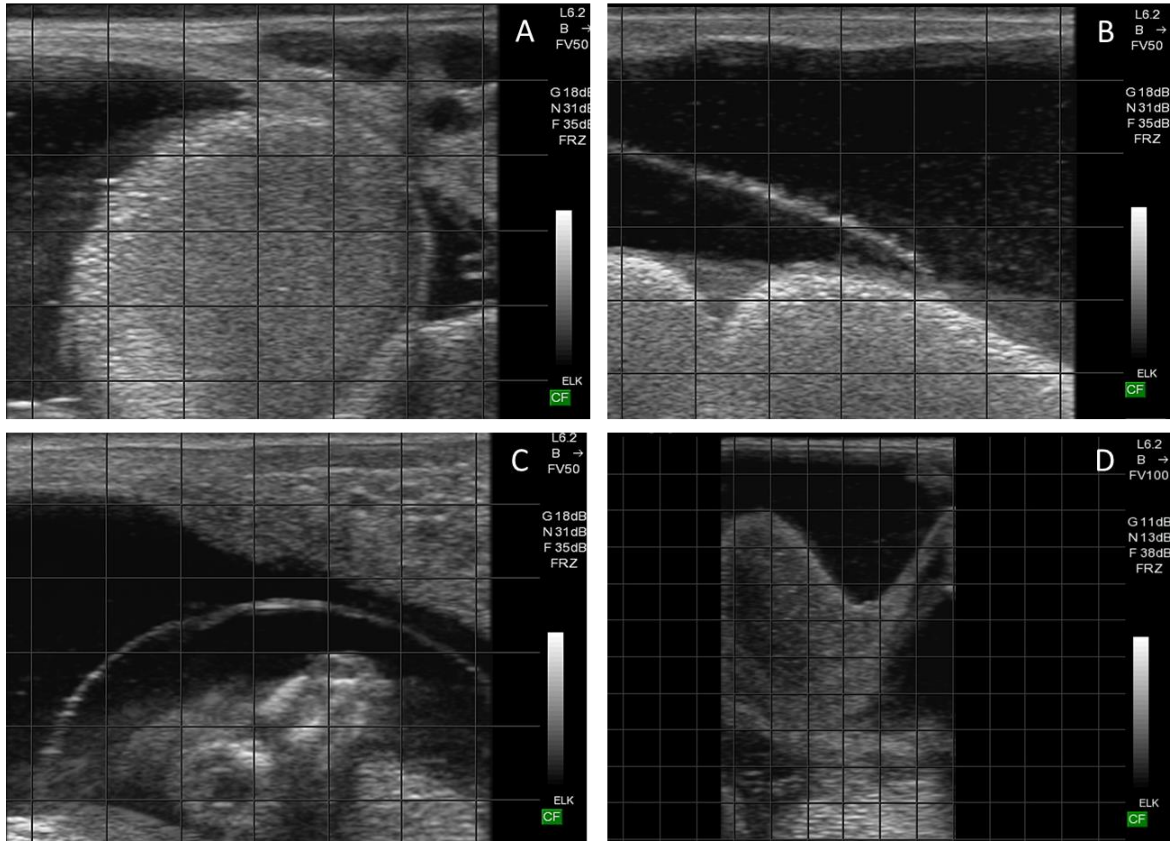


Figure 2.2. Ultrasonogram examples of confirmed-pregnant elk in Kentucky. Each panel shows evidence of pregnancy in chemically immobilized female elk in southeastern Kentucky. All ultrasonograms were captured in B-mode and show a large pocket of amniotic fluid, which is non-echogenic so it appears very dark, and the uterine wall. We also looked for placentomes (A, B), the umbilical cord (B), and visible fetuses (C, D).

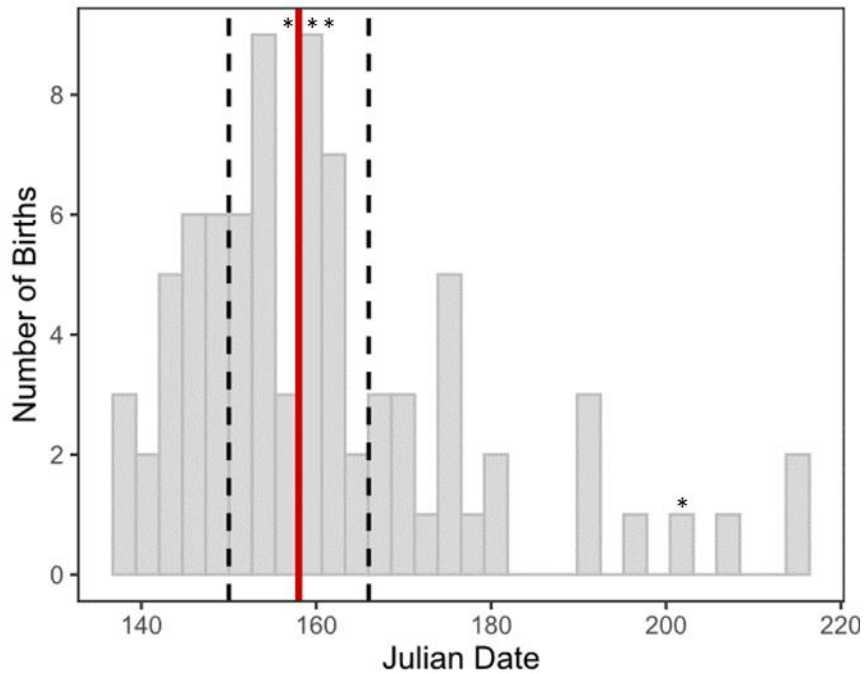


Figure 2.3. Elk calf parturition season based on calf captures during 2020 – 2021 in southeastern Kentucky. All birth dates based on vaginal implant expulsion for elk calves captured across the Elk restoration Zone in southeastern Kentucky during 2020 – 2022. The red dash line indicates the median birth date of June 7th (JD 158) and the black dashed lines indicate peak calving from May 30th to June 15th (JD 150 – 166). The stars (*) denote parturition times for yearling female elk that received VITs (JD 157, 161, 162, and 203).

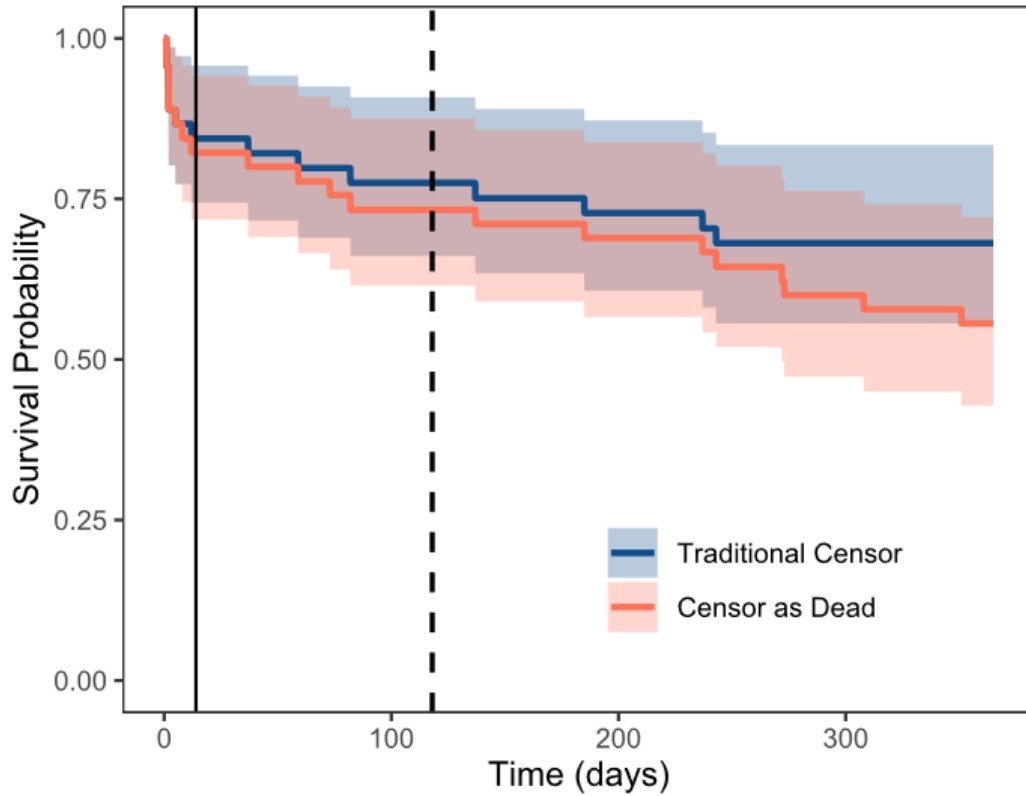


Figure 2.4. Estimated annual survival for elk calves Kentucky during 2020 – 2021 using the Kaplan-Meier estimator. The blue line and shaded area represent elk calf survival estimated from the traditional censor (TC) model, where censoring is treated as an unknown fate. The red line and shaded area represent elk calf survival estimated from the Censor as Dead (CD) model, where censoring is treated as a mortality event and used to model the “worst-case” estimated for survival. The solid line represents the neonatal survival period cutoff (14 days of life) and the dashed line represents the summer survival cutoff (first day of elk archery season at ~118 days of life).

APPENDIX 1. SUPPLEMENTAL MATERIALS FOR THE BAM VERSUS NALMED-A CHEMICAL IMMOBILIZATION ANALYSIS

Table S1.1. Model output models showing influences induction times for both BAM and NalMed-A. This includes the coefficients, Standard error, and p-values) for all model parameters from the linear models for induction time (minutes), which is the time from full sedation until the antagonists were administered). We used a threshold of $p < 0.05$ (*) to show significance.

Hypothesis	Model	β	SE	p-value
CAPTURE	Helicopter Transport Distance			
	(Intercept)	2.104	0.057	0.000
	Transp_Dist	-0.019	0.058	0.741
	Immobil_Drug	0.004	0.073	0.952
	Transp_Dist * Immobil_Drug	0.019	0.074	0.799
ANIMAL	Age Class			
	(Intercept)	2.101	0.056	0.000
	Age	0.002	0.160	0.990
	Immobil_Drug	-0.004	0.069	0.954
	Age * Immobil_Drug	-0.213	0.204	0.297
	Body Mass			
	(Intercept)	2.107	0.054	0.000
	Mass	-0.026	0.048	0.582
	Immobil_Drug	-0.030	0.067	0.649
	Mass * Immobil_drug	0.039	0.064	0.539
	Observed hemorrhage			
	(Intercept)	2.083	0.055	0.000
	Hem_Obs	0.188	0.177	0.290
	Immobil_Drug	-0.022	0.068	0.753
	Hem_Obs * Immobil_Drug	-0.051	0.217	0.815
	First Temperature Taken			
(Intercept)	2.103	0.054	0.000	
1Temp	0.009	0.053	0.866	
Immobil_Drug	-0.027	0.067	0.683	
1Temp * Immobil_Drug	-0.014	0.066	0.836	
WEATHER	Average Daily Temperature			
	(Intercept)	2.054	0.050	0.000
	Avg_Temp	-0.212	0.046	0.000
	Immobil_Drug	0.018	0.061	0.771
	Avg_Temp * Immobil_drug	0.242	0.060	0.000

Table S1.1. (continued)

Hypothesis	Model	β	SE	p-value
WEATHER (cont).	Average Daily Wind Speed			
	(Intercept)	2.102	0.053	0.000
	Wind	-0.029	0.043	0.501
	Immob_Drug	-0.027	0.065	0.677
	Wind * Immob_Drug	-0.032	0.062	0.608
	Average Daily Solar Radiation			
	(Intercept)	2.097	0.056	0.000
	Solar	-0.012	0.050	0.802
	Immob_Drug	-0.023	0.068	0.740
	Solar * Immob_Drug	0.019	0.066	0.773

Table S2.2. Parameter estimates showing the influence of capture, animal, and weather characteristics on the reversal times of BAM and NalMed-A. This includes the coefficients, standard error, and p-values for all model parameters from the linear models for reversal time (minutes), which is the time from antagonist administration until each female elk walked away). We used a threshold of $p < 0.05$ (*) to show significance.

Hypothesis	Model	β	SE	p-value	
CAPTURE	Workup Duration				
	(Intercept)	1.268	0.119	0.000	
	Workup	0.128	0.094	0.178	
	Immob_Drug	-0.119	0.147	0.418	
	Workup * Immob_Drug	0.007	0.141	0.958	
	Supplemental Oxygen				
	(Intercept)	1.079	0.270	0.000	
	Supp_O2	0.240	0.301	0.428	
	Immob_Drug	-0.159	0.349	0.649	
	Supp_O2 * Immob_drug	0.029	0.385	0.940	
	THERAPEUTICS	Penicillin			
		(Intercept)	1.249	0.128	0.000
Pen		0.188	0.366	0.608	
Immob_Drug		-0.070	0.157	0.658	
Pen * Immob_Drug		-0.501	0.464	0.283	
Banamine					
(Intercept)		1.244	0.147	0.000	
Bana		0.075	0.243	0.757	
Immob_Drug		0.065	0.180	0.718	
Bana * Immob_Drug		-0.545	0.301	0.073	
Lidocaine					
(Intercept)		0.978	0.220	0.000	
Lido		0.416	0.262	0.114	
Immob_Drug		0.105	0.287	0.714	
Lido * Immob_Drug		-0.334	0.335	0.320	
ANIMAL		Age Class			
		(Intercept)	1.291	0.128	0.000
		Age	-0.159	0.366	0.665
	Immob_Drug	-0.112	0.157	0.478	
	Age * Immob_Drug	-0.154	0.464	0.740	
	Body Mass				
(Intercept)	1.321	0.116	0.000		

Table S1.2. (continued)

Hypothesis	Model	β	SE	p-value	
ANIMAL (cont.)	Mass	-0.209	0.102	0.042	
	Immob_Drug	-0.210	0.143	0.143	
	Mass * Immob_Drug	-0.083	0.137	0.545	
	Observed Hemorrhage				
	(Intercept)	1.248	0.125	0.000	
	Hem_Obs	0.248	0.402	0.539	
	Immob_Drug	-0.142	0.155	0.362	
	Hem_Obs * Immob_Drug	0.157	0.492	0.751	
	First Temperature Taken				
	(Intercept)	1.276	0.123	0.000	
	1Temp	0.019	0.119	0.874	
	Immob_Drug	-0.130	0.152	0.393	
	1Temp * Immob_Drug	-0.012	0.149	0.934	
	WEATHER	Average Daily Temperature			
(Intercept)		1.282	0.121	0.000	
Avg_Temp		0.044	0.113	0.697	
Immob_Drug		-0.153	0.149	0.307	
Avg_Temp * Immob_Drug		0.113	0.145	0.437	
Average Daily Wind Speed					
(Intercept)		1.274	0.120	0.000	
Wind		-0.114	0.097	0.243	
Immob_Drug		-0.128	0.148	0.389	
Wind * Immob_Drug		0.056	0.141	0.693	
Average Daily Solar Radiation					
(Intercept)		1.265	0.127	0.000	
Solar		-0.019	0.113	0.869	
Immob_Drug		-0.126	0.155	0.419	
Solar * Immob_Drug	0.058	0.148	0.695		

Table S1.3. Model output (coefficients, standard error, and p-values) for all model parameters from the generalized linear models for pre-induction heart rate (beats/minute) with elk id as a mixed effect. We used a threshold of $p < 0.05$ (*) to show significance.

Hypothesis	Model	β	SE	p-value	
CAPTURE	Helicopter Transport Distance				
		(Intercept)	4.062	0.035	0.000
		Monitor_Min	-0.022	0.027	0.416
		Transp_Dist	0.004	0.033	0.910
		Immob_Drug	0.175	0.044	0.000
		Monitor_Min * Transp_Dist	0.039	0.025	0.109
		Monitor_Min * Immob_Drug	0.001	0.038	0.969
		Transp_Dist * Immob_Drug	0.002	0.042	0.969
	Monitor_Min * Transp_Dist * Immob_Drug	-0.059	0.035	0.094	
ANIMAL	Age Class				
		(Intercept)	4.083	0.037	0.000
		Monitor_Min	-0.022	0.030	0.456
		Age	0.002	0.091	0.986
		Immob_Drug	0.134	0.046	0.003
		Monitor_Min * Age	-0.048	0.064	0.459
		Monitor_Min * Immob_Drug	0.013	0.039	0.734
		Age * Immob_Drug	0.151	0.147	0.306
		Monitor_Min * Age * Immob_Drug	-0.099	0.167	0.554
		Body Mass			
		(Intercept)	4.081	0.034	0.000
		Monitor_Min	-0.031	0.027	0.242
		Mass	0.020	0.029	0.496
		Immob_Drug	0.140	0.042	0.001
		Monitor_Min * Mass	0.001	0.022	0.977
		Monitor_Min * Immob_Drug	0.020	0.037	0.586
	Mass * Immob_Drug	-0.033	0.043	0.448	
	Monitor_Min * Mass * Immob_Drug	-0.035	0.044	0.421	
	Observed Hemorrhage				
	(Intercept)	4.096	0.034	0.000	
	Monitor_Min	-0.028	0.027	0.304	
	Hem_Obs	-0.208	0.146	0.155	
	Immob_Drug	0.146	0.042	0.001	

Table S1.3. (continued)

Hypothesis	Model	β	SE	p-value	
ANIMAL (cont.)	Monitor_Min * Hem_Obs	-0.092	0.120	0.443	
	Monitor_Min * Immob_Drug	0.009	0.038	0.818	
	Hem_Obs * Immob_Drug	0.018	0.171	0.917	
	Monitor_Min * Hem_Obs * Immob_Drug	0.185	0.148	0.212	
First Temperature Taken					
	(Intercept)	4.086	0.034	0.000	
	Monitor_Min	-0.025	0.026	0.334	
	1Temp	-0.011	0.038	0.783	
	Immob_Drug	0.141	0.043	0.001	
	Monitor_Min * 1Temp	-0.059	0.027	0.027	
	Monitor_Min * Immob_Drug	0.009	0.036	0.801	
	1Temp * Immob_Drug	0.003	0.047	0.957	
	Monitor_min * 1Temp * Immob_Drug	0.085	0.037	0.021	
WEATHER	Average Daily Ambient Temperature				
		(Intercept)	4.103	0.038	0.000
		Monitor_Min	-0.048	0.031	0.122
		Avg_Temp	0.045	0.037	0.220
		Immob_Drug	0.124	0.045	0.006
		Monitor_Min * Avg_Temp	-0.020	0.032	0.539
		Monitor_Min * Immob_Drug	0.032	0.041	0.436
		Avg_Temp * Immob_Drug	-0.123	0.053	0.021
		Monitor_Min * Avg_Temp * Immob_Drug	0.042	0.054	0.434
	Average Daily Wind Speed				
		(Intercept)	4.088	0.034	0.000
		Monitor_Min	-0.050	0.030	0.099
		Wind	0.062	0.040	0.122
		Immob_Drug	0.137	0.042	0.001
		Monitor_Min * Wind	-0.036	0.043	0.400
	Monitor_Min * Immob_Drug	0.036	0.039	0.354	
	Wind * Immob_Drug	-0.131	0.048	0.006	
	Monitor_Min * Wind * Immob_Drug	0.031	0.050	0.540	
Average Daily Solar Radiation					
	(Intercept)	4.088	0.034	0.000	
	Monitor_Min	-0.028	0.027	0.289	

Table S1.3. (continued)

Hypothesis	Model	β	SE	p-value
WEATHER (cont.)	Solar	0.021	0.031	0.496
	Immob_Drug	0.124	0.042	0.003
	Monitor_Min * Solar	0.010	0.024	0.666
	Monitor_Min * Immob_Drug	0.000	0.037	0.999
	Solar * Immob_Drug	0.076	0.041	0.063
	Monitor_Min * Solar * Immob_Drug	0.000	0.037	0.999

Table S1.4. Model output (coefficients, standard error, and p-values) for all model parameters from the generalized linear models for pre-induction respiration (breaths/minute) with elk id as a mixed effect. We used a threshold of $p < 0.05$ (*) to show significance.

Hypothesis	Model Parameters	β	SE	p-value
CAPTURE	Helicopter Transport Distance			
	(Intercept)	2.895	0.069	0.000
	Monitor_Min	-0.176	0.046	0.000
	Transp_Dist	0.130	0.070	0.063
	Immob_Drug	0.162	0.087	0.062
	Monitor_Min * Transp_Dist	0.062	0.045	0.172
	Monitor_Min * Immob_Drug	-0.158	0.061	0.010
	Transp_Dist * Immob_Drug	-0.201	0.086	0.020
	Monitor_Min * Transp_Dist * Immob_Drug	-0.042	0.059	0.480
ANIMAL	Age Class			
	(Intercept)	2.937	0.079	0.000
	Monitor_Min	-0.201	0.051	0.000
	Age	-0.078	0.195	0.688
	Immob_Drug	0.168	0.095	0.077
	Monitor_Min * Age	0.003	0.114	0.982
	Monitor_Min * Immob_Drug	-0.143	0.067	0.032
	Age * Immob_Drug	0.042	0.262	0.872
	Monitor_Min * Age * Immob_Drug	-0.163	0.239	0.496
	Body Mass (kg)			
	(Intercept)	2.917	0.072	0.000
	Monitor_Min	-0.201	0.045	0.000
	Mass	0.112	0.058	0.052
	Immob_Drug	0.179	0.088	0.042
	Monitor_Min * Mass	0.007	0.037	0.860
	Monitor_Min * Immob_Drug	-0.150	0.061	0.014
Mass * Immob_Drug	-0.157	0.082	0.055	
Monitor_Min * Mass * Immob_Drug	0.012	0.062	0.842	
Observed Hemorrhage				
(Intercept)	2.912	0.074	0.000	
Monitor_Min	-0.206	0.046	0.000	
Hem_Obs	0.211	0.299	0.481	
Immob_Drug	0.209	0.091	0.022	
Monitor_Min * Hem_Obs	0.111	0.178	0.534	

Table S1.4. (continued)

Hypothesis	Model Parameters	β	SE	p-value
ANIMAL (cont.)	Monitor_Min * Immob_Drug	-0.165	0.063	0.008
	Hem_Obs * Immob_Drug	-0.458	0.346	0.186
	Monitor_Min * Hem_Obs * Immob_Drug	0.082	0.218	0.708
	First Temperature Taken			
	(Intercept)	2.934	0.072	0.000
	Monitor_Min	-0.192	0.043	0.000
	1Temp	0.118	0.075	0.117
	Immob_Drug	0.150	0.089	0.089
	Monitor_Min * 1Temp	-0.012	0.042	0.786
	Monitor_Min * Immob_Drug	-0.152	0.057	0.008
	1Temp * Immob_Drug	-0.030	0.091	0.740
	Monitor_min * 1Temp * Immob_Drug	-0.092	0.055	0.097
WEATHER	Average Daily Ambient Temperature			
	(Intercept)	2.957	0.078	0.000
	Monitor_Min	-0.214	0.057	0.000
	Avg_Temp	0.110	0.074	0.136
	Immob_Drug	0.154	0.093	0.096
	Monitor_Min * Avg_Temp	0.003	0.060	0.955
	Monitor_Min * Immob_Drug	-0.135	0.071	0.057
	Avg_Temp * Immob_Drug	-0.215	0.093	0.020
	Monitor_Min * Avg_Temp * Immob_Drug	-0.023	0.073	0.748
		Average Daily Wind Speed		
	(Intercept)	2.934	0.069	0.000
	Monitor_Min	-0.241	0.053	0.000
	Wind	0.225	0.076	0.003
	Immob_Drug	0.163	0.083	0.051
	Monitor_Min * Wind	-0.067	0.078	0.390
	Monitor_Min * Immob_Drug	-0.108	0.068	0.111
	Wind * Immob_Drug	-0.164	0.090	0.068
	Monitor_Min * Wind * Immob_Drug	0.009	0.087	0.919
	Average Daily Solar Radiation			
	(Intercept)	2.901	0.073	0.000
	Monitor_Min	-0.207	0.050	0.000
	Solar	-0.113	0.065	0.081

Table S1.4. (continued)

Hypothesis	Model Parameters	β	SE	p-value
WEATHER (cont.)	Immob_Drug	0.207	0.089	0.020
	Monitor_Min * Solar	-0.038	0.044	0.395
	Monitor_Min * Immob_Drug	-0.146	0.064	0.022
	Solar * Immob_Drug	0.058	0.084	0.487
	Monitor_Min * Solar * Immob_Drug	0.066	0.060	0.272

Table S1.5. Model output (coefficients, standard error, and p-values) for all model parameters from the generalized linear models for pre-induction body temperature (°C) with elk id as a mixed effect. We used a threshold of $p < 0.05$ (*) to show significance.

Hypothesis	Model	β	SE	p-value	
CAPTURE	Transport Distance				
	(Intercept)	39.493	0.180	0.000	
	Monitor_Min	0.053	0.056	0.338	
	Transp_Dist	-0.084	0.187	0.653	
	Immob_Drug	0.149	0.235	0.526	
	Monitor_Min * Transp_Dist	-0.021	0.051	0.684	
	Monitor_Min * Immob_Drug	0.087	0.078	0.262	
	Transp_Dist * Immob_Drug	-0.049	0.238	0.838	
	Monitor_Min * Transp_Dist * Immob_Drug	0.044	0.073	0.545	
ANIMAL	Age Class				
	(Intercept)	39.398	0.186	0.000	
	Monitor_Min	0.047	0.059	0.420	
	Age	0.944	0.496	0.057	
	Immob_Drug	0.451	0.231	0.051	
	Monitor_Min * Age	0.038	0.143	0.791	
	Monitor_Min * Immob_Drug	0.082	0.078	0.294	
	Age * Immob_Drug	-1.456	0.651	0.025	
		Monitor_Min * Age * Immob_Drug	-0.097	0.254	0.703
		Body Mass			
	(Intercept)	39.552	0.173	0.000	
	Monitor_Min	0.050	0.053	0.347	
	Mass	-0.229	0.143	0.109	
	Immob_Drug	0.222	0.217	0.307	
	Monitor_Min * Mass	-0.053	0.049	0.273	
	Monitor_Min * Immob_Drug	0.074	0.073	0.310	
Mass * Immob_Drug	-0.007	0.206	0.974		
	Monitor_Min * Mass * Immob_Drug	0.147	0.081	0.069	
	Observed Hemorrhage				
(Intercept)	39.535	0.181	0.000		
Monitor_Min	0.053	0.055	0.332		
Hem_Obs	-0.073	0.779	0.925		
Immob_Drug	0.304	0.228	0.183		
	Hem_Obs * Immob_Drug	-0.452	0.902	0.616	

Table S1.5. (continued)

Hypothesis	Model	β	SE	p-value
ANIMAL (cont.)	Monitor_Min * Hem_Obs * Immob_Drug	0.257	0.274	0.349
	First Temperature Taken			
	(Intercept)	39.641	0.081	0.000
	Monitor_Min	0.036	0.048	0.448
	1Temp	0.921	0.083	0.000
	Immob_Drug	0.074	0.103	0.470
	Monitor_Min * 1Temp	-0.118	0.046	0.010
	Monitor_Min * Immob_Drug	0.047	0.066	0.473
	1Temp * Immob_Drug	0.050	0.103	0.626
	Monitor_min * 1Temp * Immob_Drug	0.056	0.064	0.384
WEATHER	Average Daily Ambient Temperature			
	(Intercept)	39.554	0.181	0.000
	Monitor_Min	0.011	0.082	0.894
	Avg_Temp	-0.006	0.161	0.972
	Immob_Drug	0.187	0.226	0.408
	Monitor_Min * Avg_Temp	-0.072	0.101	0.477
	Monitor_Min * Immob_Drug	0.122	0.097	0.208
	Avg_Temp * Immob_Drug	0.253	0.210	0.228
	Monitor_Min * Avg_Temp * Immob_Drug	0.032	0.113	0.776
	Average Daily Wind Speed			
	(Intercept)	39.531	0.171	0.000
	Monitor_Min	0.053	0.057	0.356
	Wind	-0.023	0.152	0.880
	Immob_Drug	0.232	0.215	0.279
	Monitor_Min * Wind	-0.004	0.074	0.955
	Monitor_Min * Immob_Drug	0.063	0.076	0.410
	Wind * Immob_Drug	0.371	0.205	0.070
	Monitor_Min * Wind * Immob_Drug	-0.059	0.090	0.513
	Average Daily Solar Radiation			
	(Intercept)	39.440	0.177	0.000
	Monitor_Min	0.048	0.057	0.396
	Solar	-0.365	0.164	0.026
	Immob_Drug	0.378	0.221	0.087
	Monitor_Min * Solar	-0.028	0.050	0.578

Table S1.5. (continued)

Hypothesis	Model	β	SE	p-value
WEATHER (cont.)	Monitor_Min * Immob_Drug	0.062	0.077	0.420
	Solar * Immob_Drug	0.216	0.218	0.321
	Monitor_Min * Solar * Immob_Drug	0.076	0.072	0.296

Table S1.6. Model output (coefficients, standard error, and p-values) for all model parameters from the generalized linear models for post-induction heart rate (beats/minute) with elk id as a mixed effect. We used a threshold of $p < 0.05$ (*) to show significance.

Hypothesis	Model	β	SE	p-value	
CAPTURE	Supplemental Oxygen				
	(Intercept)	4.188	0.067	0.000	
	Monitor_Min	0.020	0.046	0.658	
	Supp_O2	-0.027	0.074	0.717	
	Immob_Drug	-0.010	0.083	0.900	
	Monitor_Min * Supp_O2	0.022	0.049	0.647	
	Monitor_Min * Immob_Drug	-0.015	0.052	0.775	
	Supp_O2 * Immob_Drug	0.011	0.091	0.901	
	Monitor_Min * Supp_O2 * Immob_Drug	-0.029	0.056	0.599	
THERAPEUTIC	Penicillin				
	(Intercept)	4.153	0.030	0.000	
	Monitor_Min	0.031	0.017	0.070	
	Pen	0.109	0.082	0.185	
	Immob_Drug	0.017	0.036	0.633	
	Monitor_Min * Pen	0.046	0.040	0.249	
	Monitor_Min * Immob_Drug	-0.031	0.020	0.125	
	Pen * Immob_Drug	-0.161	0.104	0.122	
		Monitor_Min * Pen * Immob_Drug	-0.043	0.048	0.363
		Banamine			
		(Intercept)	4.176	0.035	0.000
		Monitor_Min	0.040	0.021	0.065
		Bana	-0.021	0.057	0.708
		Immob_Drug	-0.037	0.043	0.388
		Monitor_Min * Bana	0.001	0.031	0.973
		Monitor_Min * Immob_Drug	-0.031	0.026	0.219
		Bana * Immob_Drug	0.095	0.070	0.176
		Monitor_Min * Bana * Immob_Drug	-0.023	0.037	0.540
		Lidocaine			
		(Intercept)	4.103	0.053	0.000
		Monitor_Min	-0.025	0.029	0.399
		Lido	0.085	0.063	0.175
		Immob_Drug	0.073	0.069	0.290
		Monitor_Min * Lido	0.087	0.034	0.011

Table S1.6. (continued)

Hypothesis	Model	β	SE	p-value
THERAPEUTIC (cont.)	Monitor_Min * Immob_Drug	0.051	0.037	0.172
	Lido * Immob_Drug	-0.099	0.080	0.216
	Monitor_Min * Lido * Immob_Drug	-0.120	0.043	0.005
ANIMAL	Age Class			
	(Intercept)	4.169	0.030	0.000
	Monitor_Min	0.042	0.017	0.013
	Age	-0.003	0.085	0.971
	Immob_Drug	-0.006	0.037	0.879
	Monitor_Min * Age	-0.014	0.041	0.738
	Monitor_Min * Immob_Drug	-0.043	0.020	0.030
	Age * Immob_Drug	0.023	0.111	0.837
	Monitor_Min * Age * Immob_Drug	0.035	0.065	0.595
	Body Mass			
	(Intercept)	4.159	0.029	0.000
	Monitor_Min	0.042	0.015	0.007
	Mass	0.021	0.025	0.400
	Immob_Drug	0.007	0.035	0.846
	Monitor_Min * Mass	-0.010	0.015	0.495
	Monitor_Min * Immob_Drug	-0.045	0.019	0.017
	Mass * Immob_Drug	0.017	0.032	0.600
	Monitor_Min * Mass * Immob_Drug	-0.005	0.019	0.809
	Observed Hemorrhage			
	(Intercept)	4.151	0.029	0.000
	Monitor_Min	0.028	0.016	0.085
	Hem_Obs	0.159	0.092	0.084
	Immob_Drug	0.019	0.035	0.601
	Monitor_Min * Hem_Obs	0.087	0.046	0.057
	Monitor_Min * Immob_Drug	-0.032	0.020	0.101
	Hem_Obs * Immob_Drug	-0.225	0.112	0.046
	Monitor_Min * Hem_Obs * Immob_Drug	-0.047	0.057	0.410
First Temperature Taken				
(Intercept)	4.158	0.029	0.000	
Monitor_Min	0.030	0.016	0.064	
1Temp	-0.036	0.028	0.198	

Table S1.6. (continued)

Hypothesis	Model	β	SE	p-value
ANIMAL (cont).	Immob_Drug	0.006	0.035	0.859
	Monitor_Min * 1Temp	-0.027	0.015	0.073
	Monitor_Min * Immob_Drug	-0.031	0.019	0.105
	1Temp * Immob_Drug	0.036	0.035	0.306
	Monitor_Min * 1Temp * Immob_Drug	0.032	0.019	0.091
WEATHER	Average Daily Ambient Temperature			
	(Intercept)	4.172	0.028	0.000
	Monitor_Min	0.039	0.016	0.013
	Avg_Temp	0.020	0.026	0.433
	Immob_Drug	-0.008	0.035	0.822
	Monitor_Min * Avg_Temp	-0.005	0.014	0.691
	Monitor_Min * Immob_Drug	-0.044	0.019	0.022
	Avg_Temp * Immob_Drug	-0.019	0.032	0.566
	Monitor_Min * Avg_Temp * Immob_Drug	0.018	0.017	0.295
	Average Daily Wind Speed			
	(Intercept)	4.171	0.028	0.000
	Monitor_Min	0.044	0.016	0.005
	Wind	0.053	0.025	0.034
	Immob_Drug	-0.008	0.034	0.805
	Monitor_Min * Wind	0.019	0.017	0.283
	Monitor_Min * Immob_Drug	-0.045	0.019	0.017
	Wind * Immob_Drug	-0.031	0.032	0.335
	Monitor_Min * Wind * Immob_Drug	-0.014	0.020	0.494
	Average Daily Solar Radiation			
	(Intercept)	4.170	0.029	0.000
	Monitor_Min	0.031	0.016	0.061
	Solar	0.015	0.026	0.559
	Immob_Drug	-0.012	0.035	0.741
	Monitor_Min * Solar	-0.023	0.015	0.114
	Monitor_Min * Immob_Drug	-0.032	0.019	0.105
	Solar * Immob_Drug	0.020	0.034	0.562
	Monitor_Min * Solar * Immob_Drug	0.028	0.019	0.138

Table S1.7. Model output (coefficients, standard error, and p-values) for all model parameters from the generalized linear models for post-induction respiration (breaths/minute) with elk id as a mixed effect. We used a threshold of $p < 0.05$ (*) to show significance.

Hypothesis	Model	β	SE	p-value	
CAPTURE	Supplemental Oxygen				
	(Intercept)	2.833	0.123	0.000	
	Monitor_Min	0.009	0.107	0.934	
	Supp_O2	-0.284	0.136	0.036	
	Immob_Drug	-0.134	0.152	0.377	
	Monitor_Min * Supp_O2	0.061	0.111	0.583	
	Monitor_Min * Immob_Drug	-0.087	0.116	0.452	
	Supp_O2 * Immob_Drug	0.102	0.167	0.539	
	Monitor_Min * Supp_O2 * Immob_Drug	0.040	0.122	0.743	
THERAPEUTIC	Penicillin				
	(Intercept)	2.611	0.057	0.000	
	Monitor_Min	0.069	0.035	0.048	
	Pen	-0.013	0.159	0.935	
	Immob_Drug	-0.055	0.070	0.431	
	Monitor_Min * Pen	-0.047	0.078	0.550	
	Monitor_Min * Immob_Drug	-0.067	0.042	0.109	
	Pen * Immob_Drug	-0.063	0.201	0.755	
		Monitor_Min * Pen * Immob_Drug	0.047	0.094	0.613
		Banamine			
	(Intercept)	2.656	0.067	0.000	
	Monitor_Min	0.095	0.040	0.018	
	Bana	-0.112	0.111	0.312	
	Immob_Drug	-0.108	0.082	0.185	
	Monitor_Min * Bana	-0.082	0.064	0.199	
	Monitor_Min * Immob_Drug	-0.071	0.049	0.144	
	Bana * Immob_Drug	0.120	0.137	0.380	
		Monitor_Min * Bana * Immob_Drug	0.035	0.077	0.644
		Lidocaine			
	(Intercept)	2.677	0.099	0.000	
	Monitor_Min	0.098	0.060	0.103	
	Lido	-0.092	0.117	0.429	
	Immob_Drug	-0.225	0.130	0.083	
		Monitor_Min * Lido	-0.052	0.070	0.463

Table S1.7. (continued)

Hypothesis	Model	β	SE	p-value
THERAPEUTIC (cont).	Monitor_Min * Immob_Drug	-0.146	0.078	0.060
	Lido * Immob_Drug	0.211	0.150	0.159
	Monitor_Min * Lido * Immob_Drug	0.111	0.089	0.211
ANIMAL	Age Class			
	(Intercept)	2.632	0.056	0.000
	Monitor_Min	0.074	0.033	0.026
	Age	-0.163	0.164	0.319
	Immob_Drug	-0.078	0.069	0.257
	Monitor_Min * Age	-0.109	0.099	0.274
	Monitor_Min * Immob_Drug	-0.074	0.039	0.060
	Age * Immob_Drug	0.104	0.217	0.631
	Monitor_Min * Age * Immob_Drug	0.130	0.152	0.391
	Body Mass			
	(Intercept)	2.571	0.054	0.000
	Monitor_Min	0.074	0.032	0.020
	Mass	0.093	0.047	0.048
	Immob_Drug	-0.022	0.066	0.738
	Monitor_Min * Mass	-0.029	0.032	0.369
	Monitor_Min * Immob_Drug	-0.074	0.038	0.055
	Mass * Immob_Drug	-0.081	0.061	0.188
	Monitor_Min * Mass * Immob_Drug	0.022	0.040	0.584
	Observed Hemorrhage			
	(Intercept)	2.639	0.055	0.000
	Monitor_Min	0.065	0.033	0.048
	Hem_Obs	-0.293	0.176	0.095
	Immob_Drug	-0.083	0.068	0.225
	Monitor_Min * Hem_Obs	-0.051	0.108	0.636
	Monitor_Min * Immob_Drug	-0.067	0.040	0.088
	Hem_Obs * Immob_Drug	0.212	0.214	0.323
	Monitor_Min * Hem_Obs * Immob_Drug	0.093	0.126	0.460
First Temperature Taken				
(Intercept)	2.617	0.055	0.000	
Monitor_Min	0.055	0.036	0.122	
1Temp	0.033	0.054	0.538	

Table S1.7. (continued)

Hypothesis	Model	β	SE	p-value
ANIMAL (cont).	Immob_Drug	-0.065	0.067	0.332
	Monitor_Min * 1Temp	-0.011	0.034	0.753
	Monitor_Min * Immob_Drug	-0.039	0.042	0.345
	1Temp * Immob_Drug	0.000	0.067	0.999
	Monitor_Min * 1Temp * Immob_Drug	-0.047	0.042	0.255
WEATHER	Average Daily Ambient Temperature			
	(Intercept)	2.629	0.053	0.000
	Monitor_Min	0.048	0.032	0.138
	Avg_Temp	0.104	0.048	0.029
	Immob_Drug	-0.077	0.065	0.234
	Monitor_Min * Avg_Temp	-0.045	0.029	0.124
	Monitor_Min * Immob_Drug	-0.049	0.039	0.200
	Avg_Temp * Immob_Drug	-0.123	0.061	0.045
	Monitor_Min * Avg_Temp * Immob_Drug	0.060	0.038	0.109
	Average Daily Wind Speed			
	(Intercept)	2.601	0.053	0.000
	Monitor_Min	0.061	0.032	0.058
	Wind	0.067	0.048	0.159
	Immob_Drug	-0.054	0.065	0.406
	Monitor_Min * Wind	-0.029	0.035	0.404
	Monitor_Min * Immob_Drug	-0.058	0.038	0.128
	Wind * Immob_Drug	-0.035	0.061	0.573
	Monitor_Min * Wind * Immob_Drug	-0.002	0.040	0.961
	Average Daily Solar Radiation			
	(Intercept)	2.601	0.053	0.000
	Monitor_Min	0.059	0.031	0.057
	Solar	-0.034	0.049	0.486
	Immob_Drug	-0.041	0.066	0.528
	Monitor_Min * Solar	0.004	0.027	0.890
	Monitor_Min * Immob_Drug	-0.066	0.037	0.076
	Solar * Immob_Drug	-0.008	0.064	0.903
	Monitor_Min * Solar * Immob_Drug	0.069	0.035	0.051

Table S1.8. Conditional parameters estimates or the non-linear generalized linear models used to evaluate the influences of therapeutic drugs This output includes the conditional coefficients, standard error, and p-values) for all model parameters from the generalized non-linear models for post-induction body temperature (°C) with elk id as a mixed effect. We used a threshold of $p < 0.05$ (*) to show significance.

Hypothesis	Model	β	SE	p-value
CAPTURE	Supplemental Oxygen			
	(Intercept)	38.027	0.670	0.000
	Monitor_Min - spline 1	2.670	1.724	0.121
	Monitor_Min - spline 2	-2.884	1.837	0.116
	Monitor_Min - spline 3	8.267	4.096	0.044
	Monitor_Min - spline 4	-35.548	16.039	0.027
	Monitor_Min - spline 5	146.443	61.634	0.018
	Monitor_Min - spline 6	-1493.173	548.414	0.006
	Supp_O2	1.356	0.766	0.077
	Immob_Drug	1.751	0.820	0.033
	Monitor_Min * Supp_O2 - spline 1	-3.100	1.842	0.092
	Monitor_Min * Supp_O2 - spline 2	3.207	1.910	0.093
	Monitor_Min * Supp_O2 - spline 3	-9.371	4.125	0.023
	Monitor_Min * Supp_O2 - spline 4	34.973	16.052	0.029
	Monitor_Min * Supp_O2 - spline 5	-147.596	61.640	0.017
	Monitor_Min * Supp_O2 - spline 6	1492.665	548.415	0.006
	Monitor_Min * Immob_Drug - spline 1	-4.645	2.038	0.023

Table S1.8. (continued)

Hypothesis	Model	β	SE	p-value
CAPTURE (cont.)	Monitor_Min * Immob_Drug - spline 2	4.424	1.997	0.027
	Monitor_Min * Immob_Drug - spline 3	-10.109	4.173	0.015
	Monitor_Min * Immob_Drug - spline 4	35.265	16.092	0.028
	Monitor_Min * Immob_Drug - spline 5	-147.538	61.682	0.017
	Monitor_Min * Immob_Drug - spline 6	1495.218	548.424	0.006
	Supp_O2 * Immob_Drug	-1.633	0.932	0.080
	Monitor_Min * Supp_O2 * Immob_Drug - spline 1	5.766	2.189	0.008
	Monitor_Min * Supp_O2 * Immob_Drug - spline 2	-4.226	2.094	0.044
	Monitor_Min * Supp_O2 * Immob_Drug - spline 3	10.386	4.216	0.014
	Monitor_Min * Supp_O2 * Immob_Drug - spline 4	-34.203	16.114	0.034
	Monitor_Min * Supp_O2 * Immob_Drug - spline 5	147.508	61.693	0.017
	Monitor_Min * Supp_O2 * Immob_Drug - spline 6	-1494.776	548.427	0.006
THERAPEUTIC	Penicillin			
	(Intercept)	39.100	0.363	0.000
	Monitor_Min - spline 1	-0.126	0.644	0.845
	Monitor_Min - spline 2	0.641	0.505	0.204
	Monitor_Min - spline 3	-0.977	0.500	0.051
	Monitor_Min - spline 4	-0.397	0.655	0.545

Table S1.8. (continued)

Hypothesis	Model	β	SE	p-value
THERAPEUTIC (cont.)	Monitor_Min - spline 5	-1.168	0.878	0.183
	Monitor_Min - spline 6	-0.243	0.848	0.775
	Pen	0.329	0.893	0.713
	Immob_Drug	0.572	0.432	0.185
	Monitor_Min * Pen - spline 1	-1.468	2.525	0.561
	Monitor_Min * Pen - spline 2	-1.592	1.592	0.317
	Monitor_Min * Pen - spline 3	0.642	1.482	0.665
	Monitor_Min * Pen - spline 4	0.126	2.633	0.962
	Monitor_Min * Pen - spline 5	1.342	2.720	0.622
	Monitor_Min * Pen - spline 6	-0.728	2.148	0.735
	Monitor_Min * Immob_Drug - spline 1	0.339	0.793	0.669
	Monitor_Min * Immob_Drug - spline 2	-0.196	0.617	0.751
	Monitor_Min * Immob_Drug - spline 3	-0.047	0.609	0.938
	Monitor_Min * Immob_Drug - spline 4	0.294	0.880	0.738
	Monitor_Min * Immob_Drug - spline 5	0.911	1.394	0.514
	Monitor_Min * Immob_Drug - spline 6	-3.325	2.195	0.130
	Pen * Immob_Drug	-0.805	1.079	0.455
	Monitor_Min * Pen * Immob_Drug - spline 1	1.526	3.015	0.613

Table S1.8. (continued)

Hypothesis	Model	β	SE	p-value
THERAPEUTIC (cont.)	Monitor_Min * Pen * Immob_Drug - spline 2	2.516	1.894	0.184
	Monitor_Min * Pen * Immob_Drug - spline 3	0.234	1.795	0.896
	Monitor_Min * Pen * Immob_Drug - spline 4	-0.118	2.930	0.968
	Monitor_Min * Pen * Immob_Drug - spline 5	-1.177	3.219	0.715
	Monitor_Min * Pen * Immob_Drug - spline 6	4.952	3.106	0.111
Banamine				
	(Intercept)	38.678	0.391	0.000
	Monitor_Min - spline 1	0.108	0.741	0.884
	Monitor_Min - spline 2	0.858	0.644	0.183
	Monitor_Min - spline 3	-1.696	0.608	0.005
	Monitor_Min - spline 4	0.500	0.869	0.565
	Monitor_Min - spline 5	-2.100	1.234	0.089
	Monitor_Min - spline 6	-0.774	1.471	0.599
	Bana	1.265	0.666	0.057
	Immob_Drug	0.759	0.460	0.099
	Monitor_Min * Bana - spline 1	-1.118	1.268	0.378
	Monitor_Min * Bana - spline 2	-1.008	0.949	0.288
	Monitor_Min * Bana - spline 3	1.627	0.935	0.082

Table S1.8. (continued)

Hypothesis	Model	β	SE	p-value
THERAPEUTIC (cont).	Monitor_Min * Bana - spline 4	-2.339	1.253	0.062
	Monitor_Min * Bana - spline 5	1.961	1.677	0.242
	Monitor_Min * Bana - spline 6	0.220	1.746	0.900
	Monitor_Min * Immob_Drug - spline 1	-0.394	0.937	0.674
	Monitor_Min * Immob_Drug - spline 2	-0.315	0.767	0.681
	Monitor_Min * Immob_Drug - spline 3	0.684	0.724	0.344
	Monitor_Min * Immob_Drug - spline 4	-0.603	1.094	0.581
	Monitor_Min * Immob_Drug - spline 5	2.352	1.687	0.163
	Monitor_Min * Immob_Drug - spline 6	-3.031	2.499	0.225
	Bana * Immob_Drug	-0.967	0.817	0.236
	Monitor_Min * Bana * Immob_Drug - spline 1	2.463	1.570	0.117
	Monitor_Min * Bana * Immob_Drug - spline 2	1.587	1.161	0.172
	Monitor_Min * Bana * Immob_Drug - spline 3	-1.286	1.162	0.268
	Monitor_Min * Bana * Immob_Drug - spline 4	2.892	1.592	0.069
	Monitor_Min * Bana * Immob_Drug - spline 5	-3.571	2.281	0.117
Monitor_Min * Bana * Immob_Drug - spline 6	4.404	2.820	0.118	
Lidocaine (Intercept)		39.266	0.548	0.000

Table S1.8. (continued)

Hypothesis	Model	β	SE	p-value
THERAPEUTIC (cont.)	Monitor_Min - spline 1	-0.102	1.109	0.926
	Monitor_Min - spline 2	-0.415	1.014	0.683
	Monitor_Min - spline 3	-0.447	0.985	0.650
	Monitor_Min - spline 4	-1.751	1.276	0.170
	Monitor_Min - spline 5	-0.996	1.640	0.543
	Monitor_Min - spline 6	-0.610	1.150	0.596
	Lido	-0.255	0.689	0.711
	Immob_Drug	0.147	0.682	0.829
	Monitor_Min * Lido - spline 1	0.005	1.332	0.997
	Monitor_Min * Lido - spline 2	1.051	1.159	0.365
	Monitor_Min * Lido - spline 3	-0.462	1.124	0.681
	Monitor_Min * Lido - spline 4	1.702	1.483	0.251
	Monitor_Min * Lido - spline 5	0.060	1.933	0.975
	Monitor_Min * Lido - spline 6	0.445	1.565	0.776
	Monitor_Min * Immob_Drug - spline 1	0.342	1.402	0.807
	Monitor_Min * Immob_Drug - spline 2	1.459	1.241	0.240
	Monitor_Min * Immob_Drug - spline 3	-1.028	1.210	0.396
	Monitor_Min * Immob_Drug - spline 4	3.828	1.858	0.039

Table S1.8. (continued)

Hypothesis	Model	β	SE	p-value
THERAPEUTIC (cont.)	Monitor_Min * Immob_Drug - spline 5	-1.785	2.845	0.530
	Monitor_Min * Immob_Drug - spline 6	4.896	3.761	0.193
	Lido * Immob_Drug	0.505	0.840	0.548
	Monitor_Min * Lido * Immob_Drug - spline 1	-0.158	1.667	0.924
	Monitor_Min * Lido * Immob_Drug - spline 2	-1.466	1.412	0.299
	Monitor_Min * Lido * Immob_Drug - spline 3	0.918	1.378	0.505
	Monitor_Min * Lido * Immob_Drug - spline 4	-3.762	2.077	0.070
	Monitor_Min * Lido * Immob_Drug - spline 5	1.515	3.137	0.629
	Monitor_Min * Lido * Immob_Drug - spline 6	-5.100	4.000	0.202
ANIMAL	Age Class			
	(Intercept)	38.950	0.345	0.000
	Monitor_Min - spline 1	0.078	0.646	0.904
	Monitor_Min - spline 2	0.326	0.492	0.508
	Monitor_Min - spline 3	-1.117	0.488	0.022
	Monitor_Min - spline 4	-0.057	0.682	0.934
	Monitor_Min - spline 5	-0.968	0.938	0.302
	Monitor_Min - spline 6	-0.329	0.996	0.741
	Age	1.092	0.946	0.248

Table S1.8. (continued)

Hypothesis	Model	β	SE	p-value
ANIMAL (cont.)	Immob_Drug	0.607	0.409	0.137
	Monitor_Min * Age - spline 1	-0.559	1.587	0.724
	Monitor_Min * Age - spline 2	-0.359	1.455	0.805
	Monitor_Min * Age - spline 3	1.701	1.277	0.183
	Monitor_Min * Age - spline 4	-2.386	1.732	0.168
	Monitor_Min * Age - spline 5	-0.468	2.132	0.826
	Monitor_Min * Age - spline 6	-0.051	1.578	0.974
	Monitor_Min * Immob_Drug - spline 1	0.291	0.785	0.711
	Monitor_Min * Immob_Drug - spline 2	0.270	0.590	0.647
	Monitor_Min * Immob_Drug - spline 3	0.456	0.584	0.435
	Monitor_Min * Immob_Drug - spline 4	0.086	0.831	0.918
	Monitor_Min * Immob_Drug - spline 5	0.124	1.189	0.917
	Monitor_Min * Immob_Drug - spline 6	0.264	1.271	0.835
	Age * Immob_Drug	-0.884	1.199	0.461
	Monitor_Min * Age * Immob_Drug - spline 1	-1.273	2.224	0.567
	Monitor_Min * Age * Immob_Drug - spline 2	2.324	2.340	0.320
	Monitor_Min * Age * Immob_Drug - spline 3	-6.218	2.473	0.012
	Monitor_Min * Age * Immob_Drug - spline 4	8.887	9.509	0.350

Table S1.8. (continued)

Hypothesis	Model	β	SE	p-value
ANIMAL (cont.)	Monitor_Min * Age * Immob_Drug - spline 5	-5.223	148.192	0.972
	Monitor_Min * Age * Immob_Drug - spline 6	-0.103	918.387	1.000
	Body Mass			
	(Intercept)	39.018	0.360	0.000
	Monitor_Min - spline 1	0.137	0.642	0.831
	Monitor_Min - spline 2	0.567	0.508	0.264
	Monitor_Min - spline 3	-0.759	0.485	0.117
	Monitor_Min - spline 4	-0.199	0.654	0.760
	Monitor_Min - spline 5	-0.792	0.855	0.354
	Monitor_Min - spline 6	-0.226	0.815	0.782
	Mass	-0.061	0.241	0.800
	Immob_Drug	0.568	0.419	0.175
	Monitor_Min * Mass - spline 1	-0.346	0.551	0.530
	Monitor_Min * Mass - spline 2	-0.231	0.435	0.595
	Monitor_Min * Mass - spline 3	-0.717	0.453	0.114
	Monitor_Min * Mass - spline 4	0.642	0.739	0.385
	Monitor_Min * Mass - spline 5	0.185	0.979	0.850
	Monitor_Min * Mass - spline 6	-0.269	0.801	0.737

Table S1.8. (continued)

Hypothesis	Model	β	SE	p-value
ANIMAL (cont.)	Monitor_Min * Immob_Drug - spline 1	0.067	0.773	0.931
	Monitor_Min * Immob_Drug - spline 2	0.093	0.604	0.877
	Monitor_Min * Immob_Drug - spline 3	-0.264	0.579	0.649
	Monitor_Min * Immob_Drug - spline 4	0.454	0.816	0.578
	Monitor_Min * Immob_Drug - spline 5	-0.499	1.150	0.664
	Monitor_Min * Immob_Drug - spline 6	0.623	1.281	0.627
	Mass * Immob_Drug	-0.262	0.325	0.421
	Monitor_Min * Mass * Immob_Drug - spline 1	0.223	0.709	0.753
	Monitor_Min * Mass * Immob_Drug - spline 2	0.563	0.551	0.307
	Monitor_Min * Mass * Immob_Drug - spline 3	1.110	0.556	0.046
	Monitor_Min * Mass * Immob_Drug - spline 4	-0.598	0.903	0.508
	Monitor_Min * Mass * Immob_Drug - spline 5	-0.069	1.316	0.958
	Monitor_Min * Mass * Immob_Drug - spline 6	1.584	1.684	0.347
	Observed Hemorrhage			
	(Intercept)	39.352	0.394	0.000
	Monitor_Min - spline 1	-0.238	0.688	0.729
	Monitor_Min - spline 2	-0.266	0.540	0.623
	Monitor_Min - spline 3	-0.665	0.555	0.231

Table S1.8. (continued)

Hypothesis	Model	β	SE	p-value
ANIMAL (cont.)	Monitor_Min - spline 4	-1.050	0.684	0.125
	Monitor_Min - spline 5	-0.982	0.922	0.287
	Monitor_Min - spline 6	-0.590	0.802	0.462
	Hem_Obs	-1.173	0.791	0.138
	Immob_Drug	0.206	0.451	0.648
	Monitor_Min * Hem_Obs - spline 1	4.157	4.778	0.384
	Monitor_Min * Hem_Obs - spline 2	1.301	1.963	0.508
	Monitor_Min * Hem_Obs - spline 3	-1.011	1.208	0.403
	Monitor_Min * Hem_Obs - spline 4	2.470	2.206	0.263
	Monitor_Min * Hem_Obs - spline 5	-1.205	3.995	0.763
	Monitor_Min * Hem_Obs - spline 6	4.130	9.252	0.655
	Monitor_Min * Immob_Drug - spline 1	0.608	0.820	0.458
	Monitor_Min * Immob_Drug - spline 2	1.013	0.637	0.112
	Monitor_Min * Immob_Drug - spline 3	-0.298	0.645	0.644
	Monitor_Min * Immob_Drug - spline 4	1.489	0.852	0.080
	Monitor_Min * Immob_Drug - spline 5	-0.230	1.201	0.848
	Monitor_Min * Immob_Drug - spline 6	0.661	1.141	0.562
	Hem_Obs * Immob_Drug	1.673	1.227	0.173

Table S1.8. (continued)

Hypothesis	Model	β	SE	p-value
ANIMAL (cont.)	Monitor_Min * Hem_Obs * Immob_Drug - spline 1	-6.025	5.112	0.239
	Monitor_Min * Hem_Obs * Immob_Drug - spline 2	-2.528	2.379	0.288
	Monitor_Min * Hem_Obs * Immob_Drug - spline 3	0.366	1.788	0.838
	Monitor_Min * Hem_Obs * Immob_Drug - spline 4	-5.096	3.051	0.095
	Monitor_Min * Hem_Obs * Immob_Drug - spline 5	2.466	5.968	0.679
	Monitor_Min * Hem_Obs * Immob_Drug - spline 6	-8.326	13.489	0.537
	First Temperature			
	(Intercept)	39.530	0.326	0.000
	Monitor_Min - spline 1	-0.592	0.624	0.343
	Monitor_Min - spline 2	-0.044	0.488	0.929
	Monitor_Min - spline 3	-0.783	0.477	0.100
	Monitor_Min - spline 4	-1.083	0.633	0.087
	Monitor_Min - spline 5	-0.860	0.849	0.311
	Monitor_Min - spline 6	-0.512	0.768	0.505
	1Temp	1.034	0.294	0.000
	Immob_Drug	0.007	0.376	0.986
	Monitor_Min * 1Temp - spline 1	-0.469	0.557	0.400
	Monitor_Min * 1Temp - spline 2	-1.140	0.438	0.009

Table S1.8. (continued)

Hypothesis	Model	β	SE	p-value
ANIMAL (cont.)	Monitor_Min * 1Temp - spline 3	0.579	0.439	0.187
	Monitor_Min * 1Temp - spline 4	-1.786	0.688	0.009
	Monitor_Min * 1Temp - spline 5	0.801	0.931	0.390
	Monitor_Min * 1Temp - spline 6	-0.232	1.010	0.819
	Monitor_Min * Immob_Drug - spline 1	0.818	0.748	0.275
	Monitor_Min * Immob_Drug - spline 2	0.628	0.582	0.281
	Monitor_Min * Immob_Drug - spline 3	-0.236	0.568	0.678
	Monitor_Min * Immob_Drug - spline 4	1.204	0.793	0.129
	Monitor_Min * Immob_Drug - spline 5	-0.052	1.119	0.963
	Monitor_Min * Immob_Drug - spline 6	0.158	1.099	0.886
	1Temp * Immob_Drug	0.159	0.364	0.661
	Monitor_min * 1Temp * Immob_Drug - spline 1	0.360	0.693	0.604
	Monitor_min * 1Temp * Immob_Drug - spline 2	0.569	0.557	0.307
	Monitor_min * 1Temp * Immob_Drug - spline 3	-0.578	0.559	0.302
	Monitor_min * 1Temp * Immob_Drug - spline 4	0.895	0.887	0.313
	Monitor_min * 1Temp * Immob_Drug - spline 5	-0.834	1.440	0.563
	Monitor_min * 1Temp * Immob_Drug - spline 6	-1.648	2.778	0.553
WEATHER	Avg Daily Temperature			

Table S1.8. (continued)

Hypothesis	Model	β	SE	p-value
WEATHER (cont.)	(Intercept)	39.237	0.368	0.000
	Monitor_Min - spline 1	-0.317	0.706	0.654
	Monitor_Min - spline 2	0.247	0.472	0.600
	Monitor_Min - spline 3	-0.890	0.508	0.080
	Monitor_Min - spline 4	-0.541	0.652	0.406
	Monitor_Min - spline 5	-1.564	0.971	0.107
	Monitor_Min - spline 6	-0.110	0.885	0.901
	Avg_Temp	0.373	0.581	0.522
	Immob_Drug	0.371	0.426	0.384
	Monitor_Min * Avg_Temp - spline 1	-0.540	1.028	0.599
	Monitor_Min * Avg_Temp - spline 2	-0.500	0.489	0.307
	Monitor_Min * Avg_Temp - spline 3	0.121	0.697	0.862
	Monitor_Min * Avg_Temp - spline 4	-0.265	0.670	0.692
	Monitor_Min * Avg_Temp - spline 5	-0.869	1.087	0.424
	Monitor_Min * Avg_Temp - spline 6	0.233	0.957	0.807
	Monitor_Min * Immob_Drug - spline 1	0.401	0.826	0.627
	Monitor_Min * Immob_Drug - spline 2	0.404	0.570	0.478
	Monitor_Min * Immob_Drug - spline 3	-0.242	0.596	0.685

Table S1.8. (continued)

Hypothesis	Model	β	SE	p-value
WEATHER (cont.)	Monitor_Min * Immob_Drug - spline 4	0.735	0.805	0.361
	Monitor_Min * Immob_Drug - spline 5	0.345	1.207	0.775
	Monitor_Min * Immob_Drug - spline 6	0.414	1.194	0.729
	Avg_Temp * Immob_Drug	-0.466	0.627	0.458
	Monitor_Min * Avg_Temp * Immob_Drug - spline 1	1.822	1.140	0.110
	Monitor_Min * Avg_Temp * Immob_Drug - spline 2	0.142	0.618	0.819
	Monitor_Min * Avg_Temp * Immob_Drug - spline 3	1.068	0.796	0.180
	Monitor_Min * Avg_Temp * Immob_Drug - spline 4	0.209	0.952	0.826
	Monitor_Min * Avg_Temp * Immob_Drug - spline 5	2.686	1.636	0.101
	Monitor_Min * Avg_Temp * Immob_Drug - spline 6	-5.194	2.297	0.024
Avg Daily Wind Speed				
	(Intercept)	39.059	0.358	0.000
	Monitor_Min - spline 1	-0.012	0.659	0.986
	Monitor_Min - spline 2	0.390	0.499	0.434
	Monitor_Min - spline 3	-0.833	0.528	0.115
	Monitor_Min - spline 4	-0.560	0.894	0.532
	Monitor_Min - spline 5	-0.074	1.343	0.956
	Monitor_Min - spline 6	0.321	1.415	0.821

Table S1.8. (continued)

Hypothesis	Model	β	SE	p-value
WEATHER (cont.)	Wind	0.061	0.307	0.843
	Immob_Drug	0.480	0.418	0.251
	Monitor_min * Wind - spline 1	0.021	0.588	0.972
	Monitor_min * Wind - spline 2	-0.063	0.594	0.916
	Monitor_min * Wind - spline 3	-0.298	0.612	0.626
	Monitor_min * Wind - spline 4	-0.206	1.341	0.878
	Monitor_min * Wind - spline 5	1.745	2.363	0.460
	Monitor_min * Wind - spline 6	1.006	2.548	0.693
	Monitor_Min * Immob_Drug - spline 1	0.279	0.790	0.724
	Monitor_Min * Immob_Drug - spline 2	0.308	0.598	0.607
	Monitor_Min * Immob_Drug - spline 3	-0.157	0.619	0.800
	Monitor_Min * Immob_Drug - spline 4	0.808	1.043	0.438
	Monitor_Min * Immob_Drug - spline 5	-1.184	1.734	0.495
	Monitor_Min * Immob_Drug - spline 6	-0.370	2.593	0.887
	Wind * Immob_Drug	0.445	0.379	0.241
	Monitor_Min * Wind * Immob_drug - spline 1	-0.246	0.736	0.738
	Monitor_Min * Wind * Immob_drug - spline 2	-0.339	0.688	0.623
	Monitor_Min * Wind * Immob_drug - spline 3	0.424	0.700	0.545

Table S1.8. (continued)

Hypothesis	Model	β	SE	p-value
WEATHER (cont.)	Monitor_Min * Wind * Immob_drug - spline 4	-0.461	1.458	0.752
	Monitor_Min * Wind * Immob_drug - spline 5	-2.180	2.720	0.423
	Monitor_Min * Wind * Immob_drug - spline 6	-1.407	3.760	0.708
Avg Daily Solar Radiation				
	(Intercept)	39.206	0.398	0.000
	Monitor_Min - spline 1	-0.140	0.715	0.845
	Monitor_Min - spline 2	-0.030	0.516	0.953
	Monitor_Min - spline 3	-0.887	0.557	0.111
	Monitor_Min - spline 4	-0.602	0.667	0.367
	Monitor_Min - spline 5	-1.252	0.927	0.177
	Monitor_Min - spline 6	-0.467	0.808	0.563
	Solar	0.087	0.377	0.817
	Immob_Drug	0.414	0.452	0.360
	Monitor_Min * Solar - spline 1	0.031	0.638	0.962
	Monitor_Min * Solar - spline 2	-0.931	0.465	0.045
	Monitor_Min * Solar - spline 3	-0.103	0.506	0.839
	Monitor_Min * Solar - spline 4	0.037	0.583	0.949
	Monitor_Min * Solar - spline 5	-0.513	0.819	0.530

Table S1.8. (continued)

Hypothesis	Model	β	SE	p-value
WEATHER (cont.)	Monitor_Min * Solar - spline 6	-0.566	0.721	0.432
	Monitor_Min * Immob_Drug - spline 1	0.565	0.847	0.505
	Monitor_Min * Immob_Drug - spline 2	0.486	0.624	0.436
	Monitor_Min * Immob_Drug - spline 3	0.088	0.648	0.891
	Monitor_Min * Immob_Drug - spline 4	0.394	0.862	0.647
	Monitor_Min * Immob_Drug - spline 5	1.232	1.375	0.370
	Monitor_Min * Immob_Drug - spline 6	-2.229	1.753	0.204
	Solar * Immob_Drug	-0.293	0.461	0.525
	Monitor_Min * Solar * Immob_Drug - spline 1	-0.329	0.810	0.685
	Monitor_Min * Solar * Immob_Drug - spline 2	1.455	0.611	0.017
	Monitor_Min * Solar * Immob_Drug - spline 3	-0.256	0.651	0.695
	Monitor_Min * Solar * Immob_Drug - spline 4	0.687	0.845	0.416
	Monitor_Min * Solar * Immob_Drug - spline 5	-0.808	1.547	0.601
	Monitor_Min * Solar * Immob_Drug - spline 6	4.413	2.047	0.031

Table S1.9. Model output (coefficients, standard error, and p-values) for all model parameters from the generalized non-linear models for post-induction blood oxygen saturation (SpO₂) with elk id as a mixed effect. We used a threshold of $p < 0.05$ (*) to show significance.

Hypothesis	Model	β	SE	p-value
CAPTURE	Supplemental Oxygen			
	(Intercept)	1.813	0.366	0.000
	Monitor_Min - spline 1	-0.716	0.792	0.366
	Monitor_Min - spline 2	-0.521	0.612	0.395
	Monitor_Min - spline 3	0.032	0.912	0.972
	Monitor_Min - spline 4	-2.717	3.279	0.407
	Monitor_Min - spline 5	13.761	14.087	0.329
	Monitor_Min - spline 6	-156.082	149.535	0.297
	Supp_O2	-0.670	0.439	0.127
	Immob_Drug	0.263	0.466	0.572
	Monitor_Min * Supp_O2 - spline 1	0.682	0.896	0.447
	Monitor_Min * Supp_O2 - spline 2	0.244	0.682	0.720
	Monitor_Min * Supp_O2 - spline 3	0.623	0.971	0.521
	Monitor_Min * Supp_O2 - spline 4	3.895	3.312	0.240
	Monitor_Min * Supp_O2 - spline 5	-13.053	14.102	0.355
	Monitor_Min * Supp_O2 - spline 6	157.130	149.536	0.293
	Monitor_Min * Immob_Drug - spline 1	0.383	1.010	0.704
	Monitor_Min * Immob_Drug - spline 2	0.865	0.811	0.286

Table S1.9. (continued)

Hypothesis	Model	β	SE	p-value
CAPTURE (cont.)	Monitor_Min * Immob_Drug - spline 3	-0.591	1.052	0.574
	Monitor_Min * Immob_Drug - spline 4	3.128	3.396	0.357
	Monitor_Min * Immob_Drug - spline 5	-14.535	14.176	0.305
	Monitor_Min * Immob_Drug - spline 6	156.169	149.555	0.296
	Supp_O2 * Immob_Drug	-0.096	0.541	0.860
	Monitor_Min * Supp_O2 * Immob_Drug - spline 1	-0.123	1.128	0.913
	Monitor_Min * Supp_O2 * Immob_Drug - spline 2	-0.828	0.891	0.353
	Monitor_Min * Supp_O2 * Immob_Drug - spline 3	0.561	1.123	0.618
	Monitor_Min * Supp_O2 * Immob_Drug - spline 4	-3.499	3.442	0.309
	Monitor_Min * Supp_O2 * Immob_Drug - spline 5	14.227	14.198	0.316
	Monitor_Min * Supp_O2 * Immob_Drug - spline 6	-156.267	149.556	0.296
THERAPEUTIC	Penicillin			
	(Intercept)	0.942	0.247	0.000
	Monitor_Min - spline 1	0.337	0.431	0.434
	Monitor_Min - spline 2	-0.161	0.293	0.582
	Monitor_Min - spline 3	0.927	0.342	0.007
	Monitor_Min - spline 4	1.225	0.460	0.008
	Monitor_Min - spline 5	1.047	0.709	0.140

Table S1.9. (continued)

Hypothesis	Model	β	SE	p-value
THERAPAUTIC (cont.)	Monitor_Min - spline 6	1.459	0.774	0.059
	Pen	1.054	0.449	0.019
	Immob_Drug	0.536	0.281	0.056
	Monitor_Min * Pen - spline 1	-1.865	1.035	0.072
	Monitor_Min * Pen - spline 2	0.207	0.721	0.774
	Monitor_Min * Pen - spline 3	-2.190	0.742	0.003
	Monitor_Min * Pen - spline 4	-0.033	1.288	0.980
	Monitor_Min * Pen - spline 5	-1.745	1.538	0.257
	Monitor_Min * Pen - spline 6	-1.269	1.405	0.366
	Monitor_Min * Immob_Drug - spline 1	-0.318	0.510	0.532
	Monitor_Min * Immob_Drug - spline 2	-0.057	0.361	0.874
	Monitor_Min * Immob_Drug - spline 3	-0.510	0.402	0.204
	Monitor_Min * Immob_Drug - spline 4	-0.583	0.555	0.293
	Monitor_Min * Immob_Drug - spline 5	-0.955	0.857	0.265
	Monitor_Min * Immob_Drug - spline 6	-0.609	0.907	0.502
	Pen * Immob_Drug	-1.094	0.550	0.047
	Monitor_Min * Pen * Immob_Drug - spline 1	2.046	1.339	0.126
	Monitor_Min * Pen * Immob_Drug - spline 2	0.378	0.984	0.701

Table S1.9. (continued)

Hypothesis	Model	β	SE	p-value
THERAPEUTIC (cont.)	Monitor_Min * Pen * Immob_Drug - spline 3	2.049	0.945	0.030
	Monitor_Min * Pen * Immob_Drug - spline 4	0.529	1.558	0.734
	Monitor_Min * Pen * Immob_Drug - spline 5	1.918	1.902	0.313
	Monitor_Min * Pen * Immob_Drug - spline 6	1.216	1.666	0.465
Banamine				
	(Intercept)	0.914	0.254	0.000
	Monitor_Min - spline 1	0.568	0.467	0.223
	Monitor_Min - spline 2	-0.115	0.344	0.738
	Monitor_Min - spline 3	0.726	0.394	0.065
	Monitor_Min - spline 4	1.352	0.629	0.031
	Monitor_Min - spline 5	0.922	1.365	0.499
	Monitor_Min - spline 6	1.219	3.563	0.732
	Bana	1.099	0.417	0.008
	Immob_Drug	0.449	0.288	0.119
	Monitor_Min * Bana - spline 1	-2.361	0.765	0.002
	Monitor_Min * Bana - spline 2	-0.523	0.529	0.323
	Monitor_Min * Bana - spline 3	-0.940	0.606	0.121
	Monitor_Min * Bana - spline 4	-0.930	0.888	0.295

Table S1.9. (continued)

Hypothesis	Model	β	SE	p-value
THERAPEUTIC (cont.)	Monitor_Min * Bana - spline 5	-1.006	1.602	0.530
	Monitor_Min * Bana - spline 6	-0.906	3.633	0.803
	Monitor_Min * Immob_Drug - spline 1	-0.300	0.569	0.598
	Monitor_Min * Immob_Drug - spline 2	0.108	0.425	0.799
	Monitor_Min * Immob_Drug - spline 3	-0.214	0.457	0.640
	Monitor_Min * Immob_Drug - spline 4	-0.627	0.729	0.390
	Monitor_Min * Immob_Drug - spline 5	-0.422	1.480	0.776
	Monitor_Min * Immob_Drug - spline 6	-0.162	3.600	0.964
	Bana * Immob_Drug	-0.665	0.512	0.194
	Monitor_Min * Bana * Immob_Drug - spline 1	1.605	0.957	0.094
	Monitor_Min * Bana * Immob_Drug - spline 2	-0.032	0.682	0.963
	Monitor_Min * Bana * Immob_Drug - spline 3	0.528	0.757	0.485
	Monitor_Min * Bana * Immob_Drug - spline 4	0.612	1.082	0.572
	Monitor_Min * Bana * Immob_Drug - spline 5	0.186	1.846	0.920
	Monitor_Min * Bana * Immob_Drug - spline 6	0.173	3.730	0.963
Lidocaine				
(Intercept)		1.949	0.356	0.000
Monitor_Min - spline 1		-1.570	0.638	0.014

Table S1.9. (continued)

Hypothesis	Model	β	SE	p-value
THERAPEUTIC (cont.)	Monitor_Min - spline 2	-0.816	0.479	0.088
	Monitor_Min - spline 3	0.377	0.580	0.516
	Monitor_Min - spline 4	0.543	0.866	0.531
	Monitor_Min - spline 5	0.562	1.191	0.637
	Monitor_Min - spline 6	0.805	0.981	0.412
	Lido	-0.932	0.431	0.030
	Immob_Drug	-0.633	0.413	0.126
	Monitor_Min * Lido - spline 1	1.992	0.775	0.010
	Monitor_Min * Lido - spline 2	0.619	0.567	0.275
	Monitor_Min * Lido - spline 3	0.142	0.672	0.832
	Monitor_Min * Lido - spline 4	0.663	0.991	0.504
	Monitor_Min * Lido - spline 5	0.109	1.421	0.939
	Monitor_Min * Lido - spline 6	0.134	1.311	0.919
	Monitor_Min * Immob_Drug - spline 1	1.449	0.791	0.067
	Monitor_Min * Immob_Drug - spline 2	0.365	0.643	0.570
	Monitor_Min * Immob_Drug - spline 3	0.409	0.708	0.563
	Monitor_Min * Immob_Drug - spline 4	-0.194	1.076	0.857
	Monitor_Min * Immob_Drug - spline 5	0.420	1.519	0.782

Table S1.9. (continued)

Hypothesis	Model	β	SE	p-value
THERAPEUTIC (cont.)	Monitor_Min * Immob_Drug - spline 6	0.272	1.155	0.814
	Lido * Immob_Drug	1.126	0.501	0.025
	Monitor_Min * Lido * Immob_Drug - spline 1	-1.761	0.953	0.065
	Monitor_Min * Lido * Immob_Drug - spline 2	-0.276	0.746	0.711
	Monitor_Min * Lido * Immob_Drug - spline 3	-0.594	0.817	0.468
	Monitor_Min * Lido * Immob_Drug - spline 4	-0.253	1.225	0.837
	Monitor_Min * Lido * Immob_Drug - spline 5	-1.063	1.779	0.550
	Monitor_Min * Lido * Immob_Drug - spline 6	-0.470	1.536	0.760
ANIMAL	Age Class			
	(Intercept)	1.366	0.195	0.000
	Monitor_Min - spline 1	-0.040	0.363	0.913
	Monitor_Min - spline 2	-0.381	0.253	0.133
	Monitor_Min - spline 3	0.190	0.289	0.510
	Monitor_Min - spline 4	0.973	0.430	0.024
	Monitor_Min - spline 5	0.467	0.688	0.498
	Monitor_Min - spline 6	0.674	0.804	0.402
	Age	-0.935	1.869	0.617
	Immob_Drug	0.067	0.230	0.772

Table S1.9. (continued)

Hypothesis	Model	β	SE	p-value
ANIMAL (cont.)	Monitor_Min * Age - spline 1	-0.485	2.683	0.856
	Monitor_Min * Age - spline 2	0.562	1.670	0.736
	Monitor_Min * Age - spline 3	2.297	2.042	0.261
	Monitor_Min * Age - spline 4	0.927	2.081	0.656
	Monitor_Min * Age - spline 5	1.688	2.431	0.488
	Monitor_Min * Age - spline 6	1.713	2.188	0.434
	Monitor_Min * Immob_Drug - spline 1	0.297	0.442	0.501
	Monitor_Min * Immob_Drug - spline 2	0.332	0.318	0.296
	Monitor_Min * Immob_Drug - spline 3	0.173	0.345	0.617
	Monitor_Min * Immob_Drug - spline 4	-0.129	0.512	0.801
	Monitor_Min * Immob_Drug - spline 5	-0.278	0.799	0.728
	Monitor_Min * Immob_Drug - spline 6	0.214	0.888	0.809
	Age * Immob_Drug	1.243	1.917	0.517
	Monitor_Min * Age * Immob_Drug - spline 1	-1.194	2.837	0.674
	Monitor_Min * Age * Immob_Drug - spline 2	-1.771	1.935	0.360
	Monitor_Min * Age * Immob_Drug - spline 3	-1.963	2.278	0.389
	Monitor_Min * Age * Immob_Drug - spline 4	0.367	4.310	0.932
	Monitor_Min * Age * Immob_Drug - spline 5	-15.248	36.091	0.673

Table S1.9. (continued)

Hypothesis	Model	β	SE	p-value
ANIMAL (cont.)	Monitor_Min * Age * Immob_Drug - spline 6	-0.048	9436.593	1.000
	Body Mass			
	(Intercept)	0.906	0.237	0.000
	Monitor_Min - spline 1	0.162	0.405	0.689
	Monitor_Min - spline 2	-0.056	0.270	0.835
	Monitor_Min - spline 3	0.941	0.314	0.003
	Monitor_Min - spline 4	1.304	0.416	0.002
	Monitor_Min - spline 5	1.093	0.623	0.080
	Monitor_Min - spline 6	1.248	0.644	0.052
	Mass	0.401	0.153	0.009
	Immob_Drug	0.584	0.264	0.027
	Monitor_Min * Mass - spline 1	0.119	0.313	0.704
	Monitor_Min * Mass - spline 2	-0.252	0.198	0.203
	Monitor_Min * Mass - spline 3	-0.882	0.223	0.000
	Monitor_Min * Mass - spline 4	-0.393	0.431	0.362
	Monitor_Min * Mass - spline 5	-0.701	0.688	0.308
	Monitor_Min * Mass - spline 6	-0.811	0.645	0.208
	Monitor_Min * Immob_Drug - spline 1	-0.097	0.472	0.837

Table S1.9. (continued)

Hypothesis	Model	β	SE	p-value
ANIMAL (cont.)	Monitor_Min * Immob_Drug - spline 2	-0.130	0.329	0.693
	Monitor_Min * Immob_Drug - spline 3	-0.532	0.365	0.146
	Monitor_Min * Immob_Drug - spline 4	-0.625	0.505	0.216
	Monitor_Min * Immob_Drug - spline 5	-0.925	0.778	0.234
	Monitor_Min * Immob_Drug - spline 6	-0.556	0.845	0.511
	Mass * Immob_Drug	-0.377	0.205	0.066
	Monitor_Min * Mass * Immob_Drug - spline 1	0.474	0.432	0.273
	Monitor_Min * Mass * Immob_Drug - spline 2	0.232	0.294	0.430
	Monitor_Min * Mass * Immob_Drug - spline 3	0.817	0.299	0.006
	Monitor_Min * Mass * Immob_Drug - spline 4	0.359	0.522	0.491
	Monitor_Min * Mass * Immob_Drug - spline 5	0.533	0.798	0.504
	Monitor_Min * Mass * Immob_Drug - spline 6	0.636	0.769	0.408
	Observed Hemorrhage			
	(Intercept)	1.430	0.233	0.000
	Monitor_Min - spline 1	-0.415	0.406	0.307
	Monitor_Min - spline 2	-0.429	0.285	0.132
	Monitor_Min - spline 3	0.264	0.331	0.425
	Monitor_Min - spline 4	0.816	0.457	0.074

Table S1.9. (continued)

Hypothesis	Model	β	SE	p-value
ANIMAL (cont.)	Monitor_Min - spline 5	0.605	0.679	0.373
	Monitor_Min - spline 6	0.702	0.639	0.272
	Hem_Obs	-0.078	0.478	0.871
	Immob_Drug	0.022	0.264	0.932
	Monitor_Min * Hem_Obs - spline 1	-0.991	3.327	0.766
	Monitor_Min * Hem_Obs - spline 2	0.775	1.372	0.572
	Monitor_Min * Hem_Obs - spline 3	-0.081	0.945	0.931
	Monitor_Min * Hem_Obs - spline 4	1.284	1.736	0.460
	Monitor_Min * Hem_Obs - spline 5	-2.579	3.905	0.509
	Monitor_Min * Hem_Obs - spline 6	5.128	11.576	0.658
	Monitor_Min * Immob_Drug - spline 1	0.543	0.486	0.264
	Monitor_Min * Immob_Drug - spline 2	0.214	0.354	0.545
	Monitor_Min * Immob_Drug - spline 3	0.164	0.390	0.675
	Monitor_Min * Immob_Drug - spline 4	-0.106	0.557	0.849
	Monitor_Min * Immob_Drug - spline 5	-0.394	0.844	0.641
	Monitor_Min * Immob_Drug - spline 6	-0.070	0.815	0.932
	Hem_Obs * Immob_Drug	0.059	0.774	0.939
	Monitor_Min * Hem_Obs * Immob_Drug - spline 1	0.259	3.480	0.941

Table S1.9. (continued)

Hypothesis	Model	β	SE	p-value
ANIMAL (cont.)	Monitor_Min * Hem_Obs * Immob_Drug - spline 2	0.022	1.597	0.989
	Monitor_Min * Hem_Obs * Immob_Drug - spline 3	0.255	1.245	0.838
	Monitor_Min * Hem_Obs * Immob_Drug - spline 4	-1.683	2.010	0.403
	Monitor_Min * Hem_Obs * Immob_Drug - spline 5	3.248	4.134	0.432
	Monitor_Min * Hem_Obs * Immob_Drug - spline 6	-4.456	11.623	0.701
First Temperature Taken				
	(Intercept)	1.319	0.211	0.000
	Monitor_Min - spline 1	-0.314	0.377	0.405
	Monitor_Min - spline 2	-0.336	0.265	0.205
	Monitor_Min - spline 3	0.438	0.299	0.143
	Monitor_Min - spline 4	1.038	0.428	0.015
	Monitor_Min - spline 5	0.509	0.619	0.411
	Monitor_Min - spline 6	0.826	0.649	0.203
	1Temp	-0.247	0.231	0.284
	Immob_Drug	0.166	0.244	0.496
	Monitor_Min * 1Temp - spline 1	-0.022	0.395	0.955
	Monitor_Min * 1Temp - spline 2	0.162	0.280	0.563
	Monitor_Min * 1Temp - spline 3	0.491	0.309	0.112

Table S1.9. (continued)

Hypothesis	Model	β	SE	p-value
ANIMAL (cont.)	Monitor_Min * 1Temp - spline 4	0.300	0.446	0.502
	Monitor_Min * 1Temp - spline 5	-0.022	0.746	0.977
	Monitor_Min * 1Temp - spline 6	0.802	1.065	0.452
	Monitor_Min * Immob_Drug - spline 1	0.337	0.456	0.460
	Monitor_Min * Immob_Drug - spline 2	0.160	0.332	0.630
	Monitor_Min * Immob_Drug - spline 3	0.013	0.359	0.972
	Monitor_Min * Immob_Drug - spline 4	-0.469	0.520	0.367
	Monitor_Min * Immob_Drug - spline 5	-0.247	0.760	0.745
	Monitor_Min * Immob_Drug - spline 6	0.009	0.805	0.991
	1Temp * Immob_Drug	0.039	0.271	0.887
	Monitor_min * 1Temp * Immob_Drug - spline 1	0.354	0.476	0.457
	Monitor_min * 1Temp * Immob_Drug - spline 2	-0.209	0.360	0.561
	Monitor_min * 1Temp * Immob_Drug - spline 3	-0.395	0.380	0.298
	Monitor_min * 1Temp * Immob_Drug - spline 4	0.109	0.551	0.843
	Monitor_min * 1Temp * Immob_Drug - spline 5	0.038	0.926	0.967
Monitor_min * 1Temp * Immob_Drug - spline 6	-0.775	1.379	0.574	
WEATHER	Average Daily Ambient Temperature (Intercept)	1.358	0.205	0.000

Table S1.9. (continued)

Hypothesis	Model	β	SE	p-value
WEATHER (cont.)	Monitor_Min - spline 1	-0.301	0.366	0.411
	Monitor_Min - spline 2	-0.314	0.266	0.238
	Monitor_Min - spline 3	0.166	0.295	0.574
	Monitor_Min - spline 4	1.114	0.427	0.009
	Monitor_Min - spline 5	0.105	0.648	0.871
	Monitor_Min - spline 6	0.948	0.653	0.147
	Avg_Temp	-0.353	0.289	0.222
	Immob_Drug	0.126	0.241	0.601
	Monitor_Min * Avg_Temp - spline 1	0.575	0.510	0.259
	Monitor_Min * Avg_Temp - spline 2	0.363	0.272	0.181
	Monitor_Min * Avg_Temp - spline 3	-0.256	0.358	0.475
	Monitor_Min * Avg_Temp - spline 4	0.573	0.387	0.139
	Monitor_Min * Avg_Temp - spline 5	-0.351	0.645	0.586
	Monitor_Min * Avg_Temp - spline 6	0.181	0.611	0.767
	Monitor_Min * Immob_Drug - spline 1	0.322	0.450	0.474
	Monitor_Min * Immob_Drug - spline 2	0.128	0.335	0.702
	Monitor_Min * Immob_Drug - spline 3	0.232	0.357	0.516
	Monitor_Min * Immob_Drug - spline 4	-0.458	0.518	0.377

Table S1.9. (continued)

Hypothesis	Model	β	SE	p-value
WEATHER (cont.)	Monitor_Min * Immob_Drug - spline 5	0.091	0.792	0.909
	Monitor_Min * Immob_Drug - spline 6	-0.328	0.825	0.691
	Avg_Temp * Immob_Drug	0.299	0.316	0.344
	Monitor_Min * Avg_Temp * Immob_Drug - spline 1	-0.406	0.573	0.479
	Monitor_Min * Avg_Temp * Immob_Drug - spline 2	-0.194	0.346	0.575
	Monitor_Min * Avg_Temp * Immob_Drug - spline 3	0.292	0.415	0.482
	Monitor_Min * Avg_Temp * Immob_Drug - spline 4	-0.473	0.522	0.366
	Monitor_Min * Avg_Temp * Immob_Drug - spline 5	0.401	0.911	0.659
	Monitor_Min * Avg_Temp * Immob_Drug - spline 6	0.158	0.836	0.850
Average Daily Wind Speed				
	(Intercept)	1.232	0.206	0.000
	Monitor_Min - spline 1	-0.116	0.372	0.756
	Monitor_Min - spline 2	-0.194	0.263	0.461
	Monitor_Min - spline 3	0.373	0.297	0.210
	Monitor_Min - spline 4	1.373	0.463	0.003
	Monitor_Min - spline 5	0.075	0.779	0.923
	Monitor_Min - spline 6	2.275	1.608	0.157
	Wind	0.524	0.193	0.007

Table S1.9. (continued)

Hypothesis	Model	β	SE	p-value
WEATHER (cont.)	Immob_Drug	0.264	0.241	0.272
	Monitor_min * Wind - spline 1	-0.594	0.362	0.101
	Monitor_min * Wind - spline 2	-0.068	0.298	0.821
	Monitor_min * Wind - spline 3	-1.013	0.335	0.002
	Monitor_min * Wind - spline 4	0.475	0.660	0.471
	Monitor_min * Wind - spline 5	-2.225	1.573	0.157
	Monitor_min * Wind - spline 6	3.385	4.169	0.417
	Monitor_Min * Immob_Drug - spline 1	0.173	0.453	0.703
	Monitor_Min * Immob_Drug - spline 2	-0.008	0.331	0.980
	Monitor_Min * Immob_Drug - spline 3	0.051	0.359	0.886
	Monitor_Min * Immob_Drug - spline 4	-0.792	0.551	0.151
	Monitor_Min * Immob_Drug - spline 5	0.229	0.909	0.801
	Monitor_Min * Immob_Drug - spline 6	-1.643	1.677	0.327
	Wind * Immob_Drug	-0.707	0.229	0.002
	Monitor_Min * Wind * Immob_drug - spline 1	0.467	0.449	0.299
	Monitor_Min * Wind * Immob_drug - spline 2	0.163	0.360	0.652
	Monitor_Min * Wind * Immob_drug - spline 3	1.085	0.391	0.006
	Monitor_Min * Wind * Immob_drug - spline 4	-0.106	0.721	0.883

Table S1.9. (continued)

Hypothesis	Model	β	SE	p-value
WEATHER (cont.)	Monitor_Min * Wind * Immob_drug - spline 5	2.301	1.640	0.161
	Monitor_Min * Wind * Immob_drug - spline 6	-3.496	4.200	0.405
Average Daily Solar Radiation				
	(Intercept)	1.283	0.204	0.000
	Monitor_Min - spline 1	-0.258	0.372	0.488
	Monitor_Min - spline 2	-0.288	0.273	0.291
	Monitor_Min - spline 3	0.368	0.303	0.224
	Monitor_Min - spline 4	0.973	0.430	0.023
	Monitor_Min - spline 5	0.692	0.684	0.312
	Monitor_Min - spline 6	0.508	0.725	0.483
	Solar	-0.546	0.225	0.016
	Immob_Drug	0.173	0.236	0.465
	Monitor_Min * Solar - spline 1	0.847	0.387	0.029
	Monitor_Min * Solar - spline 2	0.343	0.287	0.232
	Monitor_Min * Solar - spline 3	0.212	0.306	0.487
	Monitor_Min * Solar - spline 4	0.500	0.394	0.205
	Monitor_Min * Solar - spline 5	0.551	0.643	0.392
	Monitor_Min * Solar - spline 6	-0.245	0.824	0.766

Table S1.9. (continued)

Hypothesis	Model	β	SE	p-value
WEATHER (cont.)	Monitor_Min * Immob_Drug - spline 1	0.292	0.452	0.518
	Monitor_Min * Immob_Drug - spline 2	0.133	0.341	0.696
	Monitor_Min * Immob_Drug - spline 3	0.029	0.362	0.935
	Monitor_Min * Immob_Drug - spline 4	-0.282	0.522	0.589
	Monitor_Min * Immob_Drug - spline 5	-0.443	0.816	0.587
	Monitor_Min * Immob_Drug - spline 6	0.134	0.847	0.874
	Solar * Immob_Drug	0.641	0.270	0.018
	Monitor_Min * Solar * Immob_Drug - spline 1	-0.849	0.486	0.081
	Monitor_Min * Solar * Immob_Drug - spline 2	-0.380	0.371	0.306
	Monitor_Min * Solar * Immob_Drug - spline 3	-0.098	0.388	0.800
	Monitor_Min * Solar * Immob_Drug - spline 4	-0.740	0.515	0.151
	Monitor_Min * Solar * Immob_Drug - spline 5	-0.852	0.849	0.316
	Monitor_Min * Solar * Immob_Drug - spline 6	0.714	1.046	0.495

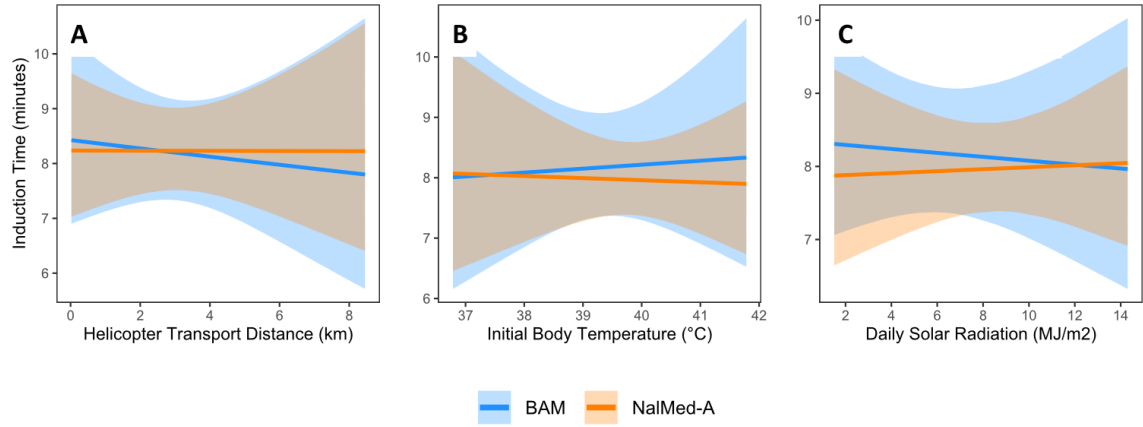


Figure S1.1. Characteristics with no notable influence on the induction of a single IM-injection of BAM and NalMed-A in female elk in southeastern Kentucky, USA with associated 95% confidence intervals, including helicopter transport distance (A), initial body temperature (B), and daily solar radiation (C).

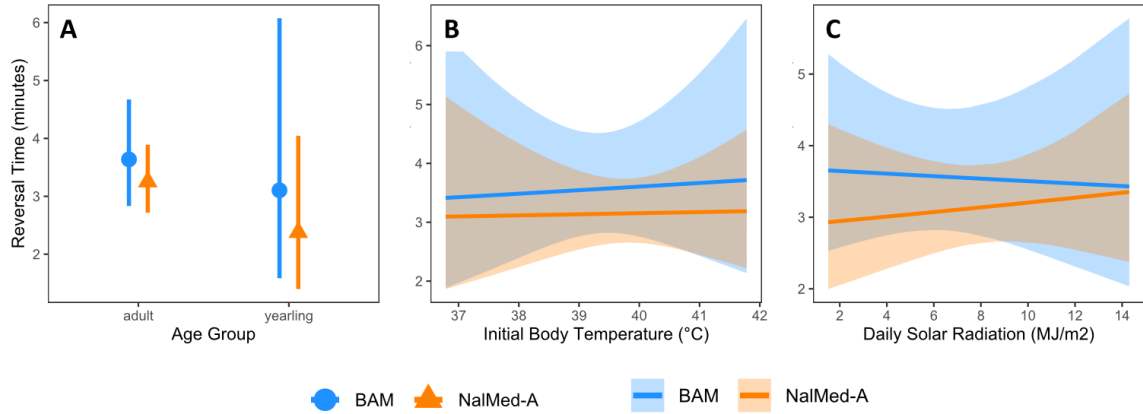


Figure S1.2. Characteristics with no notable influence on the reversal of a single IM-injection of BAM and NalMed-A in female elk in southeastern Kentucky, USA with associated 95% confidence intervals, including helicopter transport distance (A), initial body temperature (B), and daily solar radiation (C).

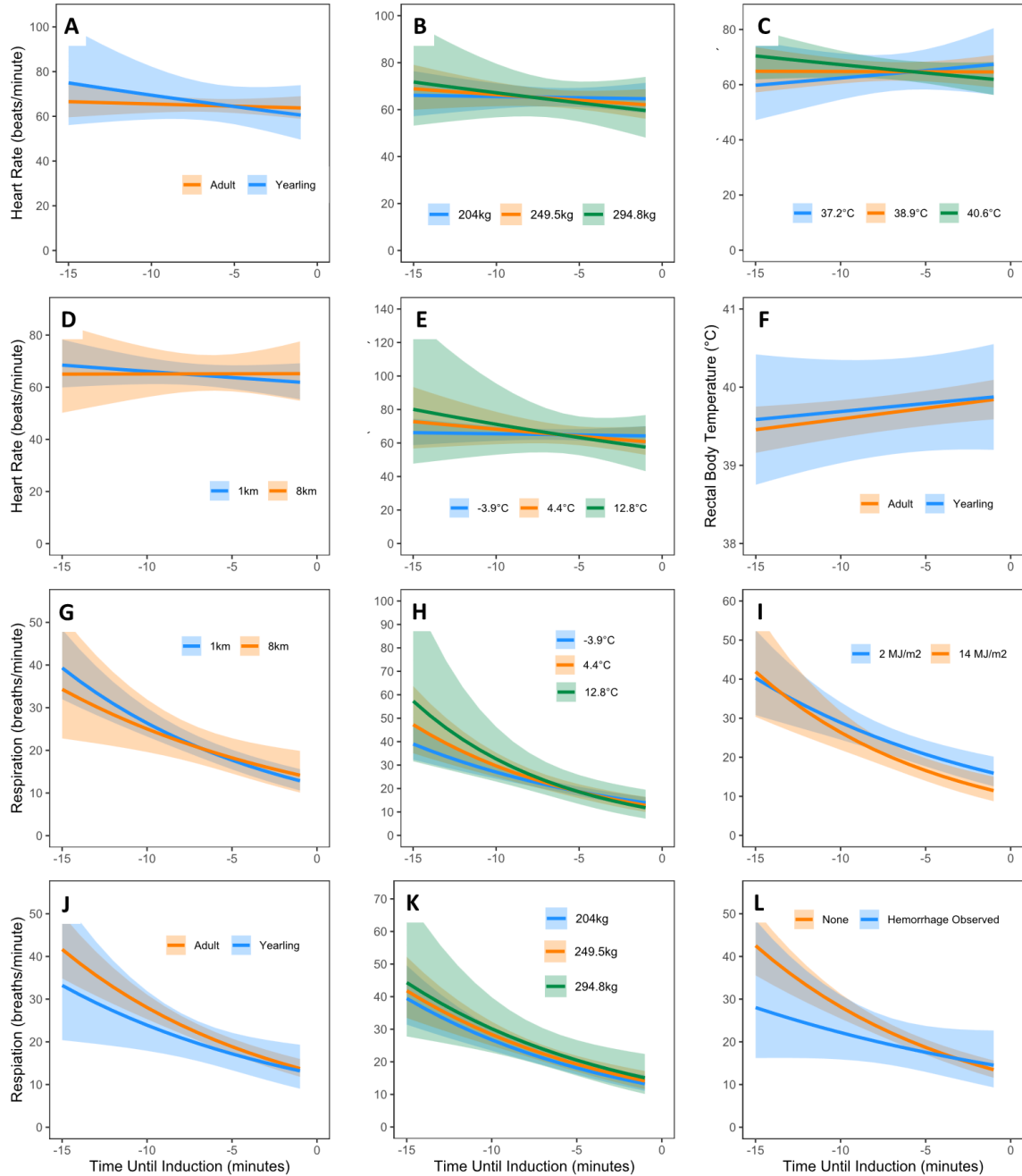


Figure S1.3. Characteristics with no notable influence on pre-induction physiological rates after a single IM-injection of BAM and NaMed-A in female elk in southeastern Kentucky, USA with associated 95% confidence intervals. Non-influential intrinsic characteristics include age group (A, F, J), body mass (B, K), observed hemorrhage (L), and initial body temperature (C). Non-influential extrinsic characteristics include helicopter transport distance (D, G), average daily ambient temperature (E, H), and daily solar radiation (I).

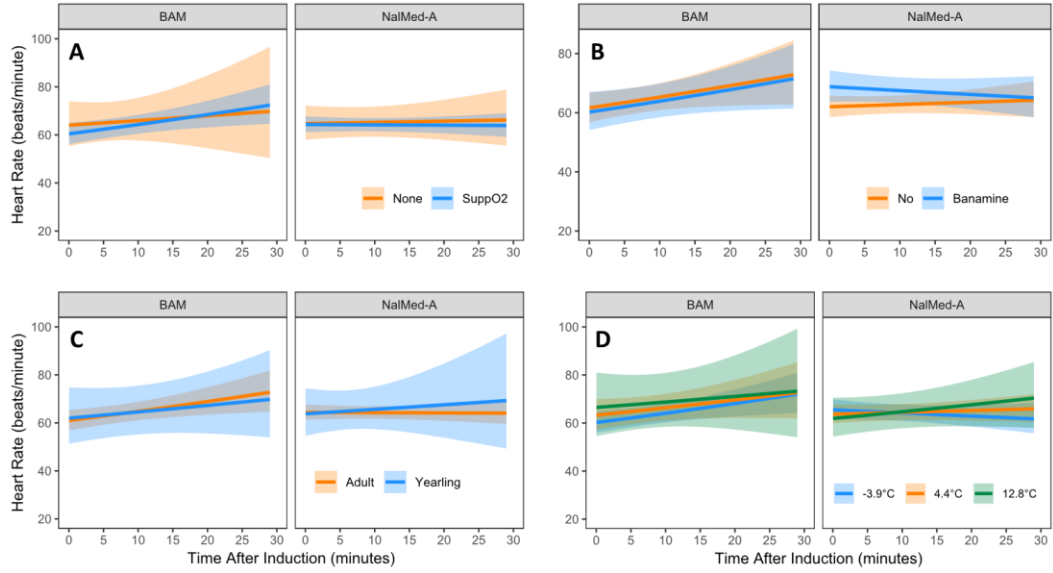


Figure S1.4. Characteristics with no notable influence on post-induction heart rates after a single IM-injection of BAM and NalMed-A in female elk in southeastern Kentucky, USA with associated 95% confidence intervals. The only non-influential intrinsic characteristic is age group (C). Non-influential extrinsic characteristics include the administration of supplemental oxygen (A) and banamine (B), and average daily ambient temperature (D).

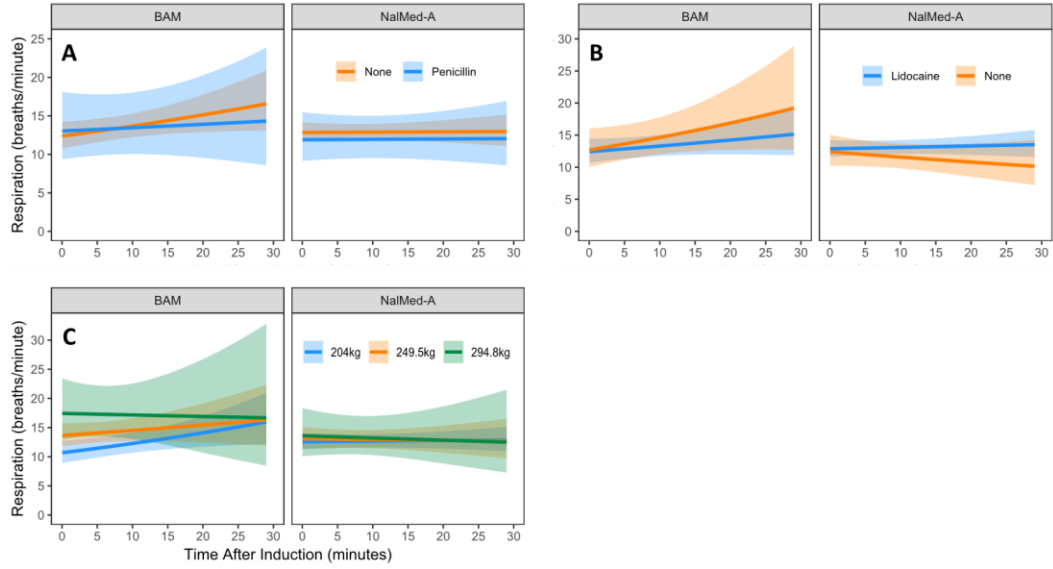


Figure S1.5. Characteristics with no notable influence on post-induction respiration after a single IM-injection of BAM and NalMed-A in female elk in southeastern Kentucky, USA with associated 95% confidence intervals. The only non-influential intrinsic characteristic is body mass (C). Non-influential extrinsic characteristics include the administration of penicillin (A) and lidocaine (B).

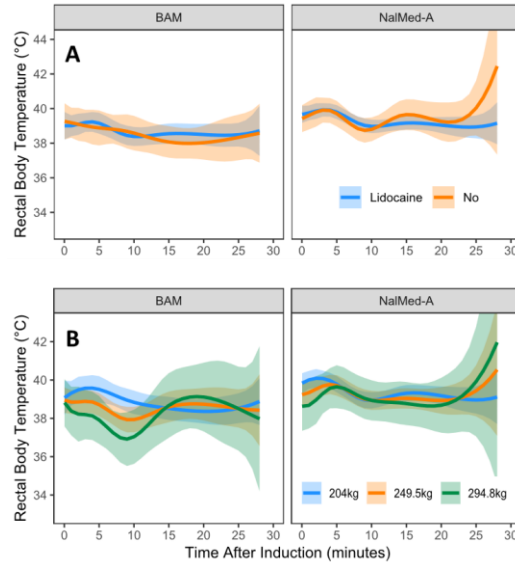


Figure S1.6. Characteristics with no notable influence on post-induction body temperature after a single IM-injection of BAM and NalMed-A in female elk in southeastern Kentucky, USA with associated 95% confidence intervals. The only non-influential intrinsic characteristic is body mass (C) and the only non-influential extrinsic characteristic is the administration of lidocaine (B).

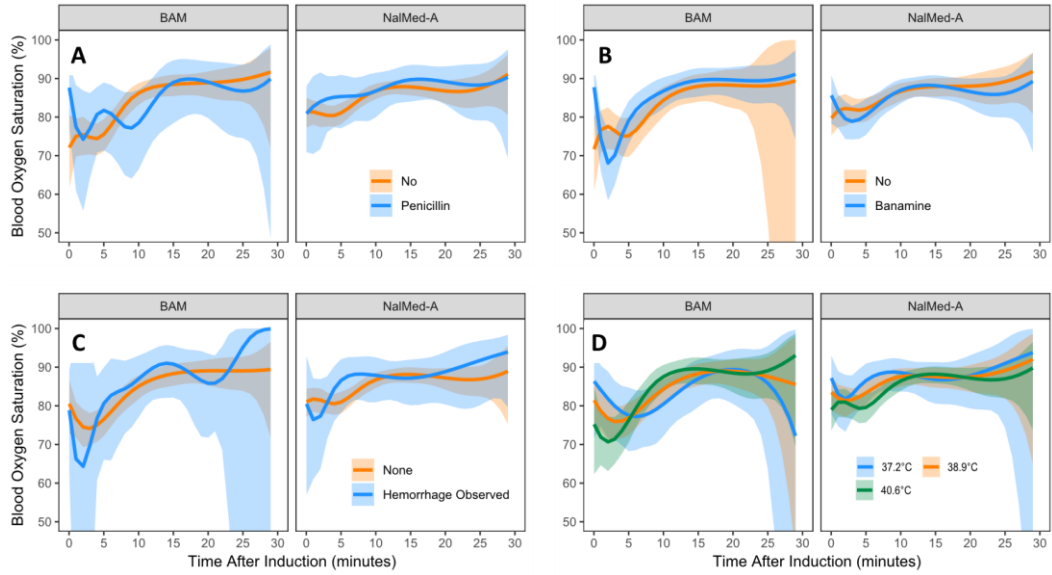


Figure S1.7. Characteristics with no notable influence on post-induction blood oxygen saturation (SpO_2) after a single IM-injection of BAM and NalMed-A in female elk in southeastern Kentucky, USA with associated 95% confidence intervals. Non-influential intrinsic characteristics include observed hemorrhage (C) and initial body temperature (D). Non-influential extrinsic cha

APPENDIX 2. ELK CALF CAPTURE AND CAUSE-SPECIFIC MORTALITY DATA

Table S2.1. Capture and cause-specific mortality data collected for elk calves captured across the Elk Restoration Zone (KERZ) during 2020 – 2022 including: 1) ear tag (plastic stud tag), 2) sex, 3) age at capture based on VIT expulsion time and capture time, 4) birth date based on VIT expulsion time, 5) mortality date for elk calves that died or were censored during the annual monitoring period, 6) mortality cause, and 7) used in analysis, which shows that only individuals captured in 2020 and 2021 were used in this analysis because 2022’s annual monitoring period has not yet ended.

146

Ear Tag	Sex	Age at Capture (days)	Birth Date	Mortality Date	Mortality Cause	Used in Analysis
06	M	0.31	5/17/2020		Survived	Yes
18	F	0.22	5/22/2020	3/26/2021	Unknown (censor)	Yes
24	F	0.85	5/23/2020		Survived	Yes
07	F	1.07	5/23/2020	10/7/2020	Disease - bacterial pneumonia	Yes
19	M	0.18	5/25/2020		Survived	Yes
23	M	0.42	5/26/2020		Survived	Yes
08	M	1.06	5/28/2020		Survived	Yes
17	F	0.74	5/30/2020	12/1/2020	Harvest	Yes
12	M	0.26	5/31/2020		Survived	Yes
04	F	0.20	6/1/2020		Survived	Yes
16	F	0.16	6/5/2020		Survived	Yes
02	F	0.34	6/6/2020	6/8/2020	Suspect trauma	Yes
03	F	0.65	6/6/2020		Survived	Yes
21	M	0.21	6/8/2020		Survived	Yes
09	M	0.57	6/9/2020		Survived	Yes
13	F	1.59	6/8/2020		Survived	Yes
15	M	1.82	6/8/2020		Survived	Yes

Table S2.1. (continued)

Ear Tag	Sex	Age at Capture (days)	Birth Date	Mortality Date	Mortality Cause	Used in Analysis
22	M	0.21	6/11/2020		Survived	Yes
20	F	0.15	6/14/2020		Survived	Yes
10	M	0.18	6/23/2020		Survived	Yes
11	M	0.38	8/2/2020	8/4/2020	Abandonment	Yes
43	M	0.08	5/19/2021	5/20/2021	Abandonment – consumed by bobcat	Yes
42	F	0.17	5/21/2021	5/7/2022	Unknown (censor)	Yes
33	M	0.46	5/24/2021	1/22/2022	Suspect Predation - coyotes	Yes
36	M	0.54	5/24/2021		Survived	Yes
45	M	0.23	5/26/2021	2/22/2022	Unknown (censor)	Yes
26	F	0.20	5/27/2021	7/3/2021	Unknown - consumed by bear	Yes
46	M	0.46	5/29/2021		Survived	Yes
27	F	0.28	5/30/2021	8/11/2021	Unknown (censor)	Yes
28	F	0.19	5/30/2021		Survived	Yes
53	F	0.17	6/1/2021		Survived	Yes
34 ^A	M	0.15	6/2/2021	8/23/2021	Suspect predation - coyotes	Yes
50	M	0.52	6/4/2021	6/6/2021	Suspect predation - bear	Yes
39	M	0.24	6/5/2021	6/6/2021	Trauma, congenital defect	Yes
51	M	0.70	6/7/2021		Survived	Yes
38	F	0.57	6/12/2021		Survived	Yes
49	M	0.15	6/13/2021		Survived	Yes
14	M	0.19	6/14/2021	6/19/2021	Predation - bear	Yes
52	M	0.15	6/15/2021		Survived	Yes

Table S2.1. (continued)

Ear Tag	Sex	Age at Capture (days)	Birth Date	Mortality Date	Mortality Cause	Used in Analysis
32	M	0.23	6/20/2021		Survived	Yes
40	M	0.11	6/23/2021	7/5/2021	Predation - bear	Yes
25	F	0.63	6/29/2021	2/21/2022	Suspect predation - coyotes	Yes
30	F	0.27	7/9/2021	9/6/2021	Suspect predation - bear	Yes
41	F	0.67	7/15/2021	4/14/2022	Unknown (censor)	Yes
44	F	0.25	8/3/2021	8/11/2021	Unknown (censor)	Yes
76	M	0.80	5/19/2022	6/12/2022	Emaciation - stuck in mud	No
82	F	0.88	5/21/2022			No
31	M	0.22	5/25/2022	7/1/2022	Suspect trauma	No
61	M	0.55	5/27/2022			No
58	M	0.24	5/28/2022			No
29	F	0.25	5/29/2022			No
74	F	0.20	5/31/2022			No
85	F	0.70	5/31/2022			No
found dead	M	0.50	6/1/2022	6/1/2022	Blunt force trauma	No
65	F	0.16	6/2/2022	6/30/2022	Disease - Salmonellosis	No
01	F	0.24	6/2/2022			No
67	M	0.98	6/2/2022			No
57 ^A	F	0.71	6/2/2022	6/15/2022	Unknown (censor)	No
77	F	0.73	6/3/2022	6/13/2022	Unknown - consumed by bobcat	No
69	M	0.61	6/4/2022	12/8/2022	Unknown - consumed by coyote	No
66	F	0.88	6/6/2022			No

Table S2.1. (continued)

Ear Tag	Sex	Age at Capture (days)	Birth Date	Mortality Date	Mortality Cause	Used in Analysis
87	M	0.15	6/7/2022			No
83	F	0.60	6/8/2022			No
55	F	0.21	6/9/2022			No
73	M	0.30	6/10/2020			No
79	M	0.32	6/11/2022			No
80	M	0.24	6/11/2022	11/15/2022	Blunt force trauma - roadkill	No
70	F	0.90	6/11/2022			No
48	M	0.49	6/15/2022			No
35	F	0.24	6/19/2022			No
75	F	0.22	6/20/2022	7/19/2022	Disease - bacterial septicemia	No
63	M	0.69	6/22/2022			No
78	F	0.16	6/23/2022	8/12/2022	Unknown (censor)	No
05	M	0.96	6/23/2022			No
59	F	0.70	6/25/2022	7/5/2022	Predation - bear	No
62	M	1.08	6/27/2022	6/30/2022	Predation - bear	No
71	M	0.60	6/30/2022	2/15/2023	Unknown (censor)	No
84	F	0.28	7/9/2022			No
72	F	0.23	7/11/2022			No
64	F	0.50	7/22/2022			No
60	M	0.28	7/26/2022	7/27/2022	Predation - bear	No

^A = birth time was estimated as halfway between calf capture time and last GPS or radio-telemetry relocation

REFERENCES

- Alexy, K. J. 2004. Meningeal worm (*Parelaphostrongylus tenuis*) and ectoparasites issues associated with elk restoration in southeastern Kentucky. Dissertation, Clemson University, Clemson, South Carolina, USA.
- AMR Vet Collective. n.d. Diff Quick® staining protocol.
<https://www.amrvetcollective.com/_resources/themes/amrvc/images/PDF/DiffQuik_protocol.pdf>.
- van Amsterdam, J., M. Pierce, and W. van den Brink. 2021. Is Europe facing an emerging opioid crisis comparable to the U.S.? *Therapeutic Drug Monitoring* 43:42–51.
- Anderson, B., R. Peng, and J. Ferreri. 2016. “weathermetrics”: functions to convert between weather metrics. <<https://github.com/geanders/weathermetrics/>>.
- Andryk, T. A., L. R. Irby, D. L. Hook, J. J. McCarthy, and G. Olson. 1983. Comparison of mountain sheep capture techniques: helicopter darting versus net-gunning. *Wildlife Society Bulletin* 11:184–187.
- Arbor Assays. 2009. DetectX® Cortisol Enzyme Immunoassay Kit. Arbor Assays, Ann Arbor, MI.
- Arnold, T. W. 2010. Uninformative parameters and model selection using akaike’s information criterion. *Journal of Wildlife Management* 74:1175–1178.
- Barbknecht, A. E., W. S. Fairbanks, J. D. Rogerson, E. J. Maichak, and L. L. Meadows. 2009. Effectiveness of vaginal-implant transmitters for locating elk parturition sites. *Journal of Wildlife Management* 73:144–148.
- Barbknecht, A. E., W. S. Fairbanks, J. D. Rogerson, E. J. Maichak, B. M. Scurlock, and L. L. Meadows. 2011. Elk parturition site selection at local and landscape scales. *Journal of Wildlife Management* 75:646–654.

- Barrett, M. W., J. W. Nolan, and L. D. Roy. 1982. Evaluation of a hand-held net-gun to capture large mammals. *Wildlife Society Bulletin* 10:108–114.
- Bartoń, K. 2023. “MuMIn”: Multi-model inference. <<https://cran.r-project.org/web/packages/MuMIn/MuMIn.pdf>>.
- Baxter, E. M., S. Jarvis, R. B. D’Eath, D. W. Ross, S. K. Robson, M. Farish, I. M. Nevison, A. B. Lawrence, and S. A. Edwards. 2008. Investigating the behavioural and physiological indicators of neonatal survival in pigs. *Theriogenology* 69:773–783.
- Bender, L. C., E. Carlson, S. M. Schmitt, and J. B. Haufler. 2002. Production and survival of elk (*Cervus elaphus*) calves in Michigan. *The American Midland Naturalist* 148:163–171.
- Bivand, R., C. Rundel, E. Pebesma, R. Stuetz, K. O. Hufthammer, P. Giraudoux, M. Davis, and S. Santilli. 2023. “rgeos”: Interface to geometry engine - open source (‘GEOS’). <<https://cran.r-project.org/web/packages/rgeos/rgeos.pdf>>.
- Bowling, W. E. 2009. Maternal antibody transfer and meningeal worm infection rates in Kentucky elk. Thesis, University of Kentucky, Lexington, Kentucky, USA.
- Brackel, K. L., E. S. Michel, B. S. Gullikson, J. A. Jenks, and W. F. Jensen. 2021. Capture method affects survival estimates and subsequent interpretation of ecological covariates for a long-lived cervid. *Ecology and Evolution* 11:6444–6455.
- Brivio, F., S. Grignolio, N. Sica, S. Cerise, and B. Bassano. 2015. Assessing the impact of capture on wild animals: The case study of chemical immobilisation on alpine ibex. *PLOS ONE* 10:e0130957.
- Brooks, M., B. Bolker, K. Kristensen, M. Maechler, A. Magnusson, M. McGillicuddy, H. Skaug, A. Nielsen, C. Berg, K. van Benthem, N. Sadat, D. Ludecke, R. Lenth, J. O’Brien, C. J. Geyer, M. Jagan, and B. Wiernik. 2022. “glmmTMB”: Generalized linear mixed models using template model builder. R Package version 1.1.4. <<https://cran.r-project.org/web/packages/glmmTMB/index.html>>.

- Burnham, K. P., D. R. Anderson, and K. P. Burnham. 2002. Model selection and multimodel inference: a practical information-theoretic approach. 2nd ed. Springer, New York, USA.
- Burnham, K. P., D. R. Anderson, and K. P. Huyvaert. 2011. AIC model selection and multimodel inference in behavioral ecology: some background, observations, and comparisons. *Behavioral Ecology and Sociobiology* 65:23–35.
- Carstensen, M., G. D. Delgiudice, B. A. Sampson, and D. W. Kuehn. 2009. Survival, birth characteristics, and cause-specific mortality of white-tailed deer neonates. *Journal of Wildlife Management* 73:175–183.
- Caslini, C., A. Comin, T. Peric, A. Prandi, L. Pedrotti, and S. Mattiello. 2016. Use of hair cortisol analysis for comparing population status in wild red deer (*Cervus elaphus*) living in areas with different characteristics. *European Journal of Wildlife Research* 62:713–723.
- Cattet, M. R. L., K. Christison, N. A. Caulkett, and G. B. Stenhouse. 2003. Physiologic responses of grizzly bears to different methods of capture. *Journal of Wildlife Diseases* 39:649–654.
- Caulkett, N., and J. M. Arnemo. 2007. Cervids (Deer). Pages 823–829 in G. West, D. Heard, and N. Caulkett, editors. *Zoo animal and wildlife immobilization and anesthesia*. 2nd edition. Blackwell Publishing Professional, Ames, Iowa, USA.
- Chitwood, M. C., M. A. Lashley, C. S. DePerno, and C. E. Moorman. 2017. Considerations on neonatal ungulate capture method: potential for bias in survival estimation and cause-specific mortality. *Wildlife Biology* 2017:wlb.00250.
- Cornell University College of Veterinary Medicine. 2016. Samples for hematology. Animal Health Diagnostic Center. <<https://www.vet.cornell.edu/animal-health-diagnostic-center/laboratories/clinical-pathology/samples-and-submissions/hematology#Bloodsmear>>.
- Cornell University College of Veterinary Medicine. 2020a. Total protein by refractometer measurement. ECLINPATH. <<https://eclinpath.com/hematology/hemogram-basics/solids-and-plasma/tp-ref-copy/>>.

- Cornell University College of Veterinary Medicine. 2020b. Hematocrit/packed cell volume. ECLINPATH. <<https://eclinpath.com/hematology/tests/hematocrit/>>.
- Cornell University College of Veterinary Medicine. 2020c. Smear examination. ECLINPATH. <<https://eclinpath.com/hematology/hemogram-basics/blood-smear-examination/>>.
- Accessed 25 Apr 2023.
- Costa, G. L., B. Nastasi, M. Musicò, F. Spadola, M. Morici, G. Cucinotta, and C. Interlandi. 2017. Influence of ambient temperature and confinement on the chemical immobilization of fallow deer (*Dama dama*). *Journal of Wildlife Diseases* 53:364–367.
- Cox, J. 2003. Community dynamics among reintroduced elk, white-tailed deer, and coyote in southeastern Kentucky. Dissertation, University of Kentucky, Lexington, Kentucky, USA.
- Cox, J. J. 2011. Tales of a repatriated megaherbivore: challenges and opportunities in the management of reintroduced elk in Appalachia. Pages 632–642 *in*. USDA Forest Service, Lexington, KY.
- Crank, D., J. Hast, J. McDermott, and M. Peterson. 2022. 2022-2023 Kentucky Department of Fish and Wildlife Resources elk report. Kentucky Department of Fish and Wildlife Resources, Frankfort, KY.
- Cristescu, B., L. M. Elbroch, T. D. Forrester, M. L. Allen, D. B. Spitz, C. C. Wilmers, and H. U. Wittmer. 2022. Standardizing protocols for determining the cause of mortality in wildlife studies. *Ecology and Evolution* 12.
- DeVivo, M. T., W. O. Cottrell, J. M. DeBerti, J. E. Duchamp, L. M. Heffernan, J. D. Kougher, and J. L. Larkin. 2011. Survival and cause-specific mortality of elk *Cervus canadensis* calves in a predator rich environment. *Wildlife Biology* 17:156–165.
- Dion, J. R., J. M. Haus, J. E. Rogerson, and J. L. Bowman. 2020. White-tailed deer neonate survival in the absence of predators. *Ecosphere* 11.

- Engebretsen, K. N., D. DeBloois, and J. K. Young. 2023. Use of radio-linked VHF technology to monitor neonate carnivores. *Wildlife Society Bulletin* 47:e1438.
- Fahlman, Å. 2014. Oxygen therapy. Pages 69–81 *in*. *Zoo animal and wildlife immobilization and anesthesia*. 2nd edition. John Wiley & Sons, Inc.
- Forrester, T. D., and H. U. Wittmer. 2019. Predator identity and forage availability affect predation risk of juvenile black-tailed deer. *Wildlife Biology* 2019.
- Fox, J., and S. Weisberg. 2011. Cox proportional-hazards regression for survival data in R. Page 20 *in*. *Appendix to An R and S-PLUS Companion to Applied Regression*. 2nd edition. <<https://socialsciences.mcmaster.ca/jfox/Books/Companion-1E/appendix-cox-regression.pdf>>. Accessed 3 Oct 2021.
- Gaillard, J.-M., M. Festa-Bianchet, and N. G. Yoccoz. 1998. Population dynamics of large herbivores: variable recruitment with constant adult survival. *Trends in Ecology & Evolution* 13:58–63.
- Ganz, T. R., M. T. DeVivo, E. M. Reese, and L. R. Prugh. 2023. Wildlife whodunnit: forensic identification of predators to inform wildlife management and conservation. *Wildlife Society Bulletin* 47.
- George, B., S. Seals, and I. Aban. 2014. Survival analysis and regression models. *Journal of Nuclear Cardiology* 21:686–694.
- Gerhart, K. L., R. G. White, R. D. Cameron, and D. E. Russell. 1996. Estimating fat content of caribou from body condition scores. *Journal of Wildlife Management* 60:713–718.
- Gettelman, T. E., C. K. Nielsen, J. M. Scimeca, and E. M. Schauber. 2022. River otter chemical immobilization and field surgery using nonscheduled drugs. *Wildlife Society Bulletin*. <<https://onlinelibrary.wiley.com/doi/10.1002/wsb.1354>>. Accessed 13 Sep 2022.
- Gilbert, S. L., M. S. Lindberg, K. J. Hundertmark, and D. K. Person. 2014. Dead before detection: addressing the effects of left truncation on survival estimation and ecological inference for neonates. *Methods in Ecology and Evolution* 5:992–1001.

- Gray, B. 2021. “cmprsk”: Subdistribution analysis of competing risks.
<<https://rdocumentation.org/packages/cmprsk/versions/2.2-11>>.
- Griffin, K. A., M. Hebblewhite, H. S. Robinson, P. Zager, S. M. Barber-Meyer, D. Christianson, S. Creel, N. C. Harris, M. A. Hurley, D. H. Jackson, B. K. Johnson, W. L. Myers, J. D. Raithel, M. Schlegel, B. L. Smith, C. White, and P. J. White. 2011. Neonatal mortality of elk driven by climate, predator phenology and predator community composition. *Journal of Animal Ecology* 80:1246–1257.
- Grimm, K. A., L. A. Lamont, W. J. Tranquilli, S. A. Greene, and S. A. Roberston, editors. 2015. Pharmacology. Pages 147–356 *in*. *Veterinary Anesthesia and Analgesia*. 5th edition. John Wiley & Sons, Inc., Ames, Iowa.
- Groombridge, J. J., C. Raisin, R. Bristol, and D. S. Richardson. 2012. Genetic consequences of reintroductions and insights from population history. Pages 395–440 *in* J. G. Ewen, D. P. Armstrong, K. A. Parker, and P. J. Seddon, editors. *Reintroduction biology: integrating science and management*. Blackwell Publishing Ltd.
<<https://onlinelibrary.wiley.com/doi/10.1002/9781444355833.ch12>>. Accessed 29 Jun 2023.
- Grovenburg, T. W., K. L. Monteith, C. N. Jacques, R. W. Klaver, C. S. DePerno, T. J. Brinkman, K. B. Monteith, S. L. Gilbert, J. B. Smith, V. C. Bleich, C. C. Swanson, and J. A. Jenks. 2014. Re-evaluating neonatal-age models for ungulates: Does model choice affect survival estimates? G. Brock, editor. *PLoS ONE* 9:e108797.
- Gruerber, C. E., S. Nakagawa, R. J. Laws, and I. G. Jamieson. 2011. Multimodel inference in ecology and evolution: challenges and solutions: Multimodel inference. *Journal of Evolutionary Biology* 24:699–711.
- Hamlin, K. L., D. F. Pac, C. A. Sime, R. M. DeSimone, and G. L. Dusek. 2000. Evaluating the accuracy of ages obtained by two methods for Montana ungulates. *Journal of Wildlife Management* 64:441–449.

- Hansen, C. M., and K. B. Beckmen. 2018. Butorphanol-azaperone-medetomidine for the immobilization of captive caribou (*Rangifer tarandus granti*) in Alaska, USA. *Journal of Wildlife Diseases* 54:650–652.
- Harms, N. J., T. S. Jung, M. Hallock, and K. Egli. 2018. Efficacy of a butorphanol, azaperone, and medetomidine combination for helicopter-based immobilization of bison (*Bison bison*). *Journal of Wildlife Diseases* 54:819–824.
- Harris, D. L., R. R. Shrode, I. W. Rupel, and R. E. Leighton. 1960. A study of solar radiation as related to physiological and production responses of lactating holstein and jersey cows. *Journal of Dairy Science* 43:1255–1262.
- Hast, J. 2019. Vital rates and habitat selection of bull elk (*Cervus canadensis nelsoni*) in southeast Kentucky. Dissertation, University of Kentucky, Lexington, Kentucky, USA. <https://uknowledge.uky.edu/animalsci_etds/113/>. Accessed 24 Feb 2021.
- Heisey, D. M., and B. R. Patterson. 2006. A Review of Methods to Estimate Cause-Specific Mortality in Presence of Competing Risks. *Journal of Wildlife Management* 70:1544–1555.
- Hill, J. D. 1976. Climate of Kentucky. Progress Report, University of Kentucky Agriculture Experiment Station, Lexington, KY.
- Hooven, N. D., K. E. Williams, J. T. Hast, J. R. McDermott, R. D. Crank, G. Jenkins, M. T. Springer, and J. J. Cox. 2022. Using low-fix rate GPS telemetry to expand estimates of ungulate reproductive success. *Animal Biotelemetry* 10:1–14.
- Jackson, P. G. G., and P. D. Cockcroft. 2002. Clinical examination of farm animals. Blackwell Science, Oxford, UK.
- Jenson, W. 1999. Aging elk. North Dakota Outdoors, North Dakota Game and Fish Department, Bismarck, ND. <<https://gf.nd.gov/sites/default/files/publications/aging-elk.pdf>>.

- Johnson, B. K., T. McCoy, C. O. Kochanny, and R. C. Cook. 2006. Evaluation of vaginal implant transmitters in elk (*Cervus elaphus nelsoni*). *Journal of Zoo and Wildlife Medicine* 37:301–305.
- Johnson, D. E. 1951. Biology of the elk calf, *Cervus canadensis nelsoni*. *Journal of Wildlife Management* 15:396.
- KDFWR Elk Program. 2020. Description of KDFWR elk model parameters. Kentucky Department of Fish and Wildlife Resources, Frankfort, KY.
<https://fw.ky.gov/Hunt/Documents/Elk/Elk_Model_Parameters_2020_update.pdf>.
- Keller, B. J., R. A. Montgomery, H. R. Campa III, D. E. Beyer Jr, S. R. Winterstein, L. P. Hansen, and J. J. Millspaugh. 2015. A review of vital rates and cause-specific mortality of elk *Cervus elaphus* populations in eastern North America. *Mammal Review* 45:146–159.
- Kindall, J. L., L. I. Muller, J. D. Clark, J. L. Lupardus, and J. L. Murrow. 2011. Population viability analysis to identify management priorities for reintroduced elk in the Cumberland Mountains, Tennessee. *Journal of Wildlife Management* 75:1745–1752.
- Kishore, J., M. Goel, and P. Khanna. 2010. Understanding survival analysis: Kaplan-Meier estimate. *International Journal of Ayurveda Research* 1:274.
- Kock, M. D., D. A. Jessup, R. K. Clark, C. E. Franti, and R. A. Weaver. 1987. Capture methods in five subspecies of free-ranging bighorn sheep: An evaluation of drop-net, drive-net, chemical immobilization and the net-gun. *Journal of Wildlife Diseases* 23:634–640.
- Kreeger, T. J., and J. M. Arnemo. 2018. Handbook of wildlife chemical immobilization. 5th edition. Published by authors.
- Kreeger, T. J., M. Huizenga, C. Hansen, and B. L. Wise. 2011. Sufentanil and xylazine immobilization of Rocky Mountain elk. *Journal of Wildlife Diseases* 47:638–642.

- Larkin, J. L., K. J. Alexy, D. C. Bolin, D. S. Maehr, J. J. Cox, M. W. Wichrowski, and N. W. Seward. 2003a. Meningeal worm in a reintroduced elk population in Kentucky. *Journal of Wildlife Diseases* 39:588–592.
- Larkin, J. L., R. A. Grimes, L. Cornicelli, J. J. Cox, and D. S. Maehr. 2001. Returning elk to Appalachia: foiling murphy’s law. Pages 101–118 *in* D. Maehr, R. F. Noss, and J. L. Larkin, editors. *Large mammal restoration: ecological and sociological challenges in the 21st century*. Island Press, Washington, D.C., USA.
- <https://books.google.com/books?hl=en&lr=&id=dtqCMuHotOsC&oi=fnd&pg=PA101&dq=foiling+murphy%27s+law&ots=mmk-RxjnRa&sig=Y5GppMZ4wBz_J5j1YkT29xoJ_-g#v=onepage&q=foiling%20murphy's%20law&f=false>.
- Larkin, J. L., D. S. Maehr, J. J. Cox, D. C. Bolin, and M. W. Wichrowski. 2003b. Demographic characteristics of a reintroduced elk population in Kentucky. *Journal of Wildlife Management* 67:467.
- Le Gouar, P., J. Mihoub, and F. Sarrazin. 2012. Dispersal and habitat selection: Behavioural and spatial constraints for animal translocations. Pages 138–164 *in* J. G. Ewen, D. P. Armstrong, K. A. Parker, and P. J. Seddon, editors. *Reintroduction biology: integrating science and management*. 1st edition. Blackwell Publishing Ltd., Oxford, UK.
- Lees, A., J. Lea, H. Salvin, L. Cafe, I. Colditz, and C. Lee. 2018. Relationship between rectal temperature and vaginal temperature in grazing *Bos taurus* heifers. *Animals* 8:156.
- Levine, R. L., S. P. H. Dwinell, B. Kroger, C. Class, and K. L. Monteith. 2022. Helicopter-based immobilization of moose using butorphanol-azaperone-medetomidine. *Wildlife Society Bulletin* 46:e1327.
- Lian, M., A. L. Evans, M. F. Bertelsen, Å. Fahlman, H. A. Haga, G. Ericsson, and J. M. Arnemo. 2014. Improvement of arterial oxygenation in free-ranging moose (*Alces alces*)

- immobilized with etorphine-acepromazine-xylazine. *Acta Veterinaria Scandinavica* 56:1–8.
- Livezey, K. B. 1990. Toward the reduction of marking-induced abandonment of newborn ungulates. *Wildlife Society Bulletin* 18:193–203.
- Logan, B. R., M.-J. Zhang, and J. P. Klein. 2006. Regression models for hazard rates versus cumulative incidence probabilities in hematopoietic cell transplantation data. *Biology of Blood and Marrow Transplantation* 12:107–112.
- Mazerolle, M. J. 2020. “AICcmodavg”: Model Selection and Multimodel Inference Based on (Q)AIC(c). <<https://www.rdocumentation.org/packages/AICcmodavg/versions/2.3-1>>.
- McDermott, J. R. 2017. Survival and cause-specific mortality of white-tailed deer (*Odocoileus virginianus*) neonates in a southeastern Kentucky population. Thesis, University of Kentucky, Lexington, Kentucky, USA. <http://uknowledge.uky.edu/forestry_etds/31/>. Accessed 7 Mar 2022.
- McDermott, J. R., W. Leuenberger, C. A. Haymes, G. B. Clevinger, J. K. Trudeau, T. C. Carter, J. T. Hast, G. S. W. Jenkins, W. E. Bowling, and J. J. Cox. 2020. Safe use of butorphanol–azaperone–medetomidine to immobilize free-ranging white-tailed deer. *Wildlife Society Bulletin* 44:281–291.
- McFarlan, A. C. 1943. *Geology of Kentucky*. University of Kentucky, Lexington, KY.
- Mercer, J. B., J. F. Andrews, and M. Székely. 1979. Thermoregulatory responses in new-born lambs during the first thirty-six hours of life. *Journal of Thermal Biology* 4:239–245.
- Meuleman, T., J. D. Port, T. H. Stanley, K. F. Williard, and J. Kimball. 1984. Immobilization of elk and moose with carfentanil. *Journal of Wildlife Management* 48:258.
- Mohri, M., K. Sharifi, and S. Eidi. 2007. Hematology and serum biochemistry of Holstein dairy calves: Age related changes and comparison with blood composition in adults. *Research in Veterinary Science* 83:30–39.

- Monteith, K. L., K. B. Monteith, J. A. Delger, L. E. Schmitz, T. J. Brinkman, C. S. Deperno, and J. A. Jenks. 2012. Immobilization of white-tailed deer with telazol, ketamine, and xylazine, and evaluation of antagonists. *The Journal of Wildlife Management* 76:1412–1419.
- Mota-Rojas, D., D. Wang, C. G. Titto, J. Martínez-Burnes, D. Villanueva-García, K. Lezama, A. Domínguez, I. Hernández-Avalos, P. Mora-Medina, A. Verduzco, A. Olmos-Hernández, A. Casas, D. Rodríguez, N. José, J. Rios, and A. Pelagalli. 2022. Neonatal infrared thermography images in the hypothermic ruminant model: Anatomical-morphological-physiological aspects and mechanisms for thermoregulation. *Frontiers in Veterinary Science* 9:963205.
- Murrow, J. L., J. D. Clark, and E. K. Delozier. 2009. Demographics of an experimentally released population of elk in Great Smoky Mountains National Park. *Journal of Wildlife Management* 73:1261–1268.
- National Oceanic and Atmospheric Administration [NOAA]. 2022. U.S. Climate Normals Quick Access (1991-2020). National Centers for Environmental Information. <<https://www.ncei.noaa.gov/access/us-climate-normals/#dataset=normals-annualseasonal&timeframe=30&location=KY&station=USW00003889>>. Accessed 25 Aug 2022.
- Nigon, E. M. 2020. Estimates of calf survival and factors influencing Roosevelt elk mortality in northwestern California. Thesis, Humboldt State University, Arcata, California, USA.
- Paterson, J. 2007. Capture myopathy.pdf. Pages 171–179 in G. West, D. Heard, and N. Caulkett, editors. *Zoo animal and wildlife immobilization and anesthesia*. 2nd edition. Blackwell Publishing Professional, Ames, Iowa, USA.
- Pebesma, E., R. Bivand, B. Rowlingson, V. Gomez-Rubio, R. Hijmans, M. Sumner, D. MacQueen, J. Lemon, F. Lindgren, J. O’Brien, and J. O’Rourke. 2005. “sp”: Classes and methods for spatial data. <<https://rdr.io/cran/sp/>>.

- Pebesma, E., and R. S. Bivand. 2005. Classes and methods for spatial data: the sp package. <https://cran.r-project.org/web/packages/sp/vignettes/intro_sp.pdf>.
- Pollock, K. H., S. R. Winterstein, C. M. Bunck, and P. D. Curtis. 1989. Survival analysis in telemetry studies: the staggered entry design. *Journal of Wildlife Management* 53:7.
- Popp, J. N., T. Toman, F. F. Mallory, and J. Hamr. 2014. A century of elk restoration in eastern North America. *Restoration Ecology* 22:723–730.
- Portier, C., M. Festa-Bianchet, J.-M. Gaillard, J. T. Jorgenson, and N. G. Yoccoz. 1998. Effects of density and weather on survival of bighorn sheep lambs (*Ovis canadensis*). *Journal of Zoology* 245:271–278.
- R Core Team. 2020. R: A language and environment for statistical computing. R Foundation for Statistical Computing, Vienna, Austria. <<https://www.R-project.org/>>.
- Raithel, J. D., M. J. Kauffman, and D. H. Pletscher. 2007. Impact of spatial and temporal variation in calf survival on the growth of elk populations. *Journal of Wildlife Management* 71:795–803.
- Read, M. R. 2003. A review of alpha₂ adrenoreceptor agonists and the development of hypoxemia in domestic and wild ruminants. *Journal of Zoo and Wildlife Medicine* 34:134–138.
- Rice, C. G. 2016. Development of a system for remotely monitoring vaginal implant transmitters and fawn survival. *Wildlife Biology* 22:22–28.
- Romano, J. E., J. A. Thompson, D. W. Forrest, M. E. Westhusin, M. A. Tomaszewski, and D. C. Kraemer. 2006. Early pregnancy diagnosis by transrectal ultrasonography in dairy cattle. *Theriogenology* 66:1034–1041.
- RStudio Team. 2021. RStudio: Integrated Development Environment for R. PBC, Moston, MA, USA. <<http://www.rstudio.com/>>.

- Sams, M. G., R. L. Lochmiller, C. W. Qualls, D. M. Leslie, and M. E. Payton. 1996. Physiological correlates of neonatal mortality in an overpopulated herd of white-tailed deer. *Journal of Mammalogy* 77:179–190.
- Seward, N. W. 2003. Calf survival, mortality, and neonatal habitat use in eastern Kentucky. Thesis, University of Kentucky, Lexington, Kentucky, USA.
- Shuman, R. M., M. J. Cherry, T. N. Simoneaux, E. A. Dutoit, J. C. Kilgo, M. J. Chamberlain, and K. V. Miller. 2017. Survival of white-tailed deer neonates in Louisiana: Neonate Survival in Louisiana. *The Journal of Wildlife Management* 81:834–845.
- Shury, T. 2007. Physical capture and restraint. Pages 109–124 in G. West, D. Heard, and N. Caulkett, editors. *Zoo animal and wildlife immobilization and anesthesia*. 2nd edition. Blackwell Publishing Professional, Ames, Iowa, USA.
- Siegal-Willott, J., S. B. Citino, S. Wade, L. Elder, L.-A. C. Hayek, and W. R. Lance. 2009. Butorphanol, azaperone, and medetomidine anesthesia in free-ranging white-tailed deer (*Odocoileus virginianus*) using radiotransmitter darts. *Journal of Wildlife Diseases* 45:468–480.
- Sikes, R. S., J. A. Bryan II, D. Byman, B. J. Danielson, J. Eggleston, M. R. Gannon, W. L. Gannon, D. W. Hale, B. R. Jasmer, D. K. Odell, L. E. Olson, R. D. Stevens, T. A. Thompson, R. M. Timm, S. A. Trehwitt, and J. R. Willoughby. 2016. 2016 Guidelines of the American Society of Mammalogists for the use of wild mammals in research and education: 97:663–688.
- Slabach, B. L. 2018. The role of sociality and disturbance in shaping elk (*Cervus canadensis*) population structure. Dissertation, University of Kentucky Libraries, Lexington, Kentucky, USA.
- Slabach, B. L., J. T. Hast, S. M. Murphy, W. E. Bowling, R. D. Crank, G. Jenkins, K. L. Johannsen, and J. J. Cox. 2018. Survival and cause-specific mortality of elk *Cervus canadensis* in Kentucky, USA. *Wildlife Biology* 2018.

- Stephenson, T. R., J. W. Testa, G. P. Adams, R. G. Sasser, C. C. Schwartz, and K. J. Hundertmark. 1995. Diagnosis of pregnancy and twinning in moose by ultrasonography and serum assay. *Alces* 31:167–172.
- Tatman, N. M., S. G. Liley, J. W. Cain, and J. W. Pitman. 2018. Effects of calf predation and nutrition on elk vital rates: Influence of nutrition and predation on elk. *Journal of Wildlife Management* 82:1417–1428.
- Therneau, T., T. Lumley, E. Atkinson, and C. Crowson. 2022. “survival”: Survival analysis. <<https://rdocumentation.org/packages/survival/versions/3.4-0>>.
- Thomas, L. F., C. M. Nunez, R. O. Dittmar, R. R. Rech, J. J. Richison, W. R. Lance, and W. E. Cook. 2022. Safety and efficacy of nalbuphine, medetomidine, and azaperone for immobilizing aoudad (*Ammotragus lervia*). *Journal of Wildlife Diseases* 58:636–640.
- Thompson, D. P., J. A. Crouse, T. J. McDonough, P. S. Barboza, and S. Jaques. 2020. Acute thermal and stress response in moose to chemical immobilization. *Journal of Wildlife Management* 84:1051–1062.
- University of Minnesota. 2022. Blood collection guidelines. Research Services. <<https://www.researchservices.umn.edu/services-name/research-animal-resources/research-support/guidelines/blood-collection#sites>>. Accessed 14 Feb 2020.
- Van de Kerk, M., B. R. McMillan, K. R. Hersey, A. Roug, and R. T. Larsen. 2020. Effect of net-gun capture on survival of mule deer. *Journal of Wildlife Management* 84:813–820.
- Viggers, K. L., D. B. Lindenmayer, and D. M. Spratt. 1993. The importance of disease in reintroduction programs. *Wildlife Research* 20:687–698.
- Webb, S. L., J. S. Lewis, D. G. Hewitt, M. W. Hellickson, and F. C. Bryant. 2008. Assessing the helicopter and net gun as a capture technique for white-tailed deer. *Journal of Wildlife Management* 72:310–314.

- Western Kentucky University Kentucky Climate Center. 2022. Monthly summaries. Kentucky Mesonet. <http://www.kymesonet.org/monthly_summaries.html>. Accessed 28 Mar 2022.
- Williams, K. E., N. D. Hooven, J. T. Hast, C. L. Casey, N. M. Nemeth, A. Weyna, M. T. Springer, and J. J. Cox. 2023. Congenital vertebral malformation in a neonatal elk (*Cervus canadensis*) in Kentucky, USA. *Journal of Wildlife Diseases* 59:532–35.
- Wolfe, L. L., M. C. Fisher, T. R. Davis, and M. W. Miller. 2014a. Efficacy of a low-dosage combination of butorphanol, azaperone, and medetomidine (BAM) to immobilize Rocky Mountain elk. *Journal of Wildlife Diseases* 50:676–680.
- Wolfe, L. L., W. R. Lance, and M. W. Miller. 2004. Immobilization of mule deer with thiafentanil (A-3080) or thiafentanil plus xylazine. *Journal of Wildlife Diseases* 40:282–287.
- Wolfe, L. L., W. R. Lance, D. K. Smith, and M. W. Miller. 2014b. Novel combinations of nalbuphine and medetomidine for wildlife immobilization. *Journal of Wildlife Diseases* 50:951–956.
- Wolfe, L. L., and M. W. Miller. 2016. Using tailored tranquilizer combinations to reduce stress associated with large ungulate capture and translocation. *Journal of Wildlife Diseases* 52:S118–S124.
- Wolfe, L. L., M. E. Wood, P. Nol, M. P. McCollum, M. C. Fisher, and W. R. Lance. 2017. The efficacy of nalbuphine, medetomidine, and azaperone in immobilizing American bison (*Bison bison*). *Journal of Wildlife Diseases* 53:304–310.
- Wright, C. A., J. T. Mcroberts, K. H. Wiskirchen, B. J. Keller, and J. J. Millspaugh. 2019. Landscape-scale habitat characteristics and neonatal white-tailed deer survival. *Journal of Wildlife Management* 83:1401–1414.

- Zhou, Q., J. Jin, L. Zhu, M. Chen, H. Xu, H. Wang, X. Feng, and X. Zhu. 2015. The optimal choice of medication administration route regarding intravenous, intramuscular, and subcutaneous injection. *Patient Preference and Adherence* 923–942.
- Zuur, A. F., E. N. Ieno, N. J. Walker, A. A. Saveliev, and G. M. Smith. 2009. *Mixed effects models and extensions in ecology with R. Statistics for biology and health*, Springer Science+Business Media, LLC, New York, New York, USA.

VITA

Kathleen E. Williams

Education and Degrees

B.S., Wildlife and Fisheries Science, August 2011 – May 2015
The Pennsylvania State University, University Park, PA
Minor in Animal Science – Beef Production and Management

Professional Positions

Wildlife Disease Biologist (Bio II), November 2022 – Present
Kentucky Department of Fish and Wildlife Resources – Frankfort, KY

Graduate Research Assistant, January 2020 – Present
Elk Calf Survival and Physiology Research
University of Kentucky – Lexington, KY

Crew Lead, May – September 2019
WA Predator-Prey Project: wolf-ungulate interactions
University of Washington – Chewelah, WA

Research Assistant – LTE, November 2018 – April 2019
WI Deer and Predator Project
Wisconsin Department of Natural Resources – Dodgeville, WI

Lead Technician, May – September 2018
WA Predator-Prey Project: wolf-ungulate interactions
University of Washington – Chewelah, WA

Lead Elk Technician, January – March 2018
Kentucky Department of Fish and Wildlife Resources – Hazard, KY

Black Bear Technician, May – August 2017
Southeastern Oklahoma Black Bear Population Demographics study
Oklahoma State University – Hodgen, OK

Deer & Elk Technician, August 2016 – April 2017
Kentucky Department of Fish and Wildlife Resources – Frankfort, KY

Elk Technician, January – August 2016
Population Dynamics of the Reintroduced Elk Herd in SE Missouri
University of Missouri – Van Buren, MO

Block Management Technician, August – December 2015
Montana Fish, Wildlife & Parks – Plentywood, MT

Fawn Technician, May – August 2015
Mule Deer/White-tailed Deer Fawn Survival Study
University of Washington – Republic, WA

Publications

- Hooven, N.D., Williams, K.E., J. Hast, J.R. McDermott, R.D. Crank, G. Jenkins, M.T. Springer, J.J. Cox. 2022. Using low-fix rate GPS telemetry to expand estimates of ungulate reproductive success. *Animal Biotelemetry* 10:1–14.
- Williams, K.E., N.D. Hooven, J.T. Hast, C.L. Casey, N.M. Nemeth, A. Weyna, M.T. Springer, J.J. Cox. 2023. Vertebral malformation in a neonatal elk born in southeastern Kentucky. Accepted - *Journal of Wildlife Diseases*.
- Hooven, N.D., K.E. Williams, J. Hast, J.R. McDermott, R.D. Crank, M.T. Springer, J.J. Cox. Multi-scale influences on elk calving site selection across a fragmented Appalachian landscape. Accepted with revisions – *Journal of Mammalogy*.

Publications – In prep/In review

- Hooven, N.D., K.E. Williams, J. Hast, J.R. McDermott, R.D. Crank, M.T. Springer, J.J. Cox. Landscape context and behavioral syndromes contribute to flexible habitat selection strategies in a large mammal. In-prep.
- Hooven, N.D., K.E. Williams, J.T. Hast, J. R. McDermott, R.D. Crank, M.T. Springer, J.J. Cox. Correlates of mid-winter pregnancy and early reproductive outcomes in a reintroduced elk (*Cervus canadensis*) population. In-review – *Mammalian Biology*.
- Murphy, S.M., K.E. Williams, M.T. Springer, J.J. Cox. FINAL ANNUAL REPORT: Elk population size estimates in Kentucky during 2019 – 2022 from statistical population reconstruction models. In-prep.